



**This electronic thesis or dissertation has been
downloaded from Explore Bristol Research,
<http://research-information.bristol.ac.uk>**

Author:

Hoare, Daniel T

Title:

Estimating London's methane emissions using a novel urban observation system

General rights

Access to the thesis is subject to the Creative Commons Attribution - NonCommercial-No Derivatives 4.0 International Public License. A copy of this may be found at <https://creativecommons.org/licenses/by-nc-nd/4.0/legalcode>. This license sets out your rights and the restrictions that apply to your access to the thesis so it is important you read this before proceeding.

Take down policy

Some pages of this thesis may have been removed for copyright restrictions prior to having it been deposited in Explore Bristol Research. However, if you have discovered material within the thesis that you consider to be unlawful e.g. breaches of copyright (either yours or that of a third party) or any other law, including but not limited to those relating to patent, trademark, confidentiality, data protection, obscenity, defamation, libel, then please contact collections-metadata@bristol.ac.uk and include the following information in your message:

- Your contact details
- Bibliographic details for the item, including a URL
- An outline nature of the complaint

Your claim will be investigated and, where appropriate, the item in question will be removed from public view as soon as possible.

Estimating London's Methane Emissions using a Novel Urban Observation System

By

Daniel Hoare

Department of Chemistry

University of Bristol

A dissertation submitted to the University of Bristol in accordance with the requirements for award of the degree of Doctor of Philosophy in the Faculty of Science.

June 2022

Corrections: December 2022

Word Count: 27937

Abstract

In recent years city governments have become more vocal and pro-active when it comes to climate policy, with cities such as London having policy in place to reach net zero emissions. In order to achieve these ambitions, cities need reliable methods to understand their emissions. In this thesis I present a novel method for estimating London's emissions, using a purpose-built measurement network and a new custom designed Bayesian modelling system. This modelling system allows for instruments that are calibrated only once before measurements begin, and then drift during a campaign. This allows for a lower cost network that requires less equipment and maintenance, so that a network can be setup more easily across the world. I apply this method to the first 6 months of data collected from the network, January-June 2021, and suggests that London's methane emissions are $47 \pm 27\%$ higher than previously reported in the national inventory.

Dedication and Acknowledgements

I would like to thank Sara and Emmi and everyone else in the GW4+ DTP for their support and community events, making me feel welcome as a PhD student. I thank my supervisor, Matt Rigby, for his guidance throughout these 4 years, and to everyone else in the Atmospheric Chemistry Research Group for being a friendly and supportive team who always had time to lend a hand when it was needed. I must also thank the rest of my London GHG colleagues for their work, as without them this project would not have been possible.

I declare that the work in this dissertation was carried out in accordance with the requirements of the University's Regulations and Code of Practice for Research Degree Programmes and that it has not been submitted for any other academic award. Except where indicated by specific reference in the text, the work is the candidate's own work. Work done in collaboration with, or with the assistance of, others, is indicated as such. Any views expressed in the dissertation are those of the author.

SIGNED: DATE:.....

Contents

1	Introduction	9
1.1	The ‘Climate Emergency’	9
1.2	Emission Monitoring	10
1.3	Inverse Modelling of GHG Emissions	13
1.3.1	Atmospheric Observations	13
1.3.2	Transport Models	15
1.3.3	Inverse methods	17
1.4	Global Emissions	18
1.5	City Emissions	19
1.6	City-scale Observations	22
1.6.1	Overview	22
1.6.2	Relation to Air Quality Networks	26
1.6.3	Hyper-local Observations	27
1.6.4	The Emerging Standard	27
1.6.5	Current Gaps	35
1.7	The structure of this thesis	37
2	The London Greenhouse Gas Project	38
2.1	Aims of the Project	38
2.2	My Role	39
2.3	Complete Network Description	40
2.3.1	Network Design	40
2.3.2	Installed Instruments	41
2.4	Conclusion	42
3	Atmospheric Modelling at the Urban Scale	43
3.1	Introduction	43
3.2	Methods	44
3.3	Results	47
3.4	Thames Barrier Modelling Summary	55
3.5	Additional NAME Modelling	56
3.6	EM27/SUN	60
3.7	Conclusion	64
4	Multi-resolution Inverse Modelling	65
4.1	Introduction	65

4.2	Bayesian Modelling	66
4.2.1	Full Model Description	66
4.2.2	Technical Considerations	68
4.3	Basis Functions and Prior Knowledge	70
4.4	Testing Drift Assumption	72
4.5	Pseudodata Inversion Tests	74
4.5.1	Introduction	74
4.5.2	Results	76
4.6	Further Work	77
4.7	Conclusions	79
5	Inferring Methane Emissions in London	81
5.1	Introduction	81
5.2	Analysing the LGHG network	81
5.3	Data from LICOR Network	82
5.4	Coherence Tests	83
5.5	London's Methane Emissions	85
5.5.1	Drift Correction	88
5.5.2	Emission Values	92
5.5.3	Comparison to Other Work	96
5.6	Further Work	96
5.7	Conclusion	97
6	Summary and Final Remarks	99
6.1	State of the Field	99
6.2	The LGHG Instrument Network	100
6.3	Upgraded Models	101
6.4	London's Emissions	101
6.5	Conclusion	102

Foreword

Welcome to my thesis, I hope that it is a pleasant read for you. I am writing here for two different primary audiences: to my assessors, to convince them that I have made a novel scientific contribution to the field worthy of a doctorate; and to future generations of students who I hope find reading this as helpful a place to start as I did with my predecessors' theses.

For the sake of clarity, I must first discuss a point of grammar. To avoid the use of passive voice, which is both unpleasant to read and misleading (the research was neither performed by this thesis, an animate object, nor did it spontaneously come in to being) I will be using pronouns that acknowledge the existence of people. To keep it clear about the work I performed, the pronoun "I" will refer to me personally and the activities I performed, the pronoun "you" refers to you, the reader, and the pronoun "we" refers to me, you and the wider scientific community.

An important point to note when reading this thesis, is that all of this work was performed as a contribution to a larger project, the London GreenHouse Gas (LGHG) network. This work took contributions from researchers of several different institutes to combine expertise to deliver a complete project. My role in this group was to provide modelling expertise throughout, and as such this is the area of the project I will be writing about in this thesis. Subjects such as instrumentation are mentioned to the point of providing required context for this thesis and the modelling requirements, and to detail any modelling contributions I provided for deployment or analysis purposes. Choices such as the use of a particular instrument, or the focus on London are outside of my remit, but I will mention reasons for these decisions where applicable to help keep you informed. More details are provided in the chapter on this.

Additionally, as a thesis, this text focuses on science and not the underlying technology and software development that took up the majority of my work hours during the PhD. In my opinion, this is an outdated flaw in the PhD process, given how fundamental code development is to modern science and the quality of code can be just as important as the statistical methods used on the output. My contribution in those regards lives on largely as internal documents and group knowledge, but I do include a few technical details within this thesis where they informed my choice

of method for the science involved. If you wish to access the code involved in this project, please contact the Atmospheric Chemistry Research Group.

1 Introduction

In this first chapter I will define the context - both in terms of the scientific theory to build upon and the sociopolitical justification - of this thesis. I will discuss why this field of research exists, the importance of its impact on society, the methods I will use in an abstract form and concrete examples from the existing literature. With this I will describe the current state of the field, and point out the gaps in the literature that still need to be filled. By the end of the chapter we will both have great excitement for how this field of science is rapidly advancing, at which point I will lay out the rest of my thesis to you, my contribution to the field.

1.1 The ‘Climate Emergency’

Anthropogenic greenhouse gas (GHG) emissions have increased at a rapid rate since the industrial revolution. The commercialisation of steam power introduced the large-scale burning of coal and the world has been largely reliant on burning fossil fuels ever since. The greenhouse effect of gases such as carbon dioxide have been known for over a century [1], but it is only in recent decades that a clear global temperature increase has been caused by the accumulated GHGs [2].

In recent years we as a society have begun to prioritise climate change. The release of the Intergovernmental Panel on Climate Change’s (IPCC) special report on 1.5 degrees of warming [2] released at the end of 2018 gained widespread media coverage alerting the public on the dangers of a warming world. By no means the first climate report written, it did make large waves and appeared to herald a turning point in popular opinion. This report was written as part of the 2015 Paris Climate Agreement, in which the parties to the United Nations Framework Convention on Climate Change (UNFCCC) agreed to limit global temperature increases to 2°C at most, and 1.5°C if possible. The special report highlighted the urgent response required to minimise the negative impacts of climate change by analysing the increased risk of harm to the environment and society from the addition 0.5 °C warming. In response, several climate movements and activists such as Greta Thunburg, Friday’s for Future and Extinction Rebellion, have grown to become household names through public demonstrations and their interactions with government.

Governments and other organisations are responding to the latest scientific reports and public opinions, with ‘climate emergency’s being declared for instance by London [3], Bristol and the University of Bristol. Some of these declarations are being backed up with emission reduction plans, such as the London 1.5 degree plan [4] and the UK’s national target to become ‘net-zero’, increased from the previous goal of an 80% reduction. Organisations such as C40, a global network of city Mayors from across the world, have been formed with the express intent on giving guidance on how emission reductions can be achieved, and to begin holding those in power to account on their policy promises.

The COVID-19 pandemic changed the way many people lived practically overnight at the start of 2020, due to efforts aimed at preventing the spread of the virus. Many countries underwent ‘lockdowns’, periods of weeks at a time where many everyday activities were restricted. This had the effect of greatly reducing the amount of vehicle and air miles travelled during these periods, which were expected to result in lower GHG emissions than in previous years. While the restrictions applied were not optimised to reduce GHG emissions, it did provoke much discussion on actions that could be taken to reduce emissions and ways to ‘build back greener’. Even during an event as tragic and all-encompassing as a deadly global pandemic, climate change is still seen as a key issue as society becomes more aware of the dangers it poses, and the efforts required to minimise harm.

1.2 Emission Monitoring

The UNFCCC came into force in 1994 with the aim of stabilising greenhouse gas emissions to prevent dangerous impacts on the environment. Annex I parties (industrialised countries who were disproportionately responsible for greenhouse gas emissions and able to act on reducing them) are required to submit annual greenhouse gas inventories which reported emissions from 1990 until the current reporting year. Such reports give great insight in to where the emissions are coming from, and thus where action must be applied to reduce emissions. The reports also provide a transparency to the process to help ensure that actions are successful and to prevent conflicts of trust between the parties.

GHG inventories are produced using the 'bottom-up' method, based on the simple idea

$$\text{total emissions} = \sum \text{activity} \cdot \text{emissions factor}, \quad (1)$$

where activity is a measure of the frequency of emissions from a particular type of event (such as the number of miles driven by petrol cars in a year) and the emissions factor is the amount of greenhouse gas produced for each event (such as the mass of carbon dioxide emitted by driving a mile in a petrol car).

At the most basic level, large-scale assumptions and averages are used to estimate both the activity and the emissions factors, with more advanced methods involving direct measurements such as placing flux sensors in the exhaust of a power plant, or detailed modelling with auxiliary data to account for geospatial heterogeneity. The majority of the annual reports to the UNFCCC from Annex I parties involves meticulously documenting the methods used to calculate the activity and emissions factor for each category. This is a requirement to ensure the reports are transparent and trustworthy, with the best methods to use varying greatly between different source sectors and the technology available to each country.

In order to help countries produce the highest quality inventories they are capable of, the IPCC provides guidelines on producing GHG inventories. The guidelines detail methods for all the required categories at various levels of bureaucratic and technical difficulties, allowing countries to pick the most appropriate methods for their own situation [5]. This reduces the research and development burden on individual states by providing tried and tested methods, and helps facilitate interstate comparison by provided a limited pool of methods. Alongside these methods for producing the inventories in the first place, there are sections dedicated to quality control and assurance. In the 2019 update of the guidelines, greater emphasis was placed on the use of verification via independent data and methodology to improve the reliability and ensure accuracy of reported emissions, and in particular the use of 'top-down' methods. This comes as a result of the increased maturity of the techniques since the initial publication of the guidelines.

Top-down methods function differently to bottom-up methods, making them useful for verification purposes. Top-down methods use direct measurements of GHGs in the atmosphere as opposed to the indirect economic measurements relied upon by

many of the bottom-up methods (if it were possible to simply measure the emissions of everything directly at source there would be no need for top-down estimates). The report includes several top-down methods, but focuses on inverse modelling, named as it is based upon solving the inverse of the equation

$$y = Hx + \epsilon, \quad (2)$$

where y is a vector of atmospheric observations, x is a vector of GHG emissions (often spatially separated), H is matrix that represents a physical model of atmospheric transport that can relate emissions over the area of interest to the atmospheric concentration at a measurement location and ϵ is a measure of uncertainties in the model and measurements. Details of this equation, and how it solved will be given in a later chapter, for now it will suffice to focus on the larger ideas behind the method.

Inverse models can be applied at scales from global to local, using the same basic principles of combining a physical model with atmospheric observations. Currently, these methods are largely in the domain of researchers and not commercial application, requiring trained experts and specialist equipment to be deployed in bespoke configurations to use successfully. Nonetheless, three countries already use inverse modelling as an additional part of the verification stage of their annual inventories - the UK, Switzerland and Australia. Of the three, the UK has the most advanced setup, with a national network of instruments, the UK Deriving Emissions linked to Climate Change Network (UK DECC Network), being used to measure number of different greenhouse gases including carbon dioxide, methane, N_2O , SF_6 and a variety of halocarbons [6].

The UK DECC network, like many observation networks for inverse modelling, measures the total concentration of each greenhouse gas and is only able to distinguish between sources if they are strongly separated in space or time, including whether the source is natural or anthropogenic. This means that gases without a natural component, or with a natural component that is assumed negligible compared to anthropogenic within the area of interest, are the best candidates for inverse modelling. Gases with large natural components, such as carbon dioxide, are not verified with inverse modelling in the UK's annual inventory although current research is working towards a method to allow for this with the current network [7]. Networks with further specialist instruments that allow for isotopes or co-emitted gases to be measured and

are being trialled in other places [8]. Different sources of greenhouse gases can carry different isotope signatures or different ratios of co-emitted gasses that can be used as information to help determine the source of the emissions. For example, the levels of ethane can be used to help determine whether methane is from a fossil fuel source. These instruments promise more information that will be able to separate sources but will not be available for the work presented in this thesis. Because of this, and that additional modelling techniques are required, these types of measurements are outside of the scope of this work and will only be mentioned in passing.

A consequence of inversion models being source-agnostic, is that they do not provide the same detailed breakdown of sectoral emissions that bottom-up methods provide. This sectoral and source breakdown is very important to creating targeted policies to control emissions, meaning that for policy makers, top-down estimates are best used in combination with the bottom up methods and not as a stand alone product. If the two methods give results that are in agreement, it gives greater confidence to the bottom-up emissions to be used to derive policy, and when the methods are in disagreement (and the top-down method has been interrogated for possible errors) this suggests that their may be incorrect assumptions in the bottom-up model. An example of this partnership between the methods being successful is the case of the UK's HFC-134a emissions inventory, where the bottom-up model was reevaluated after top-down methods inferred very different levels of emissions [9].

1.3 Inverse Modelling of GHG Emissions

An inverse model can be broadly broken down into three components: an observation system that can record atmospheric concentrations of the gas of interest at specified times and locations, an atmospheric transport model that can realistically relate greenhouse gas emissions to atmospheric concentrations, and a mathematical method that solves for the inverse - which results in inferred emissions.

1.3.1 Atmospheric Observations

A number of different techniques can be used to measure atmospheric concentrations of trace gases, which come with their own advantages and disadvantages. The best

type of instrument will depend on the scientific aims of the project, as well as practical constraints such as cost and availability.

For gases such as carbon dioxide and methane (the two gases that will be measured by the London network, and therefore the two that this section will discuss), Cavity Ring Down Spectrometry (CRDS) is a powerful technique that is widely used, such as in the UK DECC network [6]. CRDS instruments use the optical properties of lasers to rapidly measure gas concentrations. The technique measures the intensity decay of laser light in a highly reflecting optical cavity, and how it is affected by the presence of the target gas (which will absorb some of the light, increasing the decay rate). If the absorption rate of the gas at the laser wavelength is known, the ratio of decay rates allows the concentration of the gas to be measured. All of this process is handled by the measurement device. These instruments can achieve high precision as the decay rate is unaffected by variations in intensity between laser pulses, and the ability to build a compact cavity, that can allow the laser to have a path length of several kilometers within a briefcase sized enclosure. A related technique is the Optical Feedback-Cavity Enhanced Absorption Spectroscopy (OF-CEAS) [10], which uses a modified setup from the CRDS which is often simpler, and this is used in some newer trace-gas measuring instruments, such as LiCOR instruments. For inverse modelling purposes, the two techniques function much the same, and the London network will make use of both. As minimal pre-processing of the gas is required, the measurements are also near instantaneous, with measurement times on the order of seconds common in commercial instruments. This allows for high-frequency, continuous measurements that can be installed in limited physical space.

In order to further improve accuracy, it is common to install high-precision CRDS instruments with access to gas cylinders filled with pre-defined blends of air and trace-gases to apply automatic and regular calibration. This automatic process can be done on a daily schedule, which reduces the problem of 'drift' within an instrument. Drift is systematic error in the measurement that changes randomly over time, as changes in temperature and pressure, or nearby vibrations cause slight misalignment in the hardware. While high end instruments are built to minimise the amount of drift present, it is an inherent property of such high-precision multi-component instruments.

For other gases without distinctive absorption peaks at accessible wavelengths, more complicated instruments that are able to separate out traces gases from air are needed, such as gas chromatography. Different gases require different separation and measurement techniques, which result in different precision and measurement times. Some of the specific techniques are discussed elsewhere [6], but are out of the scope of this work.

Remote sensing of trace gases is possible with Fourier-Transform Infrared spectrometry (FTIR). FTIR is another light based measurement system, but uses broadband light (such as daylight) rather than lasers. It uses an inteferometer and Fourier transforms to obtain a spectrum rather than a multipass laser cavity. Instead of placing an air sample into the path of a laser, FTIR trace gas measurement systems are passive, measuring solar radiation that has passed through the atmosphere to measure trace gas concentrations throughout an entire column (or alternatively a slanted path [11]) of the atmosphere. Such system's are implemented both as ground stations such as TCCON (Total Carbon Column Observing Network) [12] and COCCON (COllaborative Carbon Column Observing Network) [13], and aboard satellites such as GOSAT [14]. FTIR instruments, especially those aboard satellites, are often less precise than CRDS instruments and sensitive to more of the atmosphere, measuring a different view of the atmosphere. These instruments are often used in global inverse modelling, with satellites also used for regional studies for areas that do not have dedicated networks of their own [15]. The main problem with these instruments is they are limited to times where there is enough sunlight available - during cloudless daytime. In the UK, especially during the winter, this is a severe limit on the amount of data that can be collected.

1.3.2 Transport Models

Atmospheric transport models range from simplified Gaussian plume models, to full fluid dynamic approaches, and both Lagrangian [15] and Eulerian [16] models have been used for inverse modelling. Lagrangian models approach atmospheric transport by looking at individual parcels of air that are advected and diffused through the atmosphere while Eulerian models place the atmosphere on a grid and model what happens within each grid cell.

Lagrangian models are very efficient when modelling transport for a small number of observation sites, as the air parcels can be started at the location of the measurement and the model run backwards in time in order to determine where the air parcels originated. In this way, it can be guaranteed that no computational resources are wasted on calculating parts of the atmosphere that are not measured by the observation system. Lagrangian models require a description of the atmosphere to inform the transport of the air parcels, such as the output of a numerical weather prediction (NWP) model. Lagrangian models are not inherently limited in resolution as they do not rely on a grid-based system, but the accuracy of the transport will be limited by the resolution of the underlying meteorology. The accuracy of a lagrangian model will also depend on assumptions used to calculate processes such as diffusion within the atmosphere.

Eulerian models are, in general, computationally expensive to run as they perform a full fluid dynamics simulation, although they do not require a NWP model to have been previously run to provide atmospheric conditions, but may use either NWP output or measurements as boundary or initial conditions. Eulerian models are useful for modelling a large number of observation sites, as the model's computational cost scales with the resolution of the model and is indifferent to the number of observation sites as the entire field is resolved. With enough sites, a Lagrangian model's cost will out-scale the initial cost of the Eulerian model. It is also possible to run a cheaper variation which uses the grid system but with pre-computed NWP data and solve only for chemical composition.

Other considerations for transport models include the desired resolution (does the model include features unique to urban environments?) and compatibility with existing data and models (if appropriate NWP output is already available). These models often require a high level of expertise to run, so technical knowledge can also limit the models practically available for a particular study. Ultimately, to be useful in inverse modelling, the transport model must be able to produce the matrix H accurately, which maps GHG emissions to atmospheric concentrations.

1.3.3 Inverse methods

A number of different methods exist for solving inverse problems in general, with several being commonly in use for GHG modelling using different assumptions and approximations. The problem of estimating greenhouse gas emissions from atmospheric observations is particularly suited to Bayesian techniques, which are able to combine information from multiple sources to obtain an answer that is more accurate than the sum of its parts. Here, I will briefly cover an overview of the inverse methods, with a more in-depth and specific discussion in a later chapter.

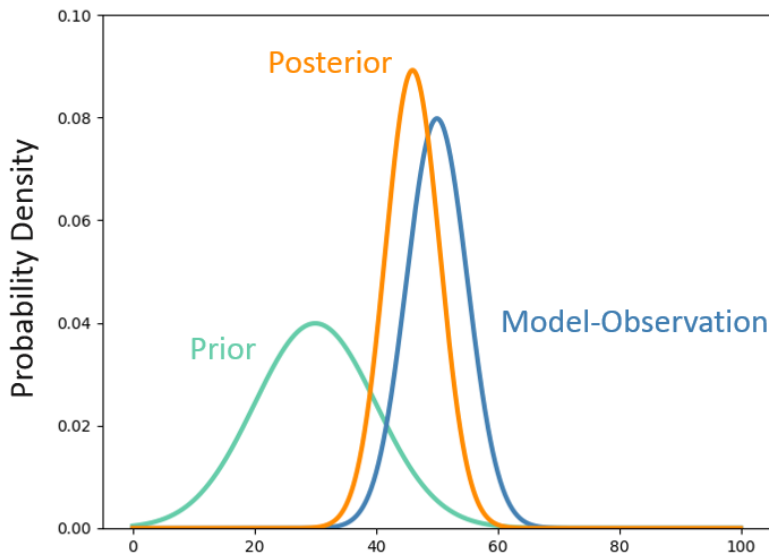


Figure 1: A 1D example of a Bayesian model, showing the prior, model-observation and posterior distributions. The posterior has the lowest uncertainty, given by the standard deviation.

A Bayesian model is based upon Baye’s Theorem, which is most relevant to this work stated as

$$P(x|y) = \frac{P(x)P(y|x)}{P(y)}, \quad (3)$$

where x represents the model inputs and y represents model outputs. $P(x|y)$ is the posterior distribution, $P(x)$ is the prior, $P(y|x)$ is the likelihood function and $P(y)$ is a normalisation term. In GHG emissions, the likelihood functions contain information about the model and measurements, and the prior information is generally taken

from existing GHG inventories. For a 1D Gaussian problem, it can be rewritten as

$$P(x|y) \propto \exp\left(-\frac{(x-x_a)^2}{2\sigma_a^2}\right) \exp\left(-\frac{(y-f(x))^2}{2\sigma_m^2}\right), \quad (4)$$

where x_a and σ_a are the mean and standard deviation of the prior distribution, σ_m is the standard deviation characterising the model-measurement uncertainty and normalisation terms have been dropped for conceptual clarity.

Figure 1 demonstrates the concept and usefulness of a Bayesian approach using a 1D Gaussian example. By choosing parameters to represent a prior and likelihood (or Model-Measurement) distribution, the posterior is calculated using 4. The calculated posterior is also Gaussian, but with a smaller width than either the prior or likelihood functions. In this case, the posterior is strongly informed by measurements and is similar to the likelihood function. Further details of the mathematics of Bayesian modelling can be found in textbooks, including the standard text [17].

In general, the distributions may take non-Gaussian forms and the problem may be many-dimensional. Gaussian distributions may give nonphysical results if negative fluxes are not an acceptable solution, and inversion modelling is often used to spatially and temporally resolve fluxes where each flux component provides an additional dimension to the problem. For these problems, numerical methods are required to sample the posterior distribution. The Metropolis-Hastings algorithm for Markov Chain Monte Carlo sampling [18] is a well established method for sampling arbitrary, high dimensional distributions, however it can be inefficient due to the underlying random nature of the sampling. More modern methods, such as the No-U-Turn sampler extension to Hamiltonian Monte Carlo sampling [19], are much more efficient in their sampling by using gradient information from the distribution to better traverse the probability space but can become stuck if the distribution is not smooth enough. Further details of the relevant methods will be discussed in the chapter on inverse modelling, for now it is sufficient to say that well-tested algorithms exist to solve the equations needed for the work in this thesis.

1.4 Global Emissions

At a global scale methane emissions are complex, with around 60% of emissions being anthropogenic and the rest natural, mostly from wetlands around the globe

[20]. Methane is the second most important greenhouse gas on a global scale, having contributed to about 20% of warming since the start of the industrial age [21]. While it is known that the main sink of methane is with hydroxyl radicals, the exact ratio of sources and sinks is unknown, and one of the great mysteries of global methane is that concentration of methane levelled off for several years in the early 2000s before continuing to rise. Many studies have looked into this, and proposed a number of different solutions such as differing levels of fossil fuel and biogenic emissions [21] or a decline in hydroxyl radicals [22].

However, some of these complexities can be ignored for moving towards city scale emissions. As a city is not a closed system, unlike the Earth as a whole, and atmospheric transport across a city can be measured in hours and days, the hydroxyl radical sink, which gives methane a lifetime on the order of one decade, is unimportant. For city studies, such as this thesis, methane can be treated as nonreactive, with no decay in concentration caused by a sink. If a city is not built atop wetlands, then there may be little natural emissions to consider. Water within a city is likely to be counted as an anthropogenic source, as it will be contaminated by human activity such as farm runoff, industry pollution or waste treatment. This means, for many cities, natural emissions are negligible, which makes it easier to estimate anthropogenic emissions. On the other hand, better constraints of anthropogenic emissions at the city level can help contribute to a better understanding of anthropogenic emissions at a global scale and help to solve the mystery of varying rate of increase in global methane concentration.

1.5 City Emissions

Urban areas are disproportionately responsible for greenhouse gas emissions. A commonly cited figure is that "urban areas are responsible for 70% of emissions", however, this figure taken from the IEA 2008 report is only in regards to energy-related carbon dioxide emissions. These emissions are a large part of total urban greenhouse gas emissions, but they are not the complete picture. A study by Marcotullio et al [23] takes a wider look at global urban emissions, analysing key GHGs (carbon dioxide, N_2O , methane and SF_6) by continent for data available for the year 2000. This study finds that urban emissions account for between 37% and 49% of emissions, depending

upon the method used. The lower figure includes only emissions from within the geographic urban extent, while the higher also includes energy used within the city but produced outside of it. This estimate does not include sectors such as aviation and shipping, which could be also attributed to the city of origin or destination.

Studies like the above highlight some of the difficulties of emissions accounting, with the central question being: which emissions count as being produced by a given city? While this is a key debate for urban policy makers, the final answer of which will have large consequences for accountability, reporting and policy goals, for us this is a simple question. A top-down emissions monitoring network only cares about emissions from within the geographic area of the city, as that is what the network measures.

Of course, there are some difficulties that arise relating to this. As we wish to use existing inventories as a prior value, and to be able to comment on the accuracy of the emissions, we care about which emissions are used to derive the emissions map. This will vary from inventory to inventory, and must be taken into account when choosing which inventories to use for inverse modelling.

For London, there are three official GHG inventories that can be analysed for urban emissions. The UK government commissions the National Atmospheric Emissions Inventory (NAEI), which is a 1km x 1km resolution gridded inventory used towards national reporting for UNFCCC and covers many gases, including carbon dioxide and methane. This is updated every year, 2 years in arrears and is publicly available from <https://naei.beis.gov.uk/>. The Greater London Authority produces the London Atmospheric Emissions Inventory (LAEI) is focused on air quality, although it includes carbon dioxide and methane for some years, and is released every few years. The area covered by this inventory is the area bounded by the M25 and the 32 boroughs. Both of these inventories provide maps based upon emission source locations, for a complete range of source sectors. The local government also produces the London Energy and Greenhouse Gas Inventory (LEGGI), which is focused on GHG emissions produced primarily through London's energy usage. It reports a single carbon dioxide equivalent emissions value composed of carbon dioxide, methane and N₂O emissions, and includes emissions from both direct emissions and indirect emissions related to

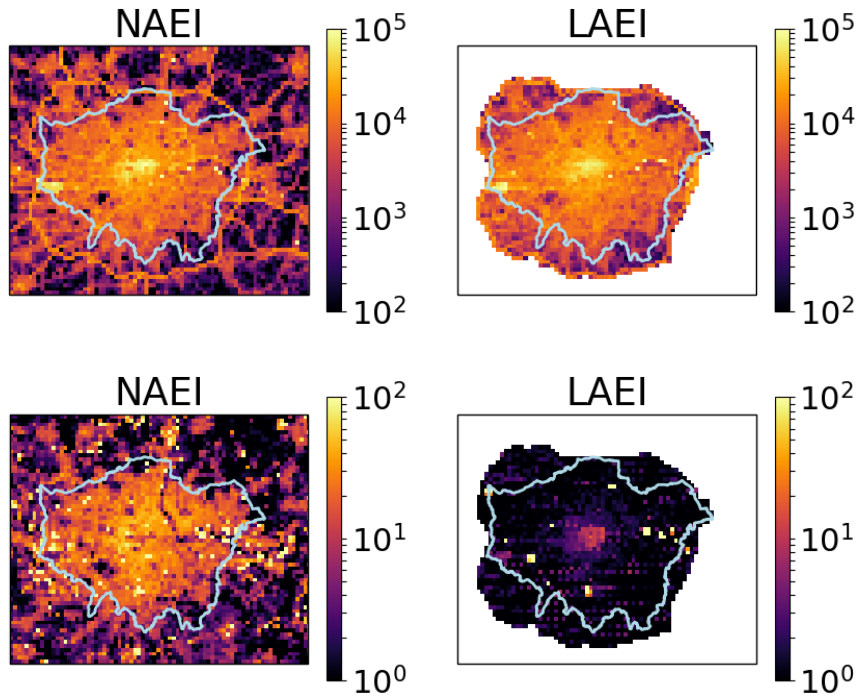


Figure 2: Comparison of emissions (tonnes/year) in two inventories, NAEI 2017 and LAEI 2013, over London for (top) carbon dioxide and (bottom) methane.

London energy usage. LEGGI summarises emissions by borough but does not provide a gridded map of emissions.

I will focus on the two gridded emissions inventories as they are both more complete in the number of sectors being measured, and are more relevant with regards to inverse modelling due to their geographic sources. At the time of writing, the latest NAEI emissions are for 2017, and the latest LAEI inventory to grid both carbon dioxide and methane is 2013. Both grids are 1km x 1km resolution, and to compare London emissions between the two, I will define London as the set of grid cells that overlap with the London boundary polygon downloaded from OpenStreetMap, which includes only the boroughs and city of London.

Figure 2 shows NAEI and LAEI emissions for carbon dioxide and methane over London. Total carbon dioxide emissions with the London region are 21.1×10^6 tonnes for NAEI and 22.7×10^6 tonnes for LAEI. Total methane emissions are 46.7×10^5 tonnes and 24.4×10^5 tonnes respectively. From both the total emissions and from visually

inspecting the maps it can be seen there is good agreement between the inventories for carbon dioxide but poor agreement for methane.

One last point to discuss with respect to these inventories is uncertainty. A NAEI factsheet (https://naei.beis.gov.uk/resources/Sector_Summary_Factsheet.html) says that the uncertainty on total emissions across the UK is 15%. However a report on the methods used to produce the maps [24], does not provide any numerical measurement of uncertainty, highlighting the complexity of the case. As the spatial mapping processing uses further approximations and techniques which introduce their own uncertainties, and also based on the map differences between NAEI and LAEI, it should be assumed that the spatial and London-scale uncertainties in the emissions map are significantly higher than 15%.

1.6 City-scale Observations

1.6.1 Overview

A growing number of cities have been targeted for urban-scale emissions studies, including London. Table 1 summarises a number of of these studies, which are discussed in further detail below. Measurement systems are classified as a Surface Network if (semi-)permanent stationary measurements are used, Satellite for any GHG satellite remote sensing, or Vehicular if aircraft, ships or other mobile transport system is used to host measurement devices. In general, Surface Networks allow for high-precision, long-term studies that can identify changing emissions over the period of years but require sustained maintenance. Vehicular systems allow for snapshots to be taken, with a lot of bespoke configuration possible to target areas of interest but do not give sustained measurements. Satellite sensing has the lowest cost barriers to entry from the user perspective (considering the common case that a user is not launching their own hardware and is using data from a satellite such as TROPOMI (TROPOspheric Monitoring Instrument)), but is also often the least sensitive way to measure GHGs.

Modelling for each city is classified as Inversion for any system that uses an inverse model to estimate emissions, Mass Balance if mass balance equations are used (i.e. accounting for the entire mass of greenhouse gas entering and leaving the

Table 1: Example Urban Emission Studies

City/Region	Gasses	Measurements	Modelling
London	CO ₂ , CH ₄	Surface Network [25], Vehicular [26, 27]	Inversion [25], Mass Balance [26, 28]
Los Angeles†	CO ₂ , CH ₄	Surface Network [29], satellite [30, 31]	Inversion [31], plume mapping [30, 29]
Oakland	CO ₂	Surface Network [32]	Multiple Linear Regression [32]
Paris	CO ₂	Surface Network [33]	Inversion [33]
Salt Lake City	CO ₂ , CH ₄	Surface Network [34], Vehicular [35]	Inversion [34], plume mapping [35]
Boston	CO ₂ , CH ₄	Surface Network [8, 36]	Inversion [8, 36]
Mumbai	CO ₂	Satellite [30]	Plume mapping [30]
Berlin	CO ₂	Satellite (OSSE) [37]	Inversion (OSSE) [37]
Indianapolis	CO ₂ , CH ₄	Surface Network [38, 39], Vehicular [40]	Mass balance [40], Inversion [38, 39]
Yangtze River Delta	CO ₂	Surface Network [41]	Inversion [41]
Cape Town	CO ₂	Surface Network [42]	Inversion [42]
Rotterdam	CO ₂ , CO	Surface Network [43]	Mass-balance [43]
North East Corridor	CO ₂	Surface Network [44, 16]	Inversion [44, 16]
Rome	CO ₂	Vehicular [45]	Mass Balance [45]
Jakarta	CO ₂ , CH ₄	Surface Network [46]	not yet available

†Including South Coast Air Basin (SoCAB)

city’s airshed), or Plume Mapping for measurement of atmospheric concentration enhancement at or down-wind of a site of interest without estimating fluxes.

Within the literature surveyed, a surface network combined with an inversion model was the most common setup for monitoring carbon dioxide and methane emissions using atmospheric observations. Within these categories there exists a lot of variation, with different network designs and models used for each city. Most studies

also focus on carbon dioxide, with much fewer looking at methane. Inversion studies can attempt to attribute emissions to different sectors using tracers, gases which are co-emitted in a known ratio for a subset of sources, such as the co-emission of CO and carbon dioxide in combustion. This method is very limited, only found to be used for measuring gas leakage in Boston using ethane co-measurements [8].

Both the largest and the smallest of the surface networks did not use inversion modelling. The smallest network consisted of two towers around Rotterdam [43], and emissions were calculated using a mass balance approach. Their success was limited by the fact the two towers did not align with the urban region directly between the two, and suggest a stationary tower combined with a mobile measurement device would allow for this to be corrected under different wind conditions. The largest network was located in Oakland, consisting of approximately 50 'opportunistically' sited sensors [32]. This network is analysed with Multiple Linear Regression in order to examine local emissions that are usually filtered out in inverse modelling, taking advantage of the uniquely high density of measurements available to them, and being closer in execution to a low cost air quality network than most other GHG systems.

Salt Lake City [34], Paris [33], Boston [36], Indianapolis [38] and the North East Corridor [16] all display similarities in the methods used. These cities and urban regions have networks consisting of several measurement sites within and surrounding the urban region. Sites within the city limits are highly sensitive to the urban emissions being monitored, and sites upwind of the city centre are used to estimate background concentrations of the greenhouse gas. This is to be taken as the emerging standard system in place for city-scale GHG observation systems, and are most similar to the LGHG system. However, even within this category, there is a large variation in number and location of measurements, and the modelling systems used to combine measurements into an emissions estimate.

Observing System Simulation Experiments (OSSEs) are also used to calculate the usefulness of future satellite missions or network configurations. They have been used to study future satellite missions and their usefulness for the urban scale, where it was found that next generation satellites could provide useful constraints on emissions [37]. Another study has used experiments to calculate the ideal ratio of number of sensors against sensor precision for a given cost [47], which concludes there are

optimal trade-offs between sensor accuracy and quantity. OSSEs are also used to test which of a number of potential sites would be beneficial, with the aim to design a network of ideally placed instruments [44]. The search for site locations was also combined with consideration of using more, but lower performance instruments which may drift more. The work explores different synthetic data inversion setups and the effect of linear drift on results, but does not include drift correction in their inversion.

The use of satellites are less common, but becoming more common as the next generation of satellites are coming online with increased resolution. For instance GOSAT (Greenhouse gases Observing SATellite) could make spot readings of about 10km [30] while OCO-2 (Orbiting Carbon Observatory-2) has a dense swathe of approximately 1.25 km by 2.2 km [48]. One study used the older GOSAT satellite in a plume mapping study that estimated carbon dioxide enhancement over Los Angeles and Mumbai and found that GOSAT would be able to observe a 22% change in Los Angeles's emissions [30]. Orbiting Carbon Observatory-2 (OCO-2) was combined with TCCON sites to perform a flux inversion across the SoCAB, which contains Los Angeles. The results were reported with an uncertainty of 25%, mostly coming from their 12 km scale transport model, which is likely too low resolution to capture urban scale transport. OCO-2 has always been used in a broader study, which looked at 20 cities across the world picked for high population densities, low levels of biogenic influence and high satellite coverage [49]. In this study, cities are treated as singular units without spatially devolved emissions to reduce uncertainty in total emission calculations and the focus is on a broad comparison of global cities.

Within the vehicular category, airborne measurements used in a mass balance model are the most common. This technique has been used in London [26], Indianapolis [40], Rome [45] and New York [50]. With this approach, an aircraft is fitted with a continuous concentration measurement device and flown around the city of focus, sometimes with multiple transects at the key locations upwind and downwind of the city. This is combined with meteorological data characterising the wind and planetary boundary layer height to calculate the mass of air passing within the volume of flight and calculate the emissions required to give the observed concentration gradient. The nature of mass balance equations assume simpler air flow than a full atmospheric model and so can result in higher uncertainty of emissions estimates. Due to the

logistics of these flights, data is often very limited and can provide only snapshots of information, which would increase uncertainty of any annual estimates if emissions vary over time, as there is no way of knowing whether the observations are typical. The New York study demonstrated that inverse modelling could be used with aircraft flights to improve results, but from 9 flights over 2 years, the authors find a variability of emissions of 31% between flights, demonstrating the downside of having such sparse data. Aircraft flights are also able to give measurements of the 'dome' of enhanced greenhouse gas concentration above a city [26], which cannot be achieved by common ground-based instruments.

In Salt Lake City, an electric Light Rail system has been fitted with continuous measurement instruments which provide plume mapping along the railway lines, showing emissions from local industrial sources [35]. These instruments can also be fitted to cars, and have been used to map plumes from local sources within urban areas such as waste treatment facilities [51]. The techniques of local source mapping has recently been extended to use drones to get a more complete spatial profile and perform mass balance equations [52].

Shipborne measurements have been used for emissions monitoring focusing on the country scale, but have been used to estimate emissions from the South of England that correspond to London [53]. This study found agreement with an airborne campaign, but with much larger uncertainties due to less geographical constraint.

1.6.2 Relation to Air Quality Networks

While observation networks designed for air quality have some similarities to GHG networks, there are several fundamental differences. An example of a low-cost, many sensor air quality network is Breathe London (<https://www.breathelondon.org/>), which provides real time measurements of NO₂ and PM_{2.5}, with more gases to become available later. Like the LGHG project, the network is composed of a number of instruments scattered throughout the city that make continuous measurements of air.

Air quality networks are generally focused on human health, measuring gases that are hazardous to people, and are interested in exposure concentrations and not emissions as is important for long lived greenhouse gases. For these reasons, air quality networks often have sensors that are close to the ground and focus on areas that

are highly contaminated by local sources where people may spend time, for example by the road in urban canyons. Each sensor measurement is seen as a snapshot of the air quality in that particular location and time, and does not necessarily say anything about the rest of the city, which is opposed to the use of footprints for GHG modelling.

1.6.3 Hyper-local Observations

As well as city wide measurements, there are also measurements that are local to neighbourhoods or roads within the city. Several studies have utilised instruments mounted on intra-city transport, such as trains [35], cars [51, 54, 55] and bikes. Such measurements give access to the spatial concentration of greenhouse gases in the surveyed area. Using a regular running train provides repeatable and frequent measurements at no extra cost, giving access to temporal information about sources in the region. Personal vehicles on the other hand, require a researcher to actively map out the routes. This means that surveys are often limited in time, but the researchers can target objects of interest and are not limited to existing routes. This leads to these measurements serving different purposes - the former can provide continuous data that is similar, but distinct to other permanent installations, while the latter is useful for spot-checking emissions and providing information about specific sources. This can give us information about sources that are out of sight for other instruments, or for sources that inverse systems have flagged as having large discrepancies from inventory records.

1.6.4 The Emerging Standard

As interest in the field of urban emissions monitoring increases, the number of research teams and different techniques applied increases. As the ultimate goal of this field is to produce emission estimates that are policy-relevant for city government, similar standards and assurances to the national IPCC monitoring will eventually need to be adopted. Without these standards, it will be difficult to compare the results of different cities and networks, and officials may be hesitant to trust and use the results. At the time of writing, organisations such as (Integrated Global Greenhouse

Information System) IG3IS and national metrology institutes are in the early phases of putting together such guides as the science matures.

Although the field is still changing quite rapidly and methods are still being improved by each new network installed, there are already trends appearing in the types of network being built. This de facto emerging standard of urban monitoring network uses from 5 to 15 tall tower analogue sites, equipped with high precision CRDS instruments, coupled to an atmospheric transport model and an inverse Bayesian model. The details and methods vary between networks, with many networks publishing papers to explain the site setup and to demonstrate their chosen models alongside initial results. I will discuss some of these papers here to highlight similarities and differences, but these papers primarily are written after the fact and focus just on the final science, and omit many of the very real practical concerns (logistical and financial) in creating these networks.

Los Angeles

Los Angeles is the test bed for the NASA JPL "Megacities Carbon Project", which aims to develop robust city-scale emission monitoring systems. The contextual framework and the plan for this project is laid out in an article by Duren and Miller [56]. This initial report from 2012 had hoped for surface networks in 25-30 megacities by 2020, and while a number of cities have started surface networks, such an uptake has not yet happened. However, the project is producing useful results from its initial cities, and is inspiration for more cities to join in, including the London network discussed in this thesis.

The Los Angeles test bed is a large budget, multi-institute collaboration designed to look at cutting edge technology and build an ideal model of a city network. Network details and initial results are discussed by [29]. For Los Angeles, the local geography is of tantamount importance. Los Angeles is a high density urban area bordered on one side by the Pacific Ocean, and on the other by a sharp mountain ridge. This mountain is large enough to significantly hinder atmospheric transport, and Los Angeles thus forms a large proportion of the South Coast Air Basin (SoCAB). Measurements made within this basin will be affected greater by emissions within the area, and lesser by emissions outside the basin as compared to flatter terrain. It also means that the local meteorology is affected, and care must be taken with transport modelling. In terms of

measuring emissions, this will cause greater signals to be seen by instruments which may allow for greater accuracy in tracking emissions changes from the city.

The network design was performed using modelled sensitivity analysis [57], and led to the conclusion that at least 8 sites would be needed to constrain fossil fuel carbon dioxide signals. Potential sites were then visited, subject to surveys, and temporary local measurements made before a permanent site was installed. Lattice-structured communication towers were used as primary installation targets, falling back to tall rooftops where needed to cover gaps in the network. This was to reduce the effect (both physics and vent emissions) of buildings on the measurements. Additional modelling was performed to assess the affect of building topology on rooftop measurements. In total 12 instruments (Picarro G2301 and G2401s, two models of CRDS instruments that both measure carbon dioxide, methane, water vapour with the G2401 also measuring carbon monoxide) were deployed across the city in the initial phase of the experiment. Each site also contained instruments to measure a range of meteorological data, however these are not used in this study but are in preparation for future studies. Each site contains two gas standards which are sampled every 22 hours, one of which is used to calibrate the instrument while the other is used in calculating uncertainty statistics.

The network sees greater spikes in concentrations during the night and early morning, when the boundary layer is stable (and thus lower) which leads to increased sensitivity to local emissions and a greater build-up of emissions in the air. The study results look at urban enhancements seen through the measurements, by comparing 'urban' signals and 'background' signals from the network and calculating the difference between them. Background signals are chosen based on statistical techniques that look for stable levels of concentrations indicative of either the ocean or continental background level. No further data, such as meteorological data, is used. Their results show some success with this simple method of calculating urban enhancements, but it is not ideal and some discrepancies were unexplained. Overall, they find that consistent urban enhancements of carbon dioxide and methane are found, varying by time of day and location in the city, with a median enhancement of ≈ 20 ppm and ≈ 150 ppb respectively for central measurements. The largest uncertainties come from background estimation and calibration, both of which are on the order of 1ppb for

carbon dioxide and 10 ppb for methane. These uncertainties are low enough to be able to measure trends in urban enhancement of both gases if emissions decrease.

This surface network has been combined with mountaintop and satellite instruments into an inverse modelling framework for a multi-tiered methane observation network [11]. The cities geography, with the high mountain range at the edge, allows for an FTIR instrument to be mounted high above the city, and used to scan reflective targets installed across the entire basin throughout the day, to retrieve spatially resolved slanted column methane measurements. The unique arrangement allows targeted measurements to be made each day, rather than relying on a once-per-day overhead passage of a satellite or a stationary ground level FTIR instrument.

The inverse model uses STILT, the Stochastic Time-Inverted Lagrangian Transport model, at a 3km resolution to model transport and emissions across the city basin. This study used readily available metrology for this 3km scale, opting for this accessible option over higher resolution custom data.

The work in Los Angeles demonstrates the type of in-depth, high precision measurements that can be made when a high level of expertise and budget are available. While this represents the highest quality of what is achievable with cutting edge science, it would not be possible for such a network to be rolled out to every large city due to these costs. Lower cost networks are needed to fill in the gaps.

Paris

Paris is the second test city, analysing emissions of carbon dioxide, being developed as part of the initial phase of the Megacities Carbon Project. The initial study is discussed in two papers that document a common inversion method and the first 2 months [33] and first year [58] of data. The data from these studies came from 5 sites, the tallest being the 300m high Eiffel Tower in the centre of the city, a 180m tall tower outside of the city limits, and 3 sites between 4 and 9 meters above ground level within the city. Picarro CRDS instruments are used at some sites and gas chromatography at others that already existed, as part of ICOS (Integrated Carbon Observation System). Data is regularly calibrated against the WMO (World Meteorological Organization) WMO-X2007 scale.

For the atmospheric model, the CHIMERE model is used at a 2km scale across the city, and 10km for the region that encloses the city. This model is driven by 15km

ECWMF (European Centre for Medium-Range Weather Forecasts) meteorology. The authors use data from AirParif for an hourly 1km emissions inventory. Data from ECWMF is used for biogenic fluxes of carbon dioxide. The inversion is performed using an analytical (Gaussian) Bayesian inversion framework. These models look only at carbon dioxide, and find that their inversions are very sensitive to diurnal cycles and spatial distribution in inventories, and that heavy handed data selection (removing on the order of 90% of the data) is needed for their inverse method to work, which looks at gradients across the city rather than raw values. These studies often remove a lot of data due to models working best under specific conditions, but requiring these to also be met when conditions are right for gradients to be measured between two sites makes this more difficult still.

Paris has also been used a test city for COCCON, the network of EM27-SUN FTIR instruments [59]. Five instruments were deployed across Paris to measure column carbon dioxide for two weeks in 2015, timed to coincide with long (14 hour) days and low cloud cover, both key issues limiting the data availability from these column instruments. The modelling used here is the same as used by the two previous studies discussed. While the campaign was too short for in-depth analysis, they find the instruments to be sensitive to regional biogenic fluxes and again suggest the use of gradients to reduce uncertainties resulting from estimating background levels.

Salt Lake City

Salt Lake City is within the Salt Lake Valley in the USA, and has five older LiCOR 6262 and 7000 infrared spectrometer carbon dioxide monitoring stations, the oldest of which has been operating for over a decade [60]. This dataset has not been subject to atmospheric and inverse modelling, but the trends have been analysed based on concentration levels above background. By looking at trends in the data, the authors of the study conclude they see signals from a power plant lowering production over the years, and the expansion of the suburban area. They were also able to compare these to temporal patterns in high resolution inventories and how the same trends are not captured in the inventories. While these are some interesting observations to make, inverse modelling could allow for greater insights still.

Inverse modelling was performed back in 2012 with the first few years of data [34]. This study used the WRF-STILT model at both 4km and 1.3km horizontal resolution

to encompass the urban region, although the high resolution was only tested for a two week period. They conclude that their method is precise enough to measure a change of no less than 15% carbon dioxide over a month from the urban region, and that column measurements would improve results, although their evidence for this comes from simulations. A new inversion scheme with a more advanced Bayesian scheme has been tested using synthetic data at Salt Lake City [61], but this has not yet been used on real data. This study finds that the inversion performs well during the afternoon but poorly at other times. The authors argue again for column measurements, stating that their lower sensitivity to PBLH is the main benefit. However, most column based measurements rely on the sun, and thus are only available during daylight hours.

A unique point about Salt Lake City, is the recent instalment of continuous measurements aboard the cities light rail network [35], building up a pictures of emission concentrations (both methane and carbon dioxide) throughout each day and train route. As the trains pass regular routes throughout the entire urban region this is useful for building up a picture of where the largest emissions are, with the study authors being able to pinpoint large point sources in the city and observe how they change over time. This system has not yet been used in an inversion network, but is still able to provide valuable information about urban emissions.

Indianapolis

The Indianapolis Flux Experiment (INFLUX) explores the limits of atmospheric methods for observing urban GHG emissions, using a high density of measurement sites across the city, with a high resolution inventory and a 1km data assimilation modelling system [38]. The core of their atmospheric modelling is based on WRF-Chem, at a 1km resolution inner grid covering the city, surrounded by 3km and 9km grids. They use a Lagrangian model as the adjoint for their inverse methods, where particle locations are recorded every minute over a 12 hour period.

Indianapolis as a city has a small high density core, and up to 50km of lower density suburban sprawl, across the flat terrain of Indiana, with no other cities within 200km which makes the modelling easier. A geographically separated source is far easier to model with the confidence that it is not being influenced by other cities as the model cannot distinguish co-located sources, and nearby sources introduce uncertainty into the results. The full network comprises 12 towers across the city,

although in the inversion study published only the 9 towers that were continuously running during the study period were used. To make the modelling easier again, the authors choose to use only afternoon times during the non-growing period for carbon dioxide. Tower sampling heights are between 40 and 136 meters, and calibrated to having a drift of less than 0.2ppm per year across the sites. Their inversion finds an increase of around 20% on the high-resolution bottom-up inventory (increase of 1.2 ± 0.23 Mt carbon). Their inversion is most sensitive to how the prior error is specified in their model (how the uncertainties are defined on a spatial and sectoral level), and less so to boundary conditions. Their 4D data assimilation shows good skill, but such a model is computationally expensive and requires large amounts of meteorological input data.

The Indianapolis inversion system has been recently advanced [39] to include solving for biogenic fluxes alongside the carbon dioxide fluxes. Inversions were performed over individual periods of 5 days, across 3 years of data (including growth periods) collected from the full 12-tower network. This study finds that for fossil fuel emissions, the inversion and high-resolution inventory agree to 3% annually. The authors do not comment on difference between their results from this and the previous study, however in the time between studies it is possible the inventory was improved, or results were different for different years, or a seasonal bias was introduced, as wintertime fossil fuel emissions were found to be higher. They do however, find a large discrepancy between their results and the cities self-reported emissions, with the self-report being 35% lower than the optimised emissions.

Boston

Boston has a small, 4-site network of measurements within the city centre and on the periphery. These have been used in an inversion system to solve for city-level emissions of methane [8]. The unique element of this study was that the measurement sites also measured atmospheric ethane, and used the ethane-to-methane ratio from the measurements and the natural gas delivered to the city in order to ascertain how much of the cities methane emissions come from natural gas. The study finds over the course of 1 year, that Boston emits 18.5 ± 3.7 g of methane per square meter with a 95% confidence interval. Of this, 60-100% of the emissions are from natural gas. Using government statistics on national gas usage, this translates to a natural gas loss

rate of 2.7 ± 0.6 % compared to inventory values of 1.1%. This is significant larger, and demonstrates a large potential problem with reported emissions of methane in a country like USA that has high levels of natural gas infrastructure, if this loss rate is indicative of a broader problem. Such a study shows the potential for measurements of additional gases to be made, in order to gain access to sectoral emission estimates that are otherwise not possible.

North East Corridor

The North-East Corridor is a testbed project following on from the LA and INFLUX networks, built around Washington D.C. and Baltimore in north east USA. An initial publication of the project was a study that devised a network design method using synthetic data and modelling to look at the potential for sites to improve emissions estimates [44]. By modelling proposed sites, and using an iterative algorithm, the method sought to find a balance between minimising the similarity of each site's measurements and gaining maximum surface sensitivity over the region. The results of the study show that siting towers too close or too far apart leads to sub-optimal emission estimates of the urban regions. They also find that adding further towers increases uncertainty reduction, but with diminishing returns. These findings confirm how such networks are expected to perform. They find that a large number of low-accuracy sensors can be comparable to a smaller number of high-accuracy sensors, but with benefits of wider spatial coverage. The study also takes a look into bias drift in the measurements, but does not attempt to correct for it, and so find that a large bias results in bias in the outputs as expected.

Four towers from this network are used in a methane inversion looking at seasonal variability in emissions [62]. This method uses STILT combined with three different publicly available meteorology sets at 3, 32 and 50km horizontal resolutions. The prior emissions used come from relatively low resolution (0.1°) inventories - EDGAR (Emission Database for Global Atmospheric Research version 4.3.2) [63] and US Environmental Protection Agency (EPA) [64]. A background site is used to set background values for their inversion in one method, or to use the lowest measured value of methane from the four sites in each month as a static monthly background. The authors note that additional measurements may allow for a more sophisticated method to be used, as background concentration can have a large effect on emission

estimates. The inversion is solved using Gaussian methods to calculate emission values with uncertainties. The study finds that there is a slight decrease in emissions during summer, coinciding with lower natural gas usage - the expected highest contributor to methane emissions in the area. However, this study looks at a single year, so may not be a robust look at seasonality. The authors find that their annual emission rates agree with those of other studies using aircraft [65] or gas ratio methods [66].

1.6.5 Current Gaps

Most networks focus on high precision, expensive, and automatically calibrated instruments. While some previous work has begun to consider instrument drift and the potential problems this brings [44], the drift is only considered in its most basic form. Further, the work looks only at the loss of performance from adding drift to an ideal system, and not into methods that are able to extract information better from drifting networks, treating drift as an insurmountable barrier. In order to lower the costs of setting up an urban monitoring network, it would be useful to be able to handle lower-cost, less frequently calibrated instruments, and thus drift needs to be something that can be handled in a way that doesn't invalidate the inversion results. Including drift corrections within the inversion modelling is one of the key targets of the London network.

As discussed, a variety of different instruments and methods have been used to look at city scale emissions, but they are often attempted independently. There is an example of satellite and TCCON sites being combined to give a more complete view [30], but for the most part satellites are not combined with in-situ measurements, or ground-based FTIR with ground-based in-situ. As these methods have different sensitivities to the atmosphere, and therefore nearby and far emissions, combining them may be able to give a more complete image of emissions, so long as the differences between measurements are correctly accounted for when comparing measurements. Part of the work in the London network will look into how useful FTIR measurements will be alongside in-situ measurements.

Most of the urban scale networks are focused on measuring carbon dioxide, with a few looking at methane and only one identified as looking at other co-tracers. This is understandable, as carbon dioxide is a larger contributor to climate change and

emissions with cities are incredibly concentrated, methane is still a potent GHG with high levels of emissions in the city - and a much shorter atmospheric lifetime which could lead to quicker reductions. LGHG will be strongly focused on methane emissions. Nitrous oxide emissions are again shorter lived but more potent, and may have significant urban emissions due to recent trends in their usage as a party drug [?]. While it is common for CRDS instruments to measure both carbon dioxide and methane, it usually requires a separate instrument to also measure nitrous oxide, adding expense and beyond the scope of the LGHG project.

More reliable methods of sectoral attribution are also required to further the usefulness of inverse modelling to policy makers. Some studies are able to use geographic location to attribute emissions to different sectors, but this relies on specific features within the layout of individual cities and may not be widely replicable. Measuring co-emitted gases (co-tracers) or measuring isotope ratios alongside concentrations are other methods that are being developed for this purpose. They have seen very limited use in urban studies, but there is much work to be done in this area before they become routine. This is beyond the scope of the LGHG project.

It is also worth noting that the field as a rule limits itself to afternoon data. While the definition of afternoon can vary between different studies, the primary goal is to avoid nighttime and the transition to day. This is because it is commonly accepted that the models will perform poorly during these times, due to the low, stable boundary layer that forms in the atmosphere. In a smaller boundary layer, the scale of physics that dominated transport at the surface is at or below the resolution of most transport models meaning they are less reliable. Atmospheric transport is also slower than in the well-mixed daytime boundary layer and measurements become dominated by local (relative to the city-scale, ie within neighbouring buildings for instance) emissions. These are difficult problems to overcome, and while in this thesis some nighttime measurements will be looked at for completeness, they are expected to be poorly modelled and difficult to work with. Improvements in this area is considered beyond the scope of this project.

1.7 The structure of this thesis

Now that we have a common understanding of the context of this field and the research that led to its creation, it is time to briefly discuss how the research will be structured and presented from this point forwards. The thesis is divided between an overview of the London Greenhouse Gas (LGHG) Project, then 3 research chapters followed by a conclusion to tie together and summarise the chapters. The research chapters will in turn discuss the skill of current atmospheric models for the new urban sites, the development of a new inverse modelling framework and some tests on synthetic data to characterise its performance, and finally what we can learn about London's emissions from this modelling coupled with the new measurement network. The first chapter is modified from a paper I published in 2020, to exclude some of the context we have laid out already, and to include further details on the method that were not possible within the publishers word limit.

The work from each chapter, while presented separately, is reliant on the work of previous chapters. The high resolution footprints from the first chapter are used to inform the resolution and structure of the inverse methods in the second chapter, which are then used to solve for emissions in the third chapter. While in truth there was some iterative nature to the research - some of the stages were developed in tandem, with prior stages being reworked to fit the needs of later stages as they progressed - the work is presented as a linear progression for clarity and ease of understanding. I note this for any readers, particularly PhD researchers, who are reading this in order to follow a similar path in their own research.

Without any further ado, I will now present to you my 'significant and original contribution' to the field of urban greenhouse gas emission monitoring.

2 The London Greenhouse Gas Project

This short chapter exists to provide context of the larger project within which I worked for this thesis. It will discuss the aims of the project, my role within it, and finish with a description of the final established network. It is the aim that providing this context and knowledge will make the decisions and work of the research chapters easier to understand.

2.1 Aims of the Project

The LGHG project is a NERC (Natural Environment Research Council) funded project lead by the University of Cambridge, with Cranfield University and Bristol University. This project was funded and began before I started, and thus I had no role in its creation. As a publicly funded project, the initially proposed details of the project are available online (<https://gtr.ukri.org/projects?ref=NE%2FR000921%2F1>) but will be summarised here for clarity, and discussed as to how they relate to the rest of the thesis.

The project gives two key motivations for its existence:

1. to follow on from the expensive Megacities projects discussed in the first chapter, but to make them cheaper and simpler with the aim of being practical for cities in the developing world, and
2. to provide policy relevant information at the city scale.

To this end, there were three primary tasks for the project to complete:

1. design and deploy a network low-cost methane, carbon monoxide and carbon dioxide sensors,
2. develop a high resolution inverse modelling method to estimate emissions from these measurements,
3. complete a case study where this model is used on a network of 20 instruments in London over a 12-month period.

The idea was that this case study could then be presented to policy makers in the Greater London Authority, which would help inform policy choices towards London's goals of lowering its emissions.

By the time I had begun my work on this project (and as will become evident in the research chapters to follow) the parameters of these tasks had changed. These changes focused on the measurement instruments that were to be used, and that rather than 20 low-cost sensors, the project began with two sets of 8 higher cost Licor instruments, one set each to measure methane and carbon dioxide (one of each to be installed side by side at each site). While this was a significant change from the original specifications, the original aims were adhered to and these instruments were to be installed with minimal extra equipment to maintain simplicity of the network, and so the modelling would have to account for instrument drift for these devices still.

During my time on the project the coronavirus pandemic caused further changes. Due to lockdowns, and the health and safety difficulties of field work during a pandemic, the installation of instruments was significantly hampered. Instruments ended up being installed several years later than originally expected, and not enough sites were secured to host all the available instruments. As a result of this, the final network (presented later in this chapter) is both far smaller than expected and a full year of data was not available for me to do the case study work on. It is my hope that at a later date, the full timeseries of data will be available for my successor to look at completely using the methods I have created in this work.

2.2 My Role

Within this framework, my role was contained within the second and third points, to develop the new modelling techniques, and apply them during the case study. The procurement and deploying of instruments was to be left to my colleagues at Cambridge and Cranfield, as they were the experts on measurement methods within the project. The sections of this work I contributed thus inform the structure and contents of this thesis, where I have two research chapters focusing on modelling development and analysis work that were completed as the network was planned and installed, and the final chapter being the work towards using London as a case study, although it was not the full 12-month study due to the delays of the pandemic.

In this section I will also describe the only work I completed on the subject of instrument and network design, which was the work to create a short list of potential

installation sites. I include this work for completeness, and to provide potential avenues for future researchers who read this work to undertake, but ultimately this did not account to much as site selection became so heavily constrained by logistical problems (just finding co-operative building owners).

2.3 Complete Network Description

I will now discuss the network as it came to be implemented. I take care to note that I had no hand in the final choice of site locations, instruments and the deployment. As well as the the newly acquired Licors, several Picarro instruments were also included in the network. One of which, at the Thames Barrier, was installed by Cranfield and used as a key part of the first research chapter. The other Picarro sites were installed separately to this project, but their data was agreed to be shared to strengthen the network.

2.3.1 Network Design

The initial network design was guided by several principles: the sites should be evenly spread around the city and should be installed in locations elevated above the surrounding urban canopy. For the latter condition, a database of building heights, and average building heights within 250 meters were obtained and given to me. For London, this database contained over 3 million buildings. The ratio of each building height to its surrounding buildings average height was calculated, to give the height ratio. This selection was narrowed by restricting the search to buildings with a height ratio of greater than 2.5. This is done in order to avoid making measurements within the roughness sublayer of the atmosphere, which is more difficult to model due to increase turbulence and small scale air movement [67].

Due to the great number of buildings available, I applied a stricter (albeit arbitrary with no physics reasoning) height ratio of 4.0, which still results in 1807 buildings on the short list to choose from. Figure 3 shows a map of these buildings across London. Ideally, one would target the buildings with the highest ratio for the clearest measurements. However, for my colleagues, gaining permissions for access to the various target sites proved to be slow and troublesome, and the greatest barrier to this process. Out of practical concerns, the instrument team targeted buildings

on the list for which they had contacts amenable to hosting research instruments, such as churches and council owned buildings. This practical concern significantly reduced the number of possible locations. Because of the logistical difficulties, and the COVID-19 pandemic, instruments weren't installed until nearly 2 years after the initial short listing process. The low number of viable instrument locations meant that no modelling or other advanced technique was applied to the network design at this stage, as sites were ultimately decided on by which ones could be accessed.

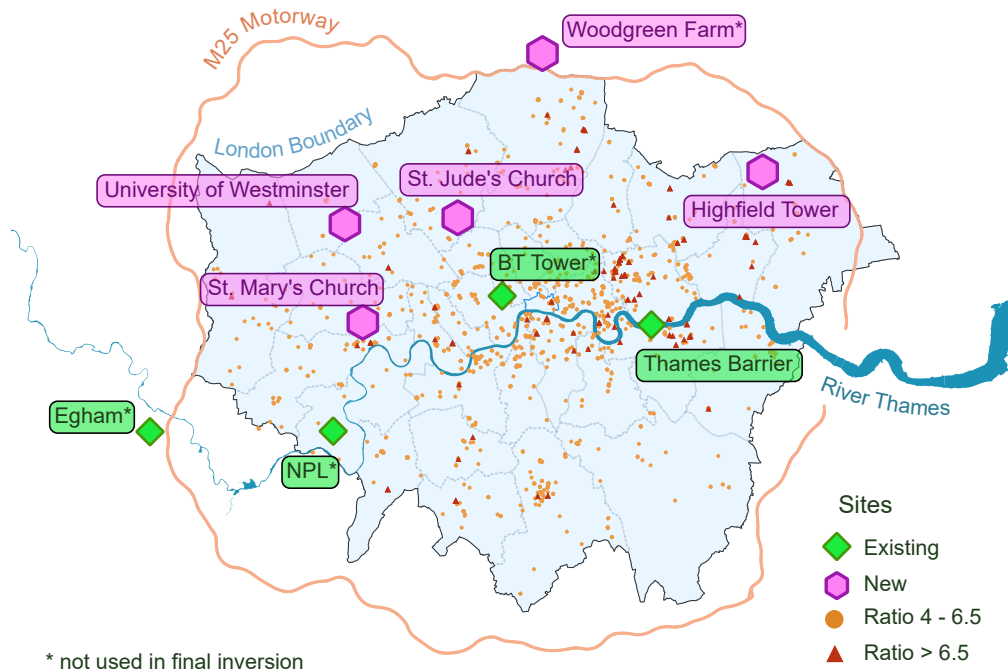


Figure 3: A map of London showing new Licor sites, existing sites with a Picarro and the shortlist of buildings used for LICOR instruments. Due to issues in data quality or availability for the final time period used, several sites are not used in the final inversion in this thesis, however, they are expected to be available for further studies.

2.3.2 Installed Instruments

A map of the London network is shown in Figure 3, and a summary of the sites available is provided in Table 2. The network in total consists of 4 sites with Picarros installed that are automatically calibrated on a regular basis and 5 sites which have the LI-CORs and no automatic calibration in place. Several of the Picarro sites

Table 2:

Site	Code	Instrument	Start Date	Height (magl)	Daily Calibration
Thames Barrier	TMB	Picarro G2401	2018-05-04	10	Yes
NPL	NPL	Picarro G2401	2020-05-01	17	Yes
University of Westminster	LWMH	LI-COR	2020-06-30	40	No
St. Jude’s Church	LSTJ	LI-COR	2020-08-14	20	No
Woodgreen Farm	LWGF	LI-COR	2020-12-05	6	No
St. Mary’s church	LSTM	LI-COR	2020-12-08	36	No
Highfield Tower	LHFT	LI-COR	2020-12-10	45	No

(Egham, NPL and BT Tower) are installed and maintained by the the teams at Royal Holloway, NPL and Imperial College London respectively. Due to issues with the timeliness of data sharing, the Egham and BT Tower sites will not be used for the initial work presented here, but will be available for a full analysis at a later date. The Thames Barrier and all LI-COR sites are installed and maintained by the LGHG instrument team led by Rod Jones and Neil Harris, and located to be evenly spread around London, as far as possible given the practical constraints we faced. It is clear from the map that there is a gap in the network for south London, which may be patched at a later date with further instruments. However, as the dominant wind direction is south-easterly this gap should still be somewhat covered by the rest of the instruments on a regular basis.

2.4 Conclusion

In this short chapter I have presented the context of this thesis, the LGHG project, and explored its goals and how they changed as I came to start this work. I have explained how they link to the work I have performed, and how that relates to what is included in this thesis. It is my hope, that by including this section here, you will have context for the research I present in the first two research chapters, and how they come together for the case study presented in the final research chapter.

3 Atmospheric Modelling at the Urban Scale

This section contains work previously published [68], alongside new material which provides further context as well as greater methodological details appropriate to a thesis chapter. As lead author of the paper, I designed, performed and wrote the analysis presented, with co-authors providing the measurement data, feedback and suggestions on drafts. ADMS-URBAN model runs and details were provided by Cambridge Environmental Research Consultants (CERC).

3.1 Introduction

NAME has been used to model national scale networks, such as the UK DECC network [69, 70] but has not before been used for this type of greenhouse gas inversions in the urban environment. The UKV meteorology produced from the MetOffice’s Unified Model, runs at a horizontal resolution of 1.5km over the UK, which is able to capture the general flow of air through a large city such as London. However, urban environments suffer from local effects due to the complication of topology associated with large buildings, streets and other structures [67]. An urban dispersion scheme is under development at the Met Office, but is still in the initial stages and has not been tested to work in backwards runs as required for inverse modelling¹. For these reasons, it is worth spending some time answering whether NAME can successfully model the atmospheric transport for the city-scale network in London. This is tested by analysing the model-data discrepancies for the initial site at the Thames Barrier, and comparing with a specialist urban scale model, ADMS-URBAN.

In this chapter, I will present analysis of modelling the first few months of data available from a continuous surface measurement site in central London. The modelled and measured time series will be compared using both the NAME model with high resolution output, as well as the ADMS-URBAN model, along with brief descriptions of each model highlighting the differences in this work. These details and the results presented constitute the previously published work. The chapter then ends with supplementary work, commenting on the model parameters used for the NAME runs as well as setting up NAME model runs for a new type of instrument, the EM27-SUN, which measures vertical column-integrated methane abundance.

¹personal correspondence

3.2 Methods

An initial instrument has been established an initial measurement site at the Thames Barrier in central London (51.497°N , 0.037°E). This site measures carbon dioxide and methane using a Picarro G2401 cavity ringdown spectrometer which performs a measurement every 5 seconds with a single measurement precision of approximately 50 parts per billion (ppb) for carbon dioxide and 1ppb for methane, well below the level of hourly variation in measurements that the modelling uses. These measurements are provided in mole fractions, which is the number of moles of the gas of interest relative to the number of moles of air. This instrument is similar to those installed throughout the national-scale UK Deriving Emissions linked to Climate Change (UK DECC) network [6]. In this article we will examine the initial period of data collected from 5 May 2018 to 31 July 2018.

In this work I geographically combine two bottom-up inventories to use as an emissions map, such that NAEI is used where present (over the UK) and Emissions Database for Global Atmospheric Research (EDGAR) used in surrounding countries to ensure coverage across the entire domain. The NAEI is a gridded inventory produced by the UK government, and provides a resolution of $1\text{km} \times 1\text{km}$ which can resolve London, while EDGAR is produced by the European Commission Joint Research Centre at $0.1^{\circ} \times 0.1^{\circ}$ (approximately $10\text{km} \times 10\text{km}$ in the UK). The latest versions of the both inventories available at the time of writing are used, which are 2016 for the NAEI and 2012 for EDGAR. Both inventories provide annual mean estimates and include no seasonal or diurnal time variations, or spatial uncertainty estimates. Within London, NAEI methane emissions are predominantly due to waste and water treatment, and leakages in the domestic gas distribution system. Emissions from the gas network are roughly distributed by population in the inventory, while waste emissions are centred on multiple emission hotspots across the city, as shown in Figure 4. These hotspots may provide a challenge for atmospheric modelling, as they are of a size similar to, or smaller than, the model resolution.

Two models are required to infer GHG emissions from atmospheric concentrations: a physical model and a statistical model. The physical model is usually an atmospheric or chemical transport model that estimates the atmospheric concentration at a given location and time using emission data and meteorological input. The statistical model

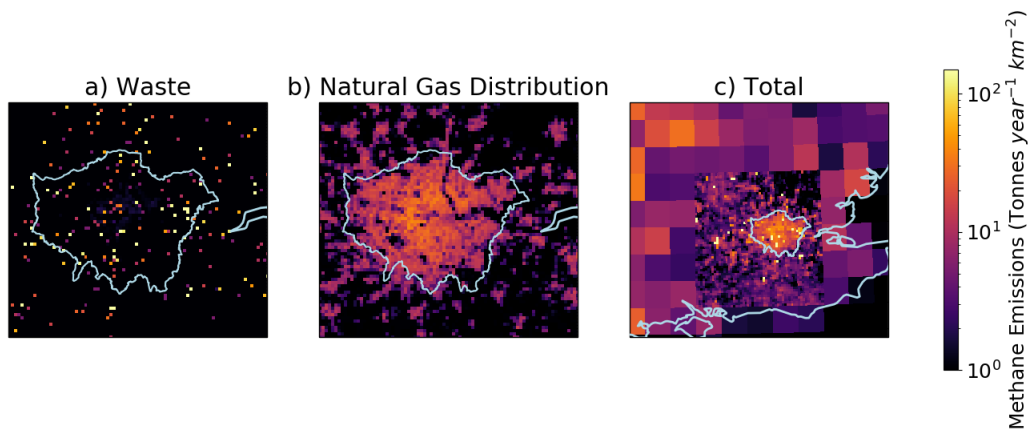


Figure 4: Methane Emissions from NAEI 2016 dataset across London for the two largest sectors, a) waste treatment and disposal, b) natural gas distribution – labelled ‘offshore’ in the inventory, and c) the total methane emissions on the model grid. Outlines show UK coast and London boundaries.

compares the modelled and observed concentrations and calculates the emissions field that enables the model to best replicate observations, subject to various constraints [71]. In this work, we focus on analysing the performance of the physical model in an urban environment.

The first of the two physical models used in this work is the Met Office Lagrangian particle dispersion model NAME [72]. Atmospheric transport is simulated in NAME as the advection and diffusion of thousands of particles, which are tracked backwards in time from the measurement location, recording where they pass near (within 100 meters of) the surface – the assumed source of emissions [69] (Figure 5). The model provides estimates of observation sensitivities known as ‘footprints’, which are 2D fields that map how much the different regions in the emissions field contribute to the observed atmospheric concentration of the gas for each measurement. The model also estimates where and when particles leave the domain, so that boundary conditions can be accounted for. Mole fractions at the measurement site can be estimated as the product of each footprint and the emissions field, plus any contribution from the mole fraction at the boundary of the domain. The domain and boundaries used in this work are shown in Figure 6. The boundary conditions are taken from the Copernicus Atmosphere Monitoring Service global methane products, which use

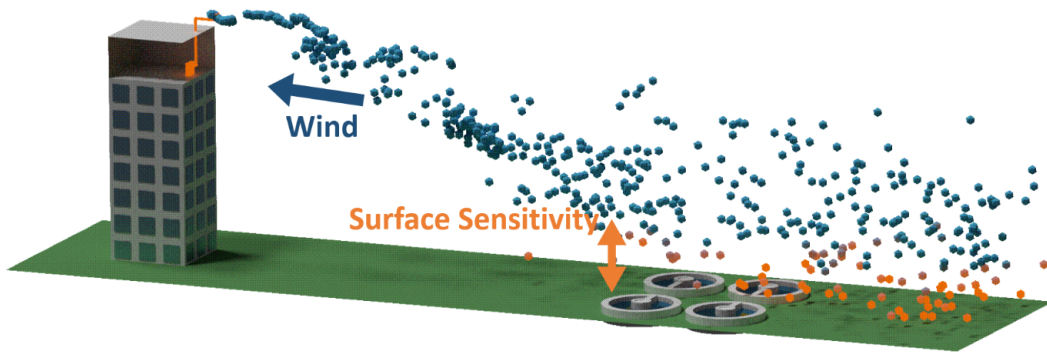


Figure 5: Schematic depiction of a Lagrangian particle dispersion model, such as NAME. Each sphere represents a modelled particle, which is released from the measurement location and transported backwards in time through advection and diffusion, and its passage near the surface is recorded to estimate where the air may have picked up methane emitted from the surface.

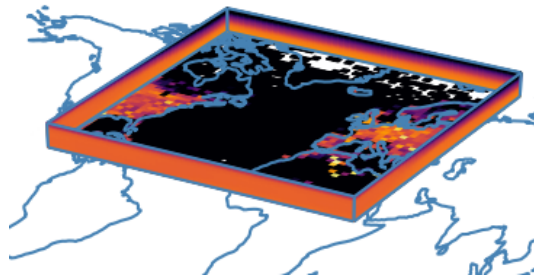


Figure 6: Domain and boundaries for NAME, height not to scale.

satellite measurements and models to produce global four-dimensional methane fields [73], adjusted to better match background measurements at Mace Head, Ireland.

The NAME model was run offline using Met Office Unified Model meteorology. I use the high resolution (1.5 km) UKV meteorological data where available and the approximately 12km resolution Global dataset elsewhere. While the UKV meteorology is high enough resolution to resolve urban scale phenomena such as the urban heat island, NAME itself does not explicitly account for urban turbulent transport. Footprints and emissions are combined in a multiple-resolution grid shown in Figure 4c, with a high-resolution ($0.032^\circ \times 0.021^\circ$, 2.5km) grid covering London and its surroundings embedded in a low-resolution ($0.352^\circ \times 0.234^\circ$, 25km) grid used for previous national modelling [74].

The second physical model used is ADMS-URBAN produced by CERC, [75, 76]. This model is designed specifically to model urban environments at a very high (street level) resolution, taking account of complex features such as the effect of buildings. ADMS-URBAN differs from NAME in several key ways: ADMS-URBAN can explicitly represent large numbers of individual sources including point sources (with specified heights) and road sources but is limited in domain, the concentration downstream of each source is represented by an analytic distribution which for point sources is Gaussian in neutral and stable conditions and skewed Gaussian in unstable conditions, but has other more complex forms for road sources. The concentration distribution is stationary in time for each successive hour and may use single-site or gridded meteorology to calculate the footprint. Here, we drive ADMS-URBAN with meteorological measurements from Heathrow Airport. These measurements are internally modified according to the difference in roughness lengths from the urban landscape at Heathrow and the Thames Barrier, resulting in a lower windspeed. This is the same setup that has been successfully used for modelling air quality in London [76]. The boundary layer height is calculated internally as opposed to NAME, which uses the value diagnosed in the Unified Model. In this study the domain for ADMS-URBAN is the same as used by the LAEI, which encompasses all London boroughs and everything within the M25. As ADMS-URBAN does not estimate the influence of fluxes outside London, or regional boundary conditions, the ADMS-URBAN footprint requires additional information, so that the total methane concentration can be simulated. In this study, we embedded ADMS-URBAN footprints within the larger-scale NAME footprints. The ADMS-URBAN footprints are coarsened to match the NAME high-resolution grid (2.5km) and thus loses some spatial information, as the grid cartographic projections are otherwise incompatible. The geographic extent of London used throughout the paper is taken from the OpenStreetMap London administration polygon, rasterised onto the NAME high-resolution grid.

3.3 Results

Examples of NAME and ADMS-Urban footprints are shown for two different meteorological conditions in Figure 7. The top row shows footprints under steady westerly winds on 10 May 2018 1500 UTC, whereas the bottom row shows footprints on 24

May 2018 1500 UTC under more complex conditions with fronts passing over London (Figure 8). Under the steady westerly winds, both footprints are qualitatively similar, with observations at the Thames Barrier being influenced by fluxes from western and central London, although the ADMS-URBAN footprint is four times more sensitive to emissions when both models are integrated over London. Under the more complex meteorological scenario, the NAME footprints indicate sensitivity to a wider area of London with nearly twice the total London sensitivity as ADMS-URBAN, presumably reflecting the range of wind directions experienced by the model particles, whereas the quasi-Gaussian plume model shows sensitivity to a narrower region upwind of the measurement site. On average, ADMS-URBAN is about twice as sensitive to London fluxes as NAME, with a mean (5th-95th percentile) total London sensitivity of 0.97 (0.24 - 2.96) $(\text{mol m}^{-2} \text{s}^{-1})^{-1}$ compared to 0.43 (0.09 - 1.39) $(\text{mol m}^{-2} \text{s}^{-1})^{-1}$ for NAME. These differences are likely due to a combination of different boundary layer and dispersion calculations, and input meteorology used by the two models.

Figure 9a shows the hourly median and 33rd-66th and 5th-95th percentile ranges of methane observations at the Thames Barrier between 5 May 2018 and 31 July 2018 inclusive. Observed mole fractions are generally higher and more variable at night than during the day, and the lowest values observed are typically observed during the daytime. This difference is thought to be largely due to diurnal changes in atmospheric stability, with stable nocturnal boundary layers trapping locally emitted methane in contrast to strong mixing of nearby sources during the day [77].

Figure 9b shows the mean observed mole fractions as a function of wind direction and wind speed which highlights that highest observed concentrations occur at low windspeeds and/or from a north-easterly direction. There are several possibilities for why north-easterly winds are associated with higher methane concentrations. The first reason is that these winds are likely to be carrying emissions from mainland Europe, with the Benelux region being particularly high in emissions according to the EDGAR inventory. In contrast, when winds come from the west, they arrive in the UK or Ireland with mole fractions consistent with the hemispheric background. A contribution from local sources is also possible, with several large methane emission hotspots within several kilometres of the Thames Barrier, according to the NAEI. For example, emissions from the Beckton Sewage Treatment Works approximately 4

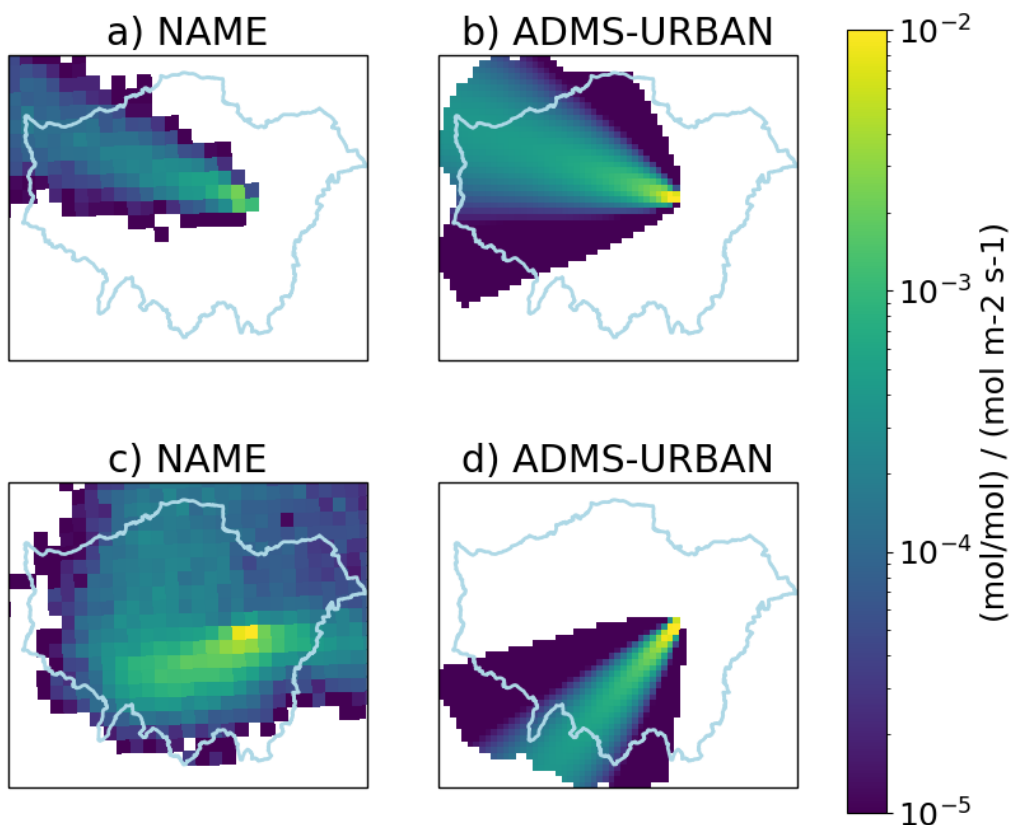


Figure 7: NAME and ADMS-URBAN footprints over London for (a,b) calm weather on 10 May 2018 1500 UTC and (c,d) a passing front on 24 May 2018 1500 UTC .ADMS-URBAN agrees qualitatively with NAME using gridded meteorological input in most weather conditions over London but differences are found in the overall magnitude of the footprint and during complex meteorological conditions (e.g. passage of fronts).

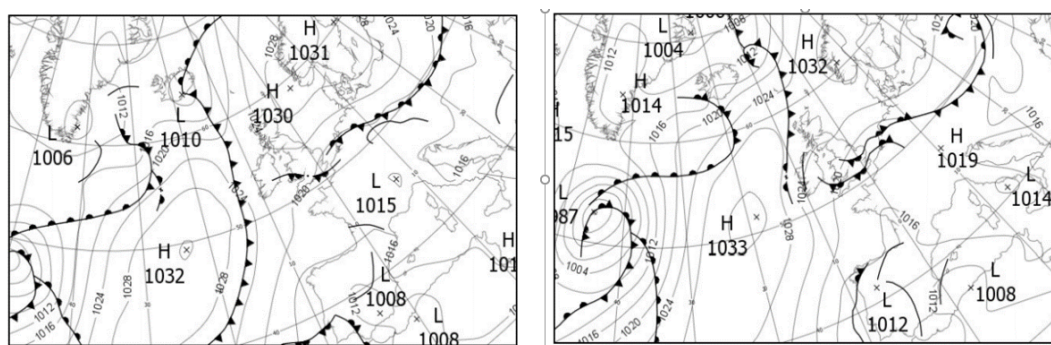


Figure 8: Met Office analysis charts for 24 May 12:00 and 25 May 00:00, showing the passage of fronts through London. Reproduced from the Met Office Daily Weather Summary 2018, Met Office Crown Copyright.

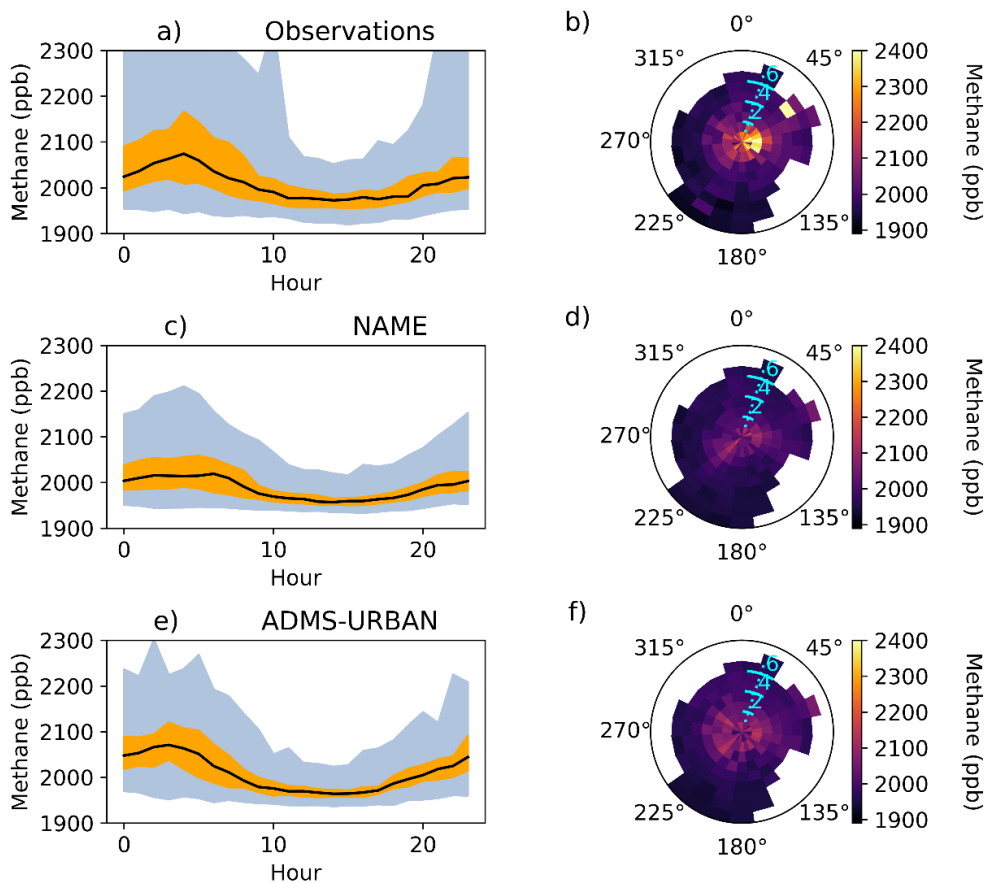


Figure 9: a,c,e) Methane hourly median (black line) and 33rd-66th (orange area) and 5th-95th (blue area) percentile range mole fractions and b,d,f) rose plot (angular: wind direction, radial: wind speed in ms^{-1}) for the Thames Barrier (51.497°N , 0.037°E) for (top) observations, (middle) NAME and (bottom) ADMS-URBAN between 5 May 2018 and 31 July 2018. Extreme values in a) are not shown to allow a clearer comparison to model values.

km away may be consistent with the maximum in the mole fraction rose at around 50° . Mole fractions associated with this wind direction tend to be highly variable, suggesting a nearby plume impinging on the measurement site, rather than a more well-mixed regional source. Data from the additional sites planned around London could help distinguish between these two cases by providing different viewpoints on local emissions.

By combining the footprints for NAME or ADMS-URBAN (embedded within NAME) with the NAEI and EDGAR emissions fields, we can produce a modelled timeseries that can be compared to the Thames Barrier data. An example for a typical two-week period is shown in Figure 10. The modelled mole fractions are attributed to three different factors: fluxes from within London, fluxes outside London and contribution from the boundary conditions at the edge of our NAME domain. The two models only differ in their modelled London contribution as the ADMS-URBAN footprints are embedded into the NAME-derived regional footprints and boundary conditions. The full period mean and 5th-95th percentiles of the mole fraction due to sources within London for NAME and ADMS are 34.2 (4.37-121) ppb and 55.9 (9.30-173) ppb respectively, compared to 45.2 (9.67-113) ppb from regional sources and 1921 (1910-1937) ppb from the boundary conditions. The modelled concentrations generally capture the observed diurnal cycle, although the magnitude of the night-time peaks can differ from the observed data by around a factor of two or more, with modelled concentrations lower, suggesting the models overestimate atmospheric transport during the night as there is no expectation of greatly increased nighttime emissions.

Figure 9c-f show the hourly medians and wind dependence for the observed, NAME and ADMS-URBAN modelled mole fractions. From the hourly medians, the night-time underestimation seen in Figure 10 is more evident. Both models show an increase in mean mole fractions at low wind speeds, but at a much lower magnitude than in the observations. This finding could be because nearby sources (within a few km) are larger than estimated in the inventory, or it could show that the models tend to over-estimate mixing during low-wind conditions, with both possibilities suggesting the high observations are not primarily due to the Benelux region. The hotspot to the north-east is also not captured in the models, which may indicate that a source

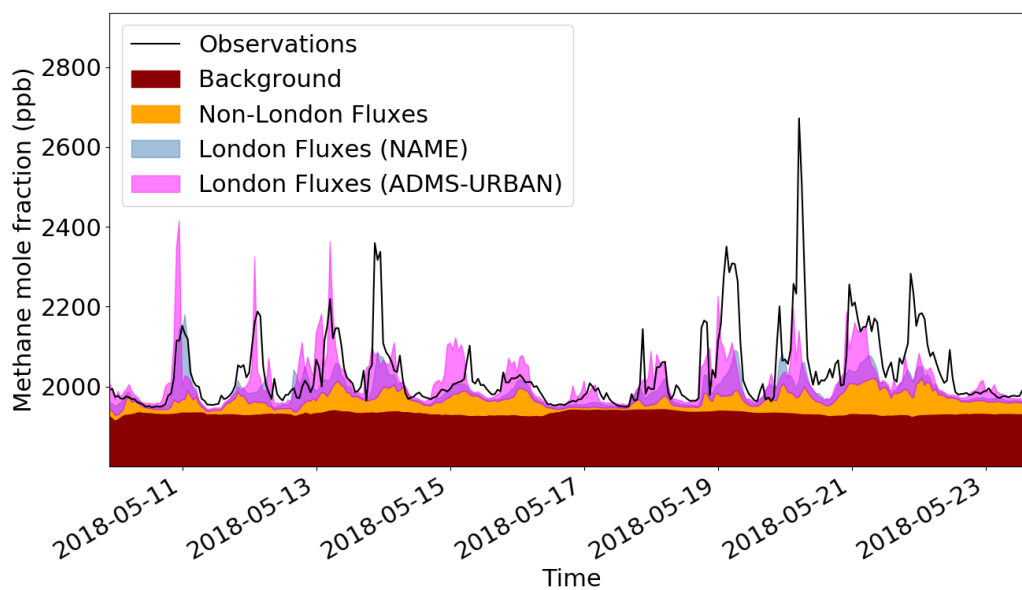


Figure 10: Timeseries comparison of modelled and observed fluxes for both NAME and ADMS-URBAN embedded in NAME. The different colours represent the contribution from different geographical regions, with the Background and Non-London Fluxes being the same between the two models. The purple segments show where the two London contributions overlap.

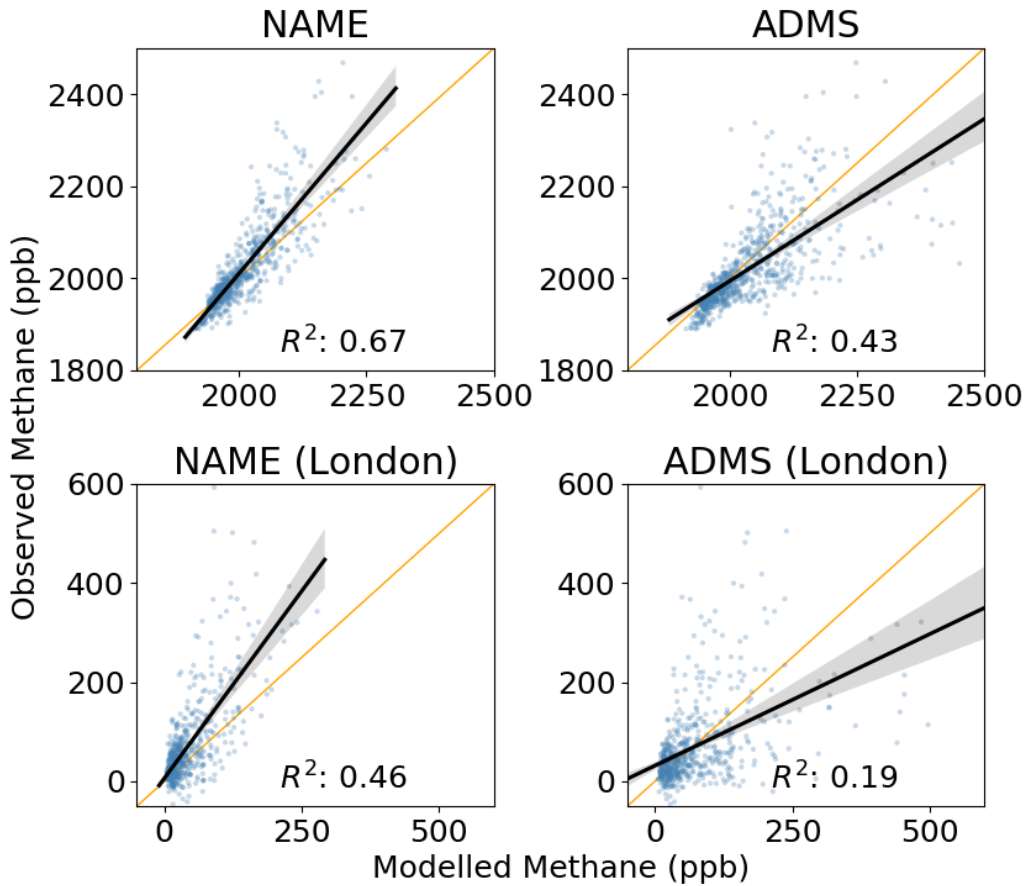


Figure 11: The top row shows the hourly mean mole fractions (contributions from London, regional sources and boundary conditions) for NAME (left) and ADMS (right). The bottom row shows the London contribution only, by subtracting the modelled non-London component from both the data and the model.

in this direction is not present or underestimated in the inventory, or it could show that model transport is generally too dispersive for this wind sector. A result like this highlights a point of interest that could be further explored with mobile instruments that can map out local emissions clearly, as this seems to be a long-running effect rather than a one-off event.

Figure 11 shows the modelled mole fractions plotted against the observations for the two dispersion models, for total concentrations and the London contribution only. For this analysis, the data were filtered to keep only points where the observational variability within each hour period was less than one half of the modelled London contribution. This removes points heavily influenced by local emissions that the models

are not expected to capture accurately, such as an exhaust vent on a neighbouring building. Such a method could result in an underestimate bias if the instrument is near a significant source that gets filtered. However, this would be avoided when multiple sites are used for the full network. Summary statistics are shown in Table 3. Overall, the models show broadly similar correlations with the data, despite their very different architectures, with the largest difference being where the ADMS-URBAN model overestimates methane concentrations. The NAME model has a slope of regression greater than 1, suggesting that the emissions or modelled sensitivity are underestimated. The opposite is true for the ADMS model, although the line of regression is skewed by a small number of points where the model greatly overpredicts methane concentrations. For both models, the R^2 value decreases when looking at just the London contribution, perhaps because they struggle to accurately represent complex urban meteorology, or because of errors in the distribution of nearby emissions sources in the NAEI. During the most well-mixed conditions (between 1100 and 1700, when hourly observation variability is below 5 ppb) the models are in closer agreement but show lower sensitivity to London emissions than at other times. Overall, model output from NAME correlates more strongly with the observations than ADMS-URBAN, perhaps due to the use of three-dimensional meteorology, compared to single site meteorology. However, ADMS-URBAN better captures the diurnal cycle present in the observations, possibly due to the different boundary layer height calculations used- although there could be many factors that contribute to both differences between the models.

These simulations show that NAME and ADMS combined with the NAEI can capture some of the major features in a methane mole fraction time series at an urban site. The two models show similar features in their simulated mole fractions, despite a different modelling approach and driving meteorology, which suggests that a substantial portion of the model-measurement mismatch is due to the differences between the truth and inventory emissions magnitude, distribution and/or temporal variability. The next step in the development of a modelling system to support the London GHG network is to develop a new statistical model, an inverse modelling system that can determine whether changes in emissions and their distribution can improve the fit between the model and the data [74]. The differences between

Table 3: Linear fit statistics for model-observation comparison. The slope is derived with the model-predicted mole fraction as the independent variable (as in Figure 8), and the bias is the mean of the data minus the model (i.e., a positive bias, or a slope greater than one shows a model underestimate and vice versa).

Model Configuration	Slope	R2	Bias (ppb)	Standard Deviation (ppb)
NAME	1.3	0.67	12	59
ADMS embedded in NAME	0.71	0.43	-17	79
NAME (London)	1.5	0.46	28	72
ADMS embedded in NAME (London)	0.53	0.19	-2.9	92
NAME (well mixed)	1.2	0.77	1.8	16
ADMS embedded in NAME (well mixed)	0.95	0.63	-6.6	20

the models will lead to differences in inferred emissions from an inverse modelling system. These differences will capture some of the sensitivity of the inverse models to atmospheric transport error and can help better inform interpretation of inferred emissions as a result.

3.4 Thames Barrier Modelling Summary

As a first step in the development of a network for monitoring of London’s carbon dioxide and methane emissions, a continuous measurement site has been established on the Thames Barrier by the instrument team. In this chapter I analysed methane data from this site during the summer of 2018 and compared the observations to two distinct atmospheric transport models, NAME and ADMS-URBAN. Results showed that over a 3-month period, the models could capture some of the broader features in the data, such as the diurnal cycle and wind-direction dependence. The consistency of the difference between the model prediction of some of these features and the data suggests that there may be a large discrepancy between the inventory emissions and actual emissions, and further study will be useful to analyse this.

Ideally, any follow-up would use both models in the inverse modelling, to provide some estimate of the sensitivity of the derived emissions to atmospheric transport model errors. This thesis will focus on the use of the NAME model from here, with follow up work using ADMS-URBAN recommended. The further work suggested in the original paper - work towards a London GHG monitoring network will involve the setup of additional measurement sites across the city, and the development of an urban-scale inverse modelling system - form the next chapters of this thesis.

Provided that the network can be supported over the coming years, the results from the emission estimates with these new measurements will be supplied to policy makers to help determine whether London's emissions reduction targets have been successful. The LGHG system also has the potential to identify missing sources or spatial discrepancies in the NAEI and may be able to give some insight into the temporal variability in emissions not accounted for in the bottom-up inventories.

3.5 Additional NAME Modelling

This subsection is supplementary information to the modelling efforts previously discussed in this section. In order to assess the model configuration of NAME for use in the new urban scenario, NAME is run as an ensemble with different input parameters. The outputs from these models are fitted against observational values, as described above, and the fit is compared between model configurations to identify which model setup performs best. All ensembles are run for comparison over May 2018 for Thames Barrier, chosen as a representative sample of the data, as this work is computationally expensive. For comparison between model and observations, the time series is filtered to remove times when the observational variation was greater than 20 ppm. This threshold is applied as times with high observational variations within the hour are most likely due to rapidly changing meteorological conditions or local pollution events that cannot be captured by the model. Different model configurations are compared using the model-measurement correlation as a metric.

The first ensemble of 9 configurations varies the number of particles and type of meteorology used, as shown in Table 4. These are all run with a 5x5 high resolution grid of approximately 2km horizontal resolution. Two separate ensembles were run for the resolution and extent of the high resolution grid, based upon the best performing

Table 4: Model configurations for the first NAME ensemble. London UKV refers to just UKV PT14 used over the south East, all UKV refers to all 16 UKV PTs used over the UK.

Model Configuration	Particles per Hour	Input met
1	3333	Global
2	10k	Global
3	20k	Global
4	3333	London UKV
5	10k	London UKV
6	20k	London UKV
7	3333	All UKV
8	10k	All UKV
9	20k	All UKV

model from the first ensemble. These parameters are picked as higher values or increased fidelity are expected to increase the skill of the mode, but with greater computational cost. Although the cutoff is arbitrary and subject, by analysing a range of values, we can pick a point before diminishing returns sets in to balance skill and cost of the model.

Figure 12 shows the comparison between members of the first ensemble. As can be seen, the number of particles makes only a minimal difference within the range chosen, suggesting that even the lowest number of particles here is sufficient for the model. The type of meteorological input used has a much greater effect, with a clear improvement in model performance when using the higher resolution data. A greater difference is seen between the global met, and the UKV met only over London, than from London only to all of the UK being covered by UKV. The interpretation here is the former directly improves the surface sensitivity of the model over the London area, which is the most significant source of emissions as seen by the model, whereas the latter is just an improvement on long range transport and modelled background values, which vary less.

For the inner grid resolution, resolutions of approximately 20km (no separate inner grid), 4km, 2km and 1km are used. The high resolution met data has a resolution

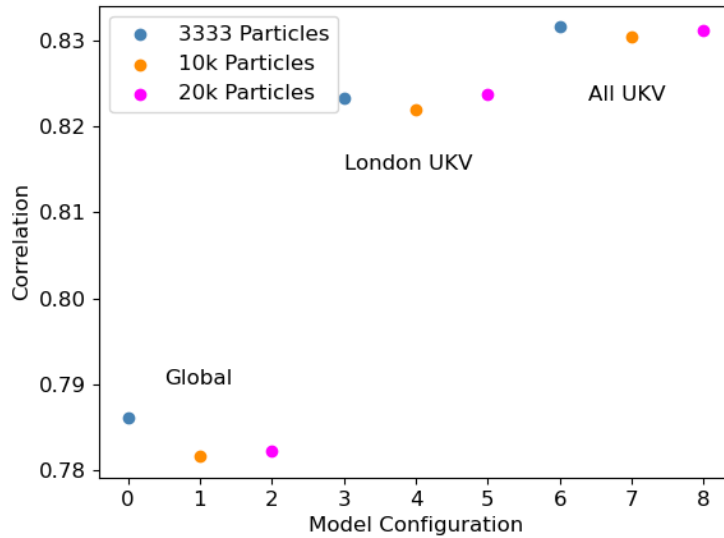


Figure 12: Model-measurement correlation for the NAME parameter scan of number of particles and input met data.

of 1.5km, and the input emissions inventory has a resolution of 1km, setting the lower limits for improvement of model-measurement mismatch. The correlations in Figure 13 show a model improvement as resolution is increased, but has converged to greatest correlation by the 2km resolution grid, with no improvement when moving to 1km. This may be due to the limit of the underlying met data, or of increased spatial uncertainty of the input emissions at its native 1km resolution.

The effect of the extent of the inner grid on model-measurement mismatch was explored by running a 2km inner grid with an extent that corresponded to a 7x7 box of the outer grid and comparing subsets of the inner grid. The correlation values and maps of the inner grids are shown in Figure 14. The grid cell that contains the Thames Barrier (B) contributes almost half of the total correlation increase of the full inner grid. The grid cell immediately to the east (C) contributes around a third of the total improvement, and the rest by the other 7 cells that include London (D). Grids for (E) and (F) are offset to the west as this is the dominant wind direction and so is expected to be more important to model better. Although these grid cells provide no further improvement to model-measurement correlation, they may allow for increased performance in the inversion stages by allowing the inverse model to more finely reassign fluxes in the area immediately surrounding London.

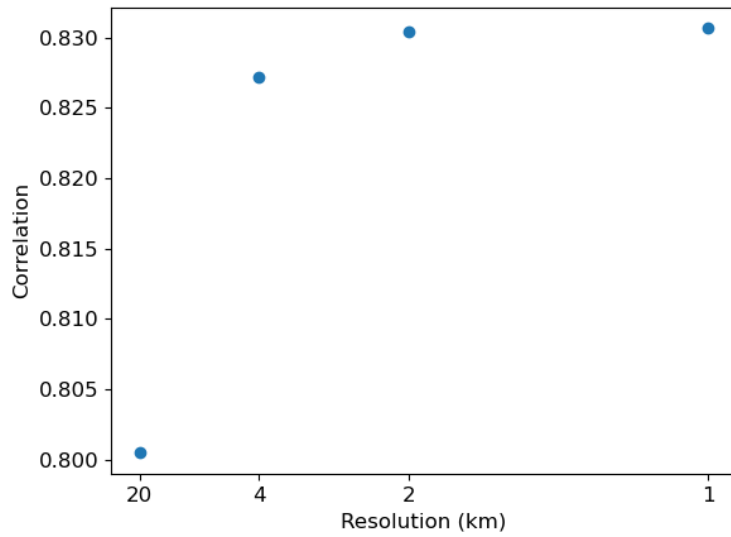


Figure 13: Model-measurement correlation for the NAME parameter scan of the resolution of the inner grid.

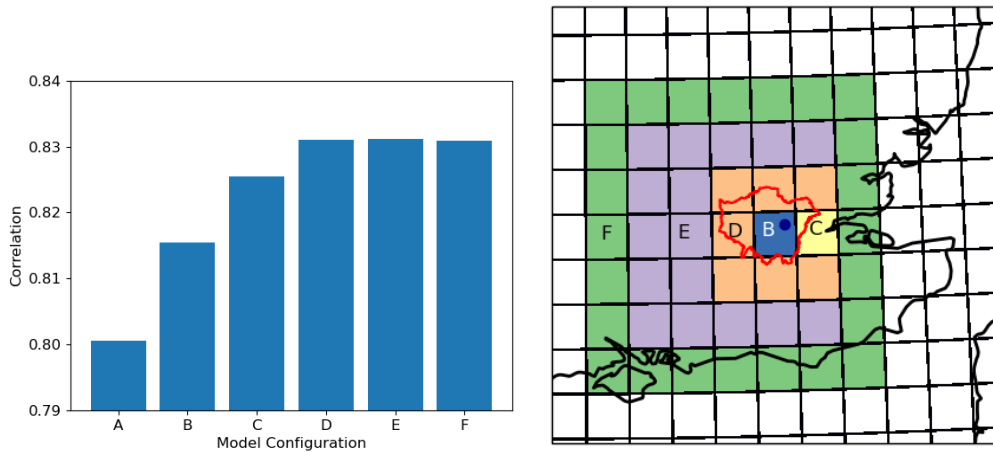


Figure 14: Left: Model-measurement correlation for the NAME parameter scan of the extent of the inner grid. Right: Map of model configurations B-F. Each configuration includes the geographic region of earlier letters. Configuration A has no inner grid.

3.6 EM27/SUN

EM27/SUN is a mobile FTIR spectrometer, used as a standard instrument for the collaborative carbon column observing network (COCCON) [13]. There is a proposal to have an EM27 instrument at both the National Physical Laboratory (NPL) and at Heathfield (HFD), as well as two additional sites in London for at least a short campaign. Here I generate synthetic data to look at possible performance of the instrument as a first step in the process.

As a remote sensing, near infrared instrument, the EM27 functions somewhat similarly to GOSAT and TROPOMI in its physics and modelling requirements. While I ultimately use these instruments as column measurements, in the modelling processes this column is split into a number of different vertical slices. Each of these slices, or levels, are modelled separately and then combined to give footprint information for the total column measurements. This process is demonstrated in figure 15.

In order to correctly use EM27 data with NAME output, several inputs are needed in addition to the column mole fraction measurement. As the column measurement does not provide enough information to fully characterise atmospheric methane alone, a prior concentration field is required, which is generated using global chemistry models. Pressure weights (P) must also be calculated, which define how much each layer of column contributes to the total. Finally, an averaging kernel (A) is needed, which contains information on how sensitive to each layer the measurement is.

These inputs are generated as part of the instrument's processing suite, but need to be manually set up in this preliminary stage. Averaging kernel look up tables, as a function of gas, altitude and solar zenith angle, were provided by Frank Hase of the Karlsruhe Institute of Technology. Prior information on methane, water and gravity profiles were taken from the closest TCCON site, Paris. These are generated on a daily basis for days with observations. As the synthetic data is generated assuming perfect clear skies, each day of synthetic data uses prior information from the next available day. The water (X^{H2O}) and gravity (g) profiles are used to calculate the pressure weights through a standard method [78]

$$c_i = \frac{1 - X_i^{H2O}}{g \cdot M_{dryair}}, \quad (5)$$

$$P_i = \frac{c_i \cdot \delta pressure}{\sum (c_i \cdot \delta pressure)}, \quad (6)$$

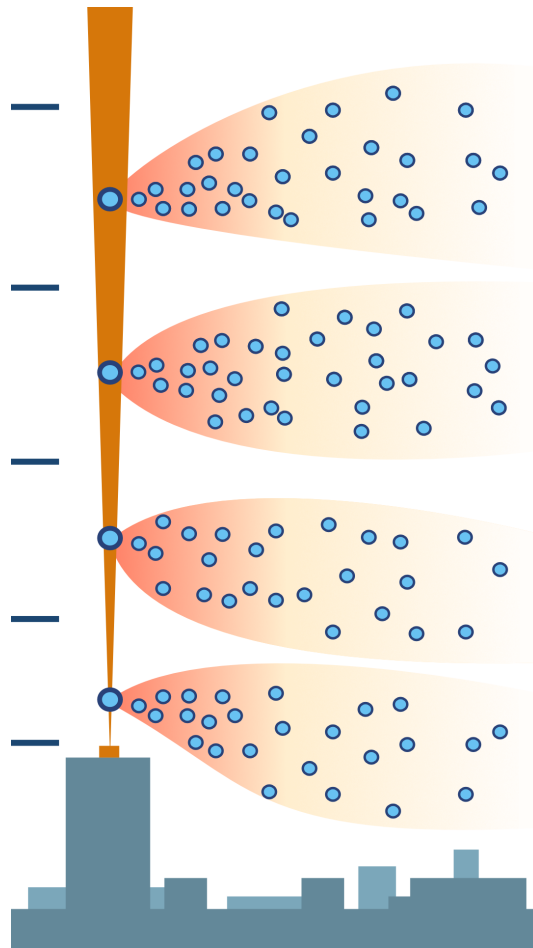


Figure 15: Diagram showing how a single column measurement for a rooftop EM27-Sun spectrometer is modelled as multiple layers in NAME. The orange beam represents the column of air measured, and the blue spheres are the modelled air particles.

where the subscript i refers to the level within the column and X is a column profile.

All the TCCON profiles are interpolated onto the same levels as the EM27 averaging kernels. For NAME, the Mk10 meteorological data (this is the product that offers global coverage over this time period) has a maximum height of 29km, so the max level used is 35, which is several kilometers below 29km depending on the day. For the levels above the model maximum the prior concentration is used in reconstructing the total column measurement. This contributes on the order of 16 ppb for our setup here.

We calculate the modelled column mole fraction using an existing method which splits out the levels that can be fully modelled from those that can't [15]

$$XCH_4^{model} = \sum_1^{35} P_i \left(A_i \cdot CH_4^{model} + (1 - A_i) \cdot CH_4^{prior} \right) + \sum_{36}^{49} P_i \cdot CH_4^{prior}, \quad (7)$$

where 49 is the highest level available in the data, which will be used in any inversions, and also to compare to other observations. When comparing the EM27 mole fraction to other ground based sites, we look for trends such as diurnal cycles and synoptic events present in the data. Finer comparison is not possible (without invoking information from the footprint as is used in the inversions) as the instruments are measuring different properties. Column and in-situ measurements are expected to be different, with column measurements showing lower mole fractions due to the decreased methane in the upper atmosphere, and lower sensitivity to local surface emissions. However, both observations should contain signals of changing emission levels, or the effects of synoptic weather events.

A timeseries of modelled data from an EM27 device are shown in figure 16. The modelled mole fractions for the EM27 instrument shows a 'v' shaped diurnal cycle, with higher methane concentrations in the evening and early morning, and midday dip. Similar patterns have been observed with the instruments in other locations. From analysing the model, it can be seen that the majority of this diurnal cycle comes from changes in sensitivity to the background conditions, with a minor effect from the change in surface sensitivity.

Figure 17 shows a comparison between the modelled local contribution of the EM27 and TMB (Thames Barrier) instruments. From this comparison it is clear that the TMB site sees a much greater signal, on the order of 20-100 ppb, compared to

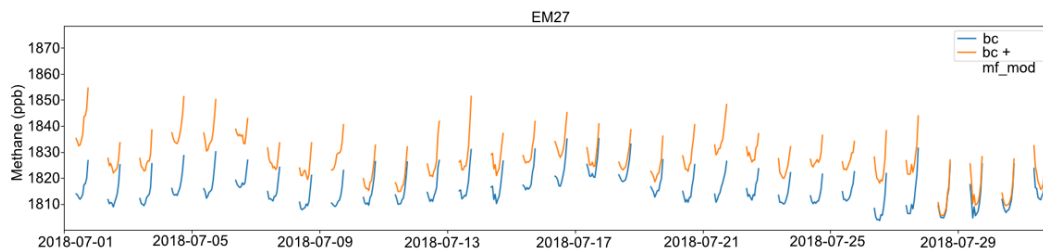


Figure 16: Simulated data for an EM27 device situated in London, showing the contributions from the boundary conditions (bc) and the modelled local contribution (mf_mod).

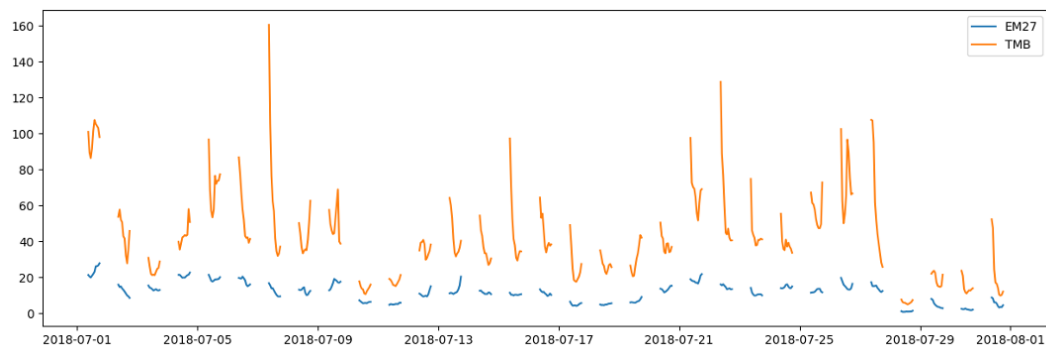


Figure 17: The modelled local contribution (mf_mod) in ppb for the EM27 instrument and the TMB instrument. TMB data is filtered to only display daytime values when EM27 model output is available for direct comparison.

the EM27 seeing around 10-20 ppb each day. It can be seen that the two instruments follow the same mesoscale pattern, as well as some shared features on a daily timescale. From this I can conclude that the models see a lot of the same information from both instruments, but with a far greater sensitivity for TMB than the EM27. Based on the methods of point measurements and column measurements, this is an expected result, but the difference seen here is quite stark. For this reason, these results suggest the TMB site is far more important for measuring London's emissions.

3.7 Conclusion

In this section I have presented the results from a published paper, detailing the skill of both NAME and ADMS to model a measurement site in central London. We find that both models are able to perform well using two different approaches, and therefore there would be an advantage to using both in attempting to infer London's greenhouse gas emissions.

I have also presented some sensitivity studies used to setup the NAME model runs for the London network, detailing several key model parameters including the number of particles, the meteorological data used and the span of the high-resolution inner grid. The final parameters are chosen to balance accuracy and performance - diminishing returns are clearly visible in the tests and using the highest settings in the model would substantially increase computational cost with little to no benefit to model accuracy.

Finally, I set out the atmospheric modelling setup for column measurements for the EM27-Sun spectrometer. Several of these devices will be installed around London and could be beneficial to supplement the LGHG network with an alternative measurement method that is less sensitive to the most local emissions which can be difficult to model. However, further modelling and use of the EM27 system is dependant on future access to measurements and the auxiliary data required to correctly model the more complicated column measurements.

4 Multi-resolution Inverse Modelling

4.1 Introduction

In this chapter I will discuss the next key component of the London GHG emissions monitoring network - the inverse model that solves Equation 2. As we have learnt from the introductory chapter of this thesis, there are a number of ways that this equation can be solved in practice. For this study, I will be drawing upon my research group's (the atmospheric chemistry research group) expertise and implementing an MCMC hierarchical Bayesian method [71]. The key advantages to this method are that I do not need my equations or distributions to follow Gaussian distributions to allow for analytical solutions, allowing more realistic distributions to be used, and the method will produce uncertainty characteristics on each variable that can be adjusted.

I will describe the model that I use for the rest of this thesis; a model which is able to work at multiple resolutions, with a high-density urban network of observations (the London Greenhouse Gas (LGHG) Project), embedded in a lower density regional network (the UK tall-tower network). Some of the urban sites may also slowly drift over time. By keeping the full size domain used in previous inverse modelling of the UK network [70, 69], the boundaries are kept far from the area of interest (London, and to a lesser extent the UK). Keeping the boundary conditions far from the area of interest is good practice to reduce the impact they have on the results, especially when we don't have direct measurements of the boundary conditions and rely on model extrapolation instead. I also use a non-uniform spatial grid to allow both a large total domain and high detail around London.

For LGHG, the model must be able to handle potentially drifting instruments. The network is composed of 5 LI-COR instruments that are not regularly calibrated and are therefore likely to drift over time. To help with this, regularly calibrated high resolution Picarro instruments will also be used in the inversion, which will help to anchor the LI-COR instruments in the model. The idea behind the anchor is to provide data as boundary conditions to the drift correction to reduce the degrees of freedom and ensure the model has enough information to solve the equations. We will use these conditions to build an urban inversion frame work for lower-cost

instruments that could be replicated with cheaper instruments still. I will also test the effectiveness of the model with some synthetic data tests. This will demonstrate the model is functioning correctly, and I will then be able to move onto using real data.

4.2 Bayesian Modelling

The introduction chapter gave a broad overview of the basics of Bayesian inverse modelling but this chapter will go into the specifics of the modelling required for the LGHG project. The project will be not using an analytical solution but instead will be using a Markov-Chain Monte Carlo (MCMC) method. I will not be diving into how to derive the underlying theory and equations behind the model - these techniques are well established and are already implemented in many packages, including the PYMC3 framework [79] that is used for this work. Instead, we care about the practicalities of these methods, the conditions in which they are likely to fail or misbehave and where they work well. I will now present the equations of the model, and then discuss some of the technical considerations for their implementation.

4.2.1 Full Model Description

The model being used in this study, as stated before, is based upon the existing setup used for regional level emission solving [15]. The main modifications I have made to the model are including a new term to account for time-varying drift in the LICOR instruments, a new method for defining the geographical basis functions and by implementing the equations in a new format to make use of the new solver available in PYMC3. This setup is designed to be used for inversions at a monthly scale, however it could be adapted to different time periods by adjusting the normalisation used, especially on the drift correction components.

The set of equations defining the Bayesian model are:

$$x(\text{basis}) \sim LN(\bar{x}, \hat{x}) \quad (8)$$

$$x_{bg}(\text{bcbasis}, \text{time}) \sim N(\bar{x}_{bg}, \hat{x}_{bg}) \quad (9)$$

$$\sigma_{model}(\text{site}) \sim LN(\sigma_{model}^-, \sigma_{model}^{\hat{}}) \quad (10)$$

$$\tilde{\phi}(\text{basis}, \text{site}, t) = \text{Quadtree}(\phi) \quad (11)$$

$$c_{i,\text{site}} = N(c_{i,\text{site}}^-, c_{i,\text{site}}^{\hat{}}) \quad (12)$$

$$\mu(\text{site}, t) = \sum_{\text{bcbasis}} (BC \cdot x_{bg}) + \sum_{\text{basis}} (\tilde{\phi} \cdot x \cdot x_{ap}) + \sum_{i=0}^2 (c_{i,\text{site}} t^i) \quad (13)$$

$$lh(\text{site}, t) \sim N(y - \mu, \sigma_y + \sigma_{model}), \quad (14)$$

where x is the scaling vector for the domain, x_{bg} is the scaling vector for the boundary conditions, σ_y and σ_{model} are the measurement and model uncertainties, $\tilde{\phi}$ is the footprint sensitivity on gridded to the computation basis, ϕ is the mean of the a priori gridded modelled mole fraction contribution calculated as $\sum_{\text{lat}, \text{lon}} (S \cdot x_{ap})$ with S being the model domain sensitivity and x_{ap} being the a priori fluxes. BC are the mole fractions at the boundaries, $c_{i,\text{site}}$ are drift coefficients, t is time and y are the observations. A bar refers to a mean parameter, and a hat to a width/standard deviation parameter. The Quadtree function aggregates the raw grid to a coarser resolution to create the basis functions for the inversion, and is uniquely calculated for each inversion. How this is implemented is described in further detail later in this chapter.

In these equations the three sums within μ refer to the boundary condition contribution, the within-domain contribution (from emissions) and the instrument drift, respectively. In the LGHG network, only the Licor instruments have a drift component, with the regular automated calibration of the other instruments assumed to fully eliminate drift. This component is vital to studying whether a cheap network made of drifting instruments can be successfully used to estimate emissions, and is one of the aims of the LGHG project. The drift is assumed to be quadratic over the time range of each inversion. The use of a second order approximation allows for instruments with relatively high levels of drifts over the time span, as large levels of drift have no reason to be linear. This assumption is tested later in this chapter, but there is no conceptual reason to prevent a different equation being used if a researcher

had access to information that suggested their instrument would drift in a different manner.

Within this framework, the values of $c_{i,site}$ are explicitly solved for in each inversion. This means the amount of drift present in each instrument is estimated for each inversion using the data given to the model. As the model is ran independently for each time period, drift information cannot be carried between different runs. It is suggested to use laboratory testing to confirm the prior values used for the mean and standard deviation values, as well as the quadratic form being appropriate. In this thesis, the corrected drift, or solved for drift, corresponds to the component $\sum_{i=0}^2 (c_{i,site}t^i)$, which is a time series representing the total amount of drift estimated for each instrument in each inversion.

The equations are normalised such that x refers to the multiplicative scaling factor applied to the prior emissions, x_{bg} is an additive percentage, both uncertainties are in ppb, t is in ‘months’ (30 day periods) and $c_{i,site}$ are in ppb/month. This normalization is used for model performance - this keeps expected adjustments of each parameter to the same order of magnitude, helping to create an ideal geometry for the probability space as explained below.

4.2.2 Technical Considerations

I have implemented my model using PYMC 3.8, a popular open source Bayesian programming package for Python. Its widespread use throughout many fields of science, and it’s open source nature, means we can be confident in its correct implementation of the algorithms it uses to solve Bayesian problems. By using a third party package I am able to get access to well tested, and advanced implementations of complex algorithms, compared to the potential issues (of bugs or computational inefficiency) of attempting to code one myself. In theory, this can also limit the possibilities of what can be achieved, but in practice PYMC has implemented all of the required features for this case.

The solver method used is a key practical consideration when using MCMC, as it can determine the computational efficiency of the problem, or even whether the problem can be reliably solved for. I will be using PYMC’s recommended solver, which is the NO-U-Turn Sampler (NUTS) [19]. NUTS is a variation of Hamiltonian Monte

Carlo, a method designed to give greater computational efficiency. Computational efficiency is a key factor in an MCMC solver, as a large number of samples must be drawn to ensure an accurate result.

Hamiltonian Monte Carlo methods are gradient methods, using Hamiltonian mechanics (differential equations of motion in momentum space) applied to probability spaces to efficiently sample a given distribution. We do not need to know the exact equations used, so instead I will discuss the broader ideas in play. In MCMC methods, common metaphors compare the probability space to a landscape filled with mountains and valleys that an agent walks around: the agent moves a given distance in a given direction and notes its altitude. The agent then repeats this action many times, slowly building up a picture of the landscape from its many samples. Where the traditional Metropolis-Hastings style approaches wander around the landscape picking directions at random each step, Hamiltonian methods pick a random direction and then kick a ball, gaining information about the terrain by how the ball rolls across it (gradient information). The individual steps of NUTS are more expensive than each step of Metropolis-Hastings, but give us much more information, leading to an overall more efficient algorithm.

Hamiltonian methods do have another draw back as well. Imagine this landscape of gentle valleys actually contains a narrow, but deep canyon in it. This canyon makes up only a very small portion of the landscape, but if the agent kicks the ball into the canyon, it's going to struggle to kick the ball back up the sheer walls to get back to the rest of the landscape. These problems with geometry having these steep local gradients can cause issues with the sampler, slowing it down or preventing it from getting a good sample of the whole space.

These problems can be identified by looking at the diagnostic properties available within PYMC3, such as the effective sample size and divergence factors, and can often be solved by implementation of scaling parameters or variable substitutions (with non-centred variables being a sensible option in many situations) in the model equations being solved. These fixes work by adjusting the geometry of the probability space the sampler has to explore without changing the underlying physical system that is being solved. In our metaphor, a change of variable would allow us to pull apart a canyon until it is once again a gentle valley.

4.3 Basis Functions and Prior Knowledge

The basis functions for the domain are based on quadtrees, which are a data structure useful for efficiently storing 2D data with spatially dependent information density. In this work, the modelled mole fraction contribution from each grid cell is used as the information density, to create a grid that is higher resolution closer to the observation sites, and lower resolution further away, in an organic way that reflects how skilled we expect the model to be for each location.

A common method, and the one I implement here, for creating a quadtree begins with a single node that encompasses the entire domain. The sum of the domain contents is checked against a predefined ‘bucket level’ and if the sum is greater than this, the domain is split into 4 equally sized child nodes. The value of the bucket level determines how coarse the final grid is, and is a subjective choice. One can use expert domain knowledge to define a grid such that any box has a contribution equal to some metric of knowability (such as model error) or it can be set to determine how many grid cells there are (more cells has a higher computational cost). This process is repeated recursively, until all of the leaves are either below the bucket level or correspond to a single grid cell. In this work, an additional initial step is optionally used to add more geographic information by defining a set of initial nodes based on country and land/sea borders as these are complex boundaries where different emissions may be expected on either side. The results of this algorithm are shown in Figure 18. A different method, that produces a similar style of grid, has been found to be effective in national studies [69].

The domain is split into a low resolution grid and a high resolution, small area grid that is embedded within the domain. The high resolution grid is calculated in advance for the specific setup (city of interest), and requires the footprints and flux fields to match in both low resolution and high resolution. The quadtree algorithm is applied to both grids separately, and then the aggregated basis functions are combined in the same way as the prior fields. This process requires consistent bookkeeping set up between all parts of the data pre- and post- processing, but does not change the functioning of the model as the underlying matrix calculations are performed the same way.

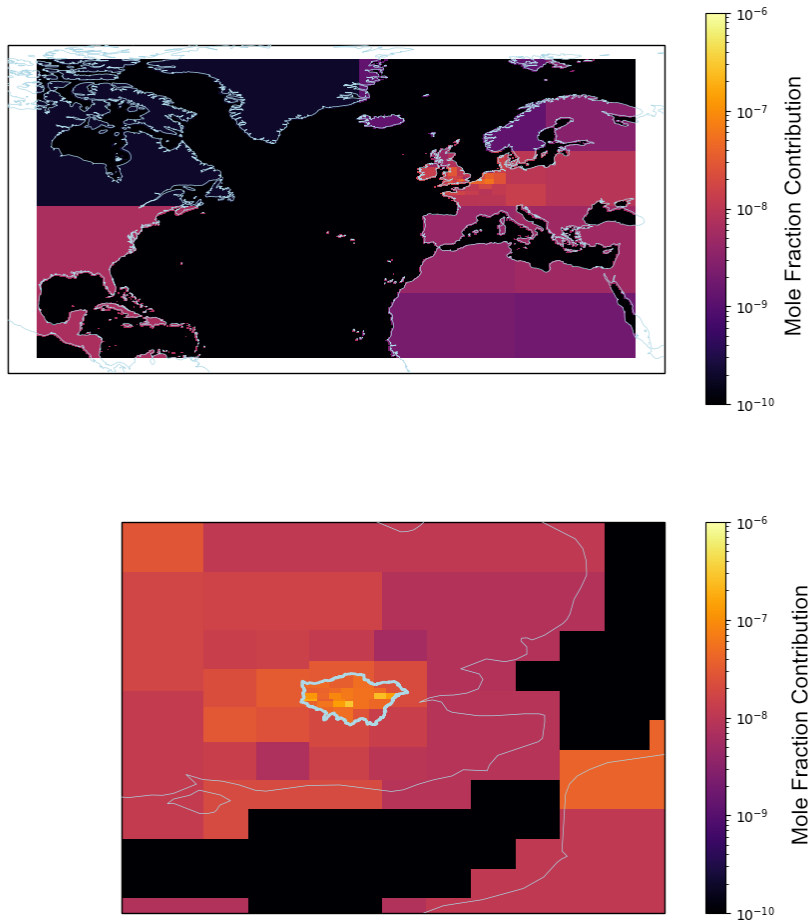


Figure 18: The model domain with grid cells aggregated through the quadtree function. This example has been pre-seeded with a land-sea basis and a London basis to give non-rectangular divisions for these important regions.

The boundary condition basis functions are kept simple, and are divided between North, East, South and West boundaries, which assumes the spatial structure of the background fields is correct. As I have no observational data near the boundaries of the model domain, I limit the degrees of freedom in changing the background and place greater trust in the priors compared to the emissions field. These background fields are taken from the CAMS inversion global products.

The prior fluxes are a combination of EDGAR [80] and NAEI emissions [available from <https://naei.beis.gov.uk/>] products. NAEI is the preferred emissions inventory, as it is high resolution and uses UK specific values in its design. However, it does not cover any area outside of the UK, while EDGAR is a global inventory. Embedding NAEI within the EDGAR fields, allows for higher resolution and UK specific prior values to be used for the UK while covering the complete domain. NAEI is embedded by converting both models onto compatible grids (those used by the model) and then simply swapping cutting EDGAR values out of the UK region and replacing them with NAEI values. As the two inventories use different methods, this Frankenstein style emissions map would not be useful for comparative analysis as is, but functions as a useful prior to start an inversion on, especially as the non-UK regions have a lower contribution to the observed and modelled values and thus matter less.

4.4 Testing Drift Assumption

Before working with full inversions that include the drift correction function, the assumption of 2nd order polynomial drift should be assessed. At the very first stage, I looked at the data collected when instruments were being setup in the lab qualitatively to ensure that quadratic curves could be fitted to the data on monthly time periods. After no problems were found at this stage, a more formal study was performed. Between 12-06-2019 and 27-11-2019, two LiCor instruments (LICOR01016, LICOR01033) were co-located with the Picarro at Thames Barrier. As the Picarro is automatically calibrated each day, this provides a stable 'truth' against which to test the LiCor instruments. A simplified Bayesian model, consisting of just the drift correction portion of the main model, is used to calculate a second order polynomial drift between the LiCor and Picarro hourly mean measurements. Alongside the drift, there is a random error component between the instruments, this is partially handled

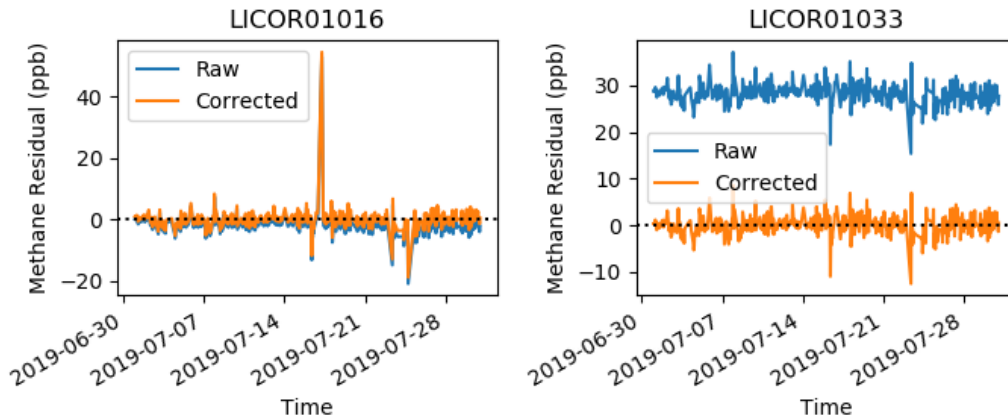


Figure 19: Residual of drift-corrected LiCor measurements compared to the Picarro 'truth' for methane.

by the Bayesian model including a small standard deviation in the likelihood function, and partially by filtering the data to be compared by the Thames Barrier variation to remove the local pollution events which cause the biggest discrepancies. This filtering was found to necessary as just one or two outliers was found to bias this simple model, as it assumes the random error between the instruments is small.

Figure 19 shows the difference between the Picarro and drift-corrected LiCor measurements once the drift-correction had been applied to the month of July. Both LiCors have significantly different drift patterns, but both are slowly drifting and can be corrected. The CO_2 measurements of these instruments has much larger drift, and is shown similarly in Figure 20. Although a large portion of the drift is corrected with a 2nd order polynomial, high order non-linear drift can be seen to remain.

The results of these tests suggests that for methane, a second-order polynomial drift is sufficient to capture the instruments behaviour. Most instruments demonstrated a small offset, but offsets of around 30 ppb were seen. Total drift over the course of a month remained under 5 ppb. The justification is weaker for the carbon dioxide measurements, but still provides most of the drift being accounted for. The issue here is that the instrument offers much worse performance for measuring carbon dioxide compared to methane. As the focus will be on methane for the rest of this thesis, this is not an issue that will be dealt with here. Further studies could also look into the effect of non-linearity correction, but as the largest values often get removed from

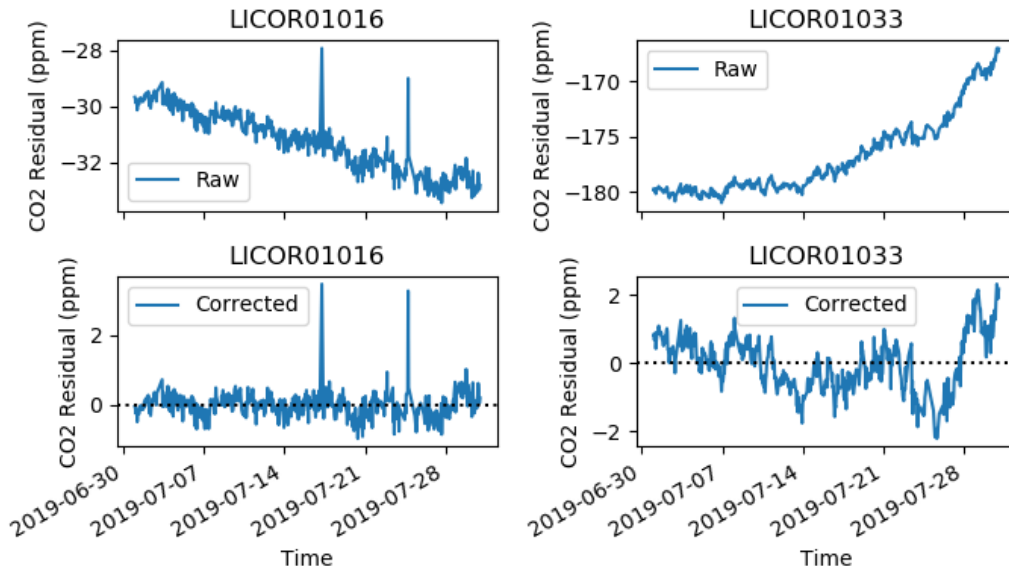


Figure 20: Residual of drift-corrected LiCor measurements for carbon dioxide.

model runs as the model cannot be trusted with them, it becomes less important. It would also add more degrees of freedom, and any study would have to assure sufficient data was present to model both the drift and non-linearity.

4.5 Pseudodata Inversion Tests

4.5.1 Introduction

To ensure that the inversion system is functioning well before unleashing the complexity of real data upon it, an experiment should be performed with a known solution to test for correctness. I generate pseudodata/synthetic observations = from a prescribed emissions field combined with the model footprints, then I perform an inversion with a different flux field as a prior to test convergence to the correct answer. Pseudodata tests have been used in previous inversion systems, for example by applying a checker-board pattern to the prior flux to generate the 'true' flux [74].

Existing studies that have performed test runs with synthetic data tend to rely on using analytical methods where possible [57, 81, 44]. With the analytical Bayesian inversions, it is possible to exactly calculate the posterior error covariance matrix. From this matrix, and from the prior error covariance matrix, it is straight forward to calculate an uncertainty reduction. The uncertainty reduction is a common metric

used to assess the skill of the inversion. Other studies [47] begin with an analytical method but run into computational difficulties, with the size of their matrices preventing practical calculations of the posterior error covariance. In this case, an alternative error metric is used: the ratio of geometric distances between the true emissions and the prior and posterior emissions. This method is not chosen for this work, as it does not make use of information from the full distributions available. With the Monte Carlo approach taken in this thesis, I am unable to use analytical methods but I know the prior distribution and store all samples of the posterior distribution. From this the highest density intervals of both distributions can be calculated and used to measure the uncertainty reduction of the inversion.

Pseudodata tests have to be further expanded to also include tests for the drift correction component. One study [44] has previously looked at drifting instruments, but took a simplified approach by considering uniformly, linearly drifting instruments. They find that larger biases decrease the skill of the inversion as would be expected, but they make no attempt to correct for the drift as is done here. There are several aims to be considered for testing the skill of drift-correcting inversions. Most fundamentally, the inversion needs to be able to retrieve the correct fluxes as this is the ultimate goal of the model. The drift correction should also be accurate to prevent biases in the results. Both of these aims are easy to test in a synthetic data inversion. For testing for the retrieved drift, comparison should be made between the true and retrieved values as time-series curves, rather than by comparing the quadratic coefficients. The latter method is inadvisable due to the anti-correlation of coefficients, where a change in one can be compensated by the opposite change in another to produce a drift that is practically the same. Using orthogonal basis functions would prevent this issue, but the simplicity of quadratic drift makes it more appealing overall.

For the LGHG project, tests will also be performed to see how the size of the network affects the results, as well as the contributions from both the calibrated and uncalibrated instruments. It must be ensured that running with the drifting London sites does not decrease the skill of the model.

4.5.2 Results

The synthetic inversion tests are kept simple to understand the basic behaviour of the system. Synthetic observations are generated for sites by keeping the background prior constant, and multiplying the flux prior by a fixed value in the range 1.1-2.0. Gaussian noise is added to all observations, with a mean of 0.0 and standard deviations between 2.0 ppb and 15.0 ppb (but constant over each set of observations). For the potential LI-COR sites, quadratic drift with coefficients randomised between -10.0 and 10.0 is added.

First I look at whether the drifting component of the model is functioning correctly - as it is the most novel and untested section of the model. Inversions are run with variable number of sites, with combinations of only drifting sites, drifting sites paired with a non-drifting site and the non-drifting site alone. Both the Thames Barrier and Mace Head sites are used as the non-drifting site, to test whether the site needs to be in London to correctly anchor the drifting sites.

From these tests, I analyse the qualitative behaviour of the inversion system with the resulting drift shown in Figure 21. I find that without an anchor site, the time varying components of the drift are retrieved with high uncertainty, but the offset bias is not retrieved, and instead the background is adjusted to get a match. With two drifting sites, the offset between sites is retrieved within uncertainty but again the mean is compensated by the background. Flux retrieval is largely successful despite this error in the mean offset. When an anchor site is added to the system, all components of the drift are retrieved, with low levels of uncertainty and more accurate flux retrieval. Both choices of anchor site (central London and Mace Head) were able to achieve these results, showing that the site does not need to be co-located with the drifting sites to function well.

With the drift compensation functioning correctly, and with its limits explored, I can now look at the emission levels. Figure 22 shows the results of several inversions in terms of total emissions for London high resolution grid and the UK low resolution grid. This is run at true (synthetic) emissions being a factor 1.1, 1.3 and 2.0 higher than the prior emissions, and with measurement uncertainties of 2.0 ppb and 15.0 ppb for each factor. I find that the correct emissions are retrieved for all scenarios, with a lower emission uncertainty in London compared to the UK. This is to be expected

as only one non-London site is being used (Mace Head) for these tests. Emission estimates have much higher uncertainties when measurement uncertainties are higher, as expected, but still produce results that agree with the truth values, demonstrating that a higher uncertainty is not detrimental to the technique but does limit how precisely we can narrow down emissions.

Next I look into the effects of the site density in London. I calculate uncertainty reduction using the equation

$$\text{uncertainty reduction} = 1 - \frac{\text{posterior uncertainty}}{\text{prior uncertainty}}, \quad (15)$$

and compare this geographically between two different scenarios. A value of 0 demonstrates no improvement in the posterior, and values approaching 1 demonstrate a great improvement on the prior resulting from the inversion. The first scenario is using the national network only, the second is using 4 of the proposed London sites. The results are shown in Figure 23. As we can see, not only is the output grid higher resolution due to the greater knowledge available combined with the quadtree algorithm, but London has a greater uncertainty reduction. Some small sections of London show a decrease in uncertainty reduction with more sites, this is likely a sign that not enough information (low emissions or low footprint sensitivity) is available to calculate the posterior with high skill at that resolution in those locations. One way to further improve this model would be to add an additional stage to the quadtree algorithm that would recombine cells with little information contained in them to counteract this.

The results of these tests demonstrate that the novel drift correction is functioning well, and adding the London sites with drift improves upon the results available with the previous national network. At a range of different true emissions and measurement uncertainty scenarios, the model functions with high skill, successfully retrieving the true emissions within posterior uncertainties.

4.6 Further Work

The work presented here needs further development to be used for estimating carbon dioxide emissions, largely due to the diurnal variation in emissions. This means that the underlying input needs to be presented at, and work with, a higher time resolution

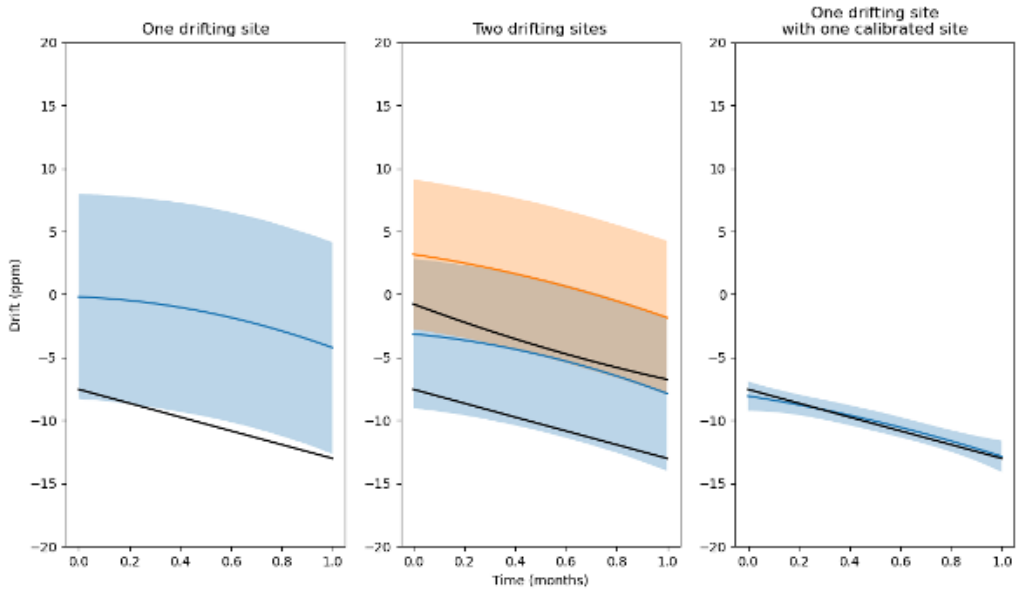


Figure 21: Drift correction during an inversion, with and without a non-drifting site. The black line shows the true drift added to the data. Coloured lines and shaded regions show mean and 2 standard deviation uncertainty on retrieved values.

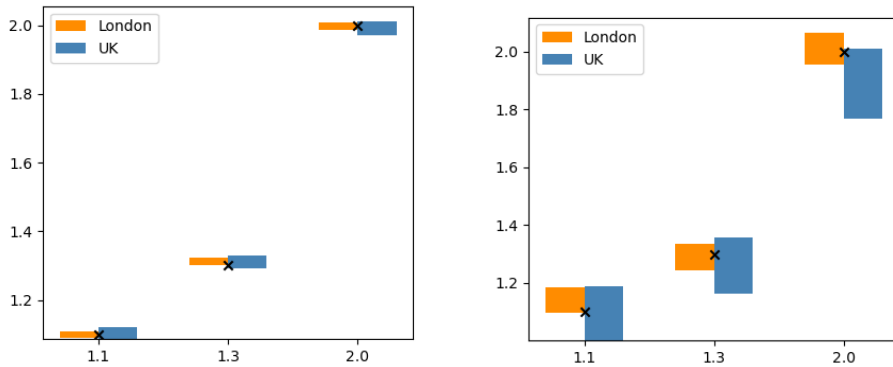


Figure 22: Normalised emission estimates (5th-95th percentile ranges) from synthetic data inversions, using data with an hourly standard deviation of (left) 2ppb and (right) 15 ppb.

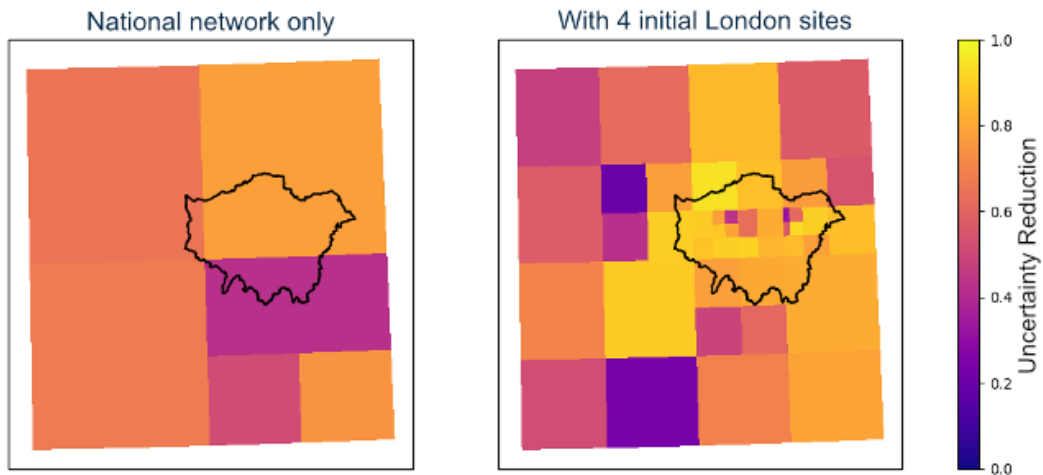


Figure 23: Fractional uncertainty reduction from a synthetic data inversion showing increased reduction and higher resolution is possible with more London sites.

- a 30 day average footprint will present problems for a diurnal emissions profile. Adding seasonal time scale variation needed for carbon dioxide emissions into the inverse method may cause interactions between the retrieved emissions time profile and the time profile of the drift correction - some fine tuning may be needed to reliably separate the two effects. Some extra data or restriction on the model may be needed to prevent the model compensating for one with the other.

Spatial basis functions can have a large effect on the results of an inversion, and the quadtree algorithm presented here is a simple approach. It is possible that more sophisticated, or multi-step, algorithms would be able to provide more useful basis functions - by making each component (grid cell) more equal by combining those that fall below the bucket level for instance. An improvement in performance is by no means guaranteed however, and due to limited resources I did not explore this further in this thesis as the current method showed no signs of this being a problem - all the synthetic data tests show good retrievals of the truth.

4.7 Conclusions

In this chapter I presented the framework of the inverse method that will be used within the final chapter of the thesis. It is largely based off of existing, proven methods,

but has been adapted and expanded to include a drift component and a new method to calculate geographical basis functions.

I have analysed some of the initial data of the new Licor instruments co-located with existing Picarro to deduce the amount of instrument drift that I expect to see. This leads to a simple quadratic drift form within the inverse model, which is a simple model that can easily be incorporated into the equations. The potential problem of using this form is that there will be some anti-correlation between the linear and quadratic terms in the inversion, which could effect the performance of the model. This also means the drift correction should be analysed as a time-series rather than by its individual parameters. However, it is not expected that these issues will prevent high skill in the model.

Finally, I tested the new inverse model in several scenarios with synthetic data, using different additional sites and a range of uncertainties and true emission levels. From these results, it can be seen that the model performs drift correction well when an 'anchor' site is included - one that is not drifting that the model can use as a boundary condition. Without an anchor site the time varying component of the drift is captured, but the offset from the drift is balanced against correcting the background signal. I have also shown that including London sites increases the resolution and skill of the model to resolve London emissions, and that the model is able to correctly recover the true emissions in test conditions, within posterior uncertainties. From this, I conclude that the model is ready to be used on real data to estimate London's methane emissions.

5 Inferring Methane Emissions in London

5.1 Introduction

In this section I will use the methods and framework outlined in the previous two chapters, with the newly installed measurement network, in order to infer the methane emissions of London. I begin by looking at how much data we have from the installed network, then I outline and discuss the inversion modelling setup used to infer London's emissions, including several sensitivity tests to investigate the robustness of the results. I finish the chapter by analysing the results for possible explanations for differences between inventory and posterior emissions.

5.2 Analysing the LGHG network

With the instruments installed across London, I can begin analysing the data taken from these sites, and applying the models from the previous two chapters. I begin by using the methods from the first chapter to produce high-resolution NAME footprints for each of the sites. Due to complications arising from the pandemic, ADMS-URBAN modelling is not available for this chapter, and I recommend that inclusion of that model to this work be a point for a future researcher to look into.

In Figure 24 we see the time-averaged NAME footprint for all of the sites in the London network for a typical month. This map gives us an idea of where the network is more likely to make accurate estimates of greenhouse gas emissions and where uncertainty reduction is likely to be higher - the higher the sensitivity the higher the expected skill of the inverse model in general. Two main features we see from this plot are: the increased sensitivity in west London due to an increased concentration of sites, with a corresponding lack of sensitivity in south-east London due to a lack of sites; and the increased sensitivity to the south-west of each site due to the prevailing winds. In this month we also see an increased sensitivity to the north-east, likely the result of a winter weather system passing through the UK at some point during the month shown, which is regular if infrequent occurrence in London.

This all suggests that I should be able to resolve most of the London, particularly the central and western regions, very well, but with less skill in the south-east of the city. As we saw in Figure 2, there are several large sources of methane documented

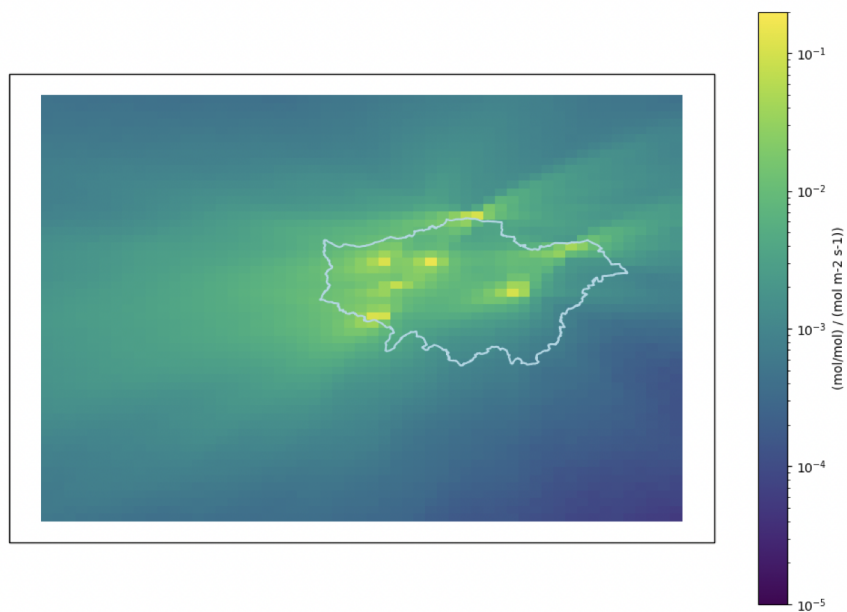


Figure 24: Average NAME footprint of the seven main London sites for January 2021, showing the high resolution model domain with the London boundaries outlined.

in the southern and eastern portions of London. A lack of sensitivity in these areas is likely to make it harder to accurately infer these emissions and lead to a higher uncertainty in our final results.

5.3 Data from LICOR Network

Before I continue to use the full network to achieve our goals of obtaining an emissions estimate for London, it would be prudent to take a pause to look at the data from the new sites. The quality of the data we put into the inverse model will directly affect the quality of the output estimates I get. I also need to know how to filter the data in order to prevent local emissions and spikes that cannot be correctly resolved from entering the model as this would bias the outputs.

Figure 25 shows the average daily cycle of models and observations for the new data. The average is calculated over the first 3 months of 2021. A short time period prevents any potential large seasonal or other longterm changes affecting the data. The sites follow a general pattern of peaking during the early hours of the morning, and a minimum in the early afternoon - the pattern expected when concentration is dominated by the boundary layer height and emissions are homogeneous throughout

a day. Some sites, such as TMB and LSTJ show a very close match between the modelled and observed values, while other sites such as LWMH and LWGF show a model under-prediction. These sites also have a larger observational uncertainty - this could mean local emissions that the model is unable to pick up. This is expected for LWGF, as this instrument is close to the ground on a farm, which is known to have large volumes of manure on site, which would be a local source of methane. For this reason, and large variance in the high resolution data, LWGF is excluded from the model runs as we do not expect the model to accurately capture the local pollution events that dominate the data.

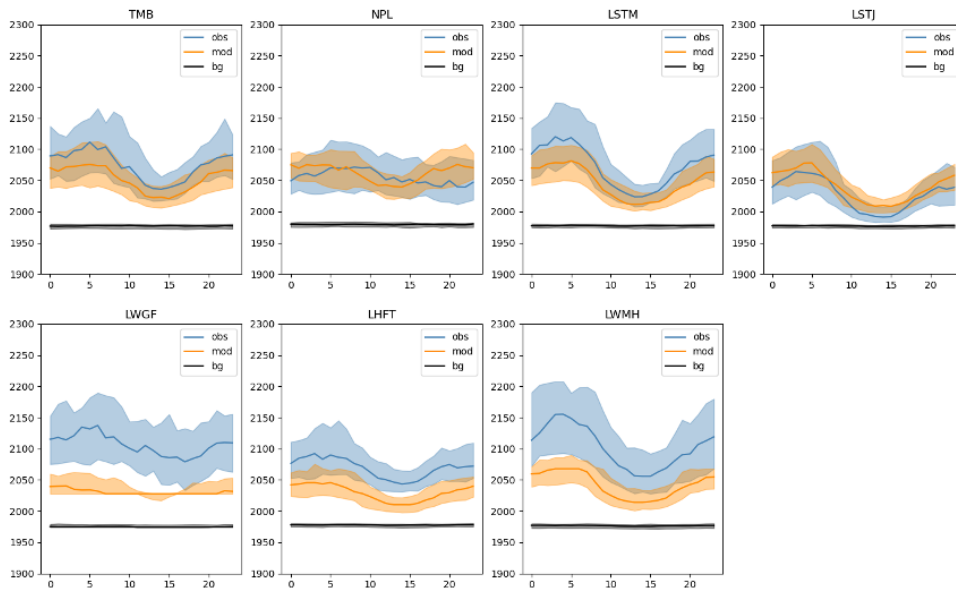


Figure 25: Average daily cycle for modelled and measured observations for each of the London sites, over the first 3 months of 2021. Shading indicates 33-66 percentile range.

5.4 Coherence Tests

In the previous chapter I tested how robust the model is to various effects, such as number of sites and instrument drifts. However, it is inevitable that when we apply real data to a model, there will be effects that have not been included in the cleaner, artificial data. It could be that instrument drift takes a different form from the model I applied based on the results of a single test site. Perhaps it is that the

prior emissions map is significantly wrong such that the inversion gets stuck in local minima before finding the 'correct' value. Or that the real data of a site is adversely affected by instrument malfunction or unforeseen strong local meteorological effects.

Part of this problem is negated by applying quality assurance procedures to the raw data before it is used. The instrument team use their expert analysis to check for spurious or suspect data points. We can apply multiple distinct emission maps to see how great of an effect they have on the end results, we can check against multiple different transport models with their different physics schemes.

Even with all these different procedures in place to protect against spurious results, it is good to apply some simple coherence tests to the inversion outputs themselves. These tests are to be considered necessary but not sufficient - if the results fail the tests they must be treated with scepticism, but passing them does not guarantee the results are error free. This is why in the previous chapter I tested the model on synthetic data first, to ensure it works as expected under laboratory conditons.

The basic test I will apply to the inversions at this point, is to compare inversions with an additional site added or removed. The results of such an inversion should be consistent, in a perfect world adding an extra site would simply decrease the uncertainty of the previous result. The more sites involved in the inversion, the smaller this effect should be. Large differences in results by changing a single tower could be the result of strong sources previously unseen by the network, or by issues with the data of that site, or perhaps difficulties in simulating that particular site.

An initial coherence test is shown in Figure 26. This is a set of monthly inversions performed over 2019 and 2020 on initial data from Picarro sites, with a few missing months due to pandemic-related data availability issues. The grey bars represent prior emissions values from NAEI, the blue bars are using the national network (DECC) only, with the others representing one or both of the initial London non-drifting sites. In this case I would expect to see that by adding London sites the London emissions uncertainty in the posterior would decrease, and that results from each London site separately would agree with each other. When we look at the results this is what we see - the inversion with this set of data is passing my basic checks.

There is one point to note however, and that is the disagreement between the London sites in 2020-09. This was not an expected result, as the TMB results disagree

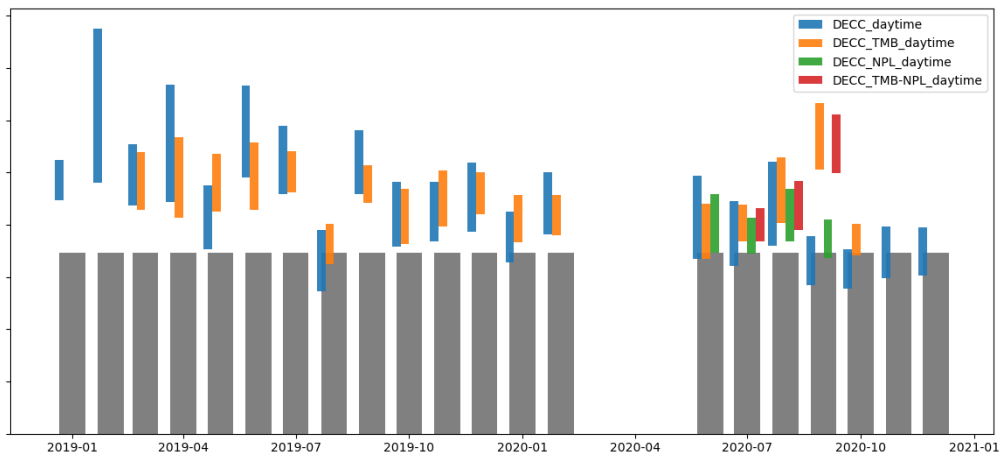


Figure 26: A monthly inversion performed using initial London GHG network data. Grey bars show prior emissions. The emission values are purposefully omitted as only the relative values are relevant here.

with both the national network and NPL results. By taking a closer look at the data, there are several extremely large, and possibly quite local, pollution events in the TMB timeseries which are likely driving up the emissions estimates. For this month as well the NPL data is only available for the first half of the month, before these pollution events are seen. These local pollution events are not present in inventories and can be difficult to capture in inversions, but should be easier to discern as more sites are added to the network in London, giving us a closer look at how emissions change. This also points to how the inverse system can be biased by large local pollution events, and that correctly filtering the data for events that may not be accurately modelled (such as by using variation in hourly data) are key to getting accurate emissions estimates in systems like LondonGHG.

5.5 London's Methane Emissions

Now I am ready to begin exploring the emissions estimates from using the full London Greenhouse Gas network. This section will focus on emissions from the first half of 2021, as this period has the most complete data record available at the time of writing. As a result of data not being available to myself at the time this was carried out, the NPL data is not used in these inversions.

Before I share any results in this section, I believe it is important to first clarify a matter of geography. One of the difficulties of comparing different emission estimates, whether inventory or inversion, is that direct comparisons only work when estimates use the same scope. In this case, the scope of emissions is defined by the geographic location of the sources. Figure 27 displays maps showing the geographic extents I consider as the "UK" and as "London". Emissions estimates cited in the following section for London are those summed within the highlighted grid cells, and for the UK as the same from its highlighted grid cells (excluding London emissions). To make it clear, the "UK" values do not include emissions from London, and the total emissions can be found from summing the two values. The priors likewise are the prior emissions maps summed across the same grid cells - this may lead to a small difference in totals between the results cited here and the UK's official estimates.



Figure 27: Map showing the geographic definitions of the UK (yellow) and London (inner black with blue border) used in this work. Coastlines are shown in red.

A set of inversions with slightly differing configurations are run over this period - this allows us to gain some insight into what is affecting the results. These runs include the baseline run of the DECC and London sites together with drifting LICORs, a run

with only the DECC sites, a run with only the London sites, a run where there is no drift corrected in any instrument, and a run where the TMB fixed instrument is also allowed to drift. The last run allows us to check whether unnecessary drift is being added by the model. These inversions all filter the data to use only daytime values - this is standard practice in the field as during the night there is extreme variance in observations due to the combination of London's local emissions and the stable boundary conditions of the night, and it is not expected that the model would be skilled with these conditions. A final run of the baseline configuration, but including all data is also tested.

First step is to check that the components of the model are sensible and correct. The main point to check is that the posterior modelled concentrations correctly match the observations, as this is the primary aim of the model. Figure 28 shows a typical set of observations and posterior modelled values. These plots show a good agreement between the observations and model outputs. Figure 29, which shows scatter plots of the modelled vs observed methane levels during one month for each run, demonstrates how the the posterior shows a great improvement on the prior values. From this plot it is clear that for all setups, the prior data has an underestimate in the methane levels, but the inverse model is able to adjust the priors to obtain similar levels of agreement between model and observation.

It is interesting to note that these plots show very similar posterior agreements between the different setups, suggesting the model is not particularly sensitive to the different input parameters being adjusted (sites used and the drift being solved for). While they don't tell us about which priors have been adjusted to create a solution, it does suggest a large amount of freedom in the system if drift is as important to the results as expected. This is something we will need to take a look at.

With this we have confirmed that the inverse model is achieving its goal - of adjusting priors to make the modelled and observed methane values agree. The next step is to ensure that it has done this in a reasonable manner, and that it hasn't found non-physical solutions to the problems. The correct setup of priors, such as using log-normal distributions to ensure no negative emissions should prevent a number of non-physical solutions such inverse models may find, but I should not be so arrogant to assume that this has prevented all possible problems.

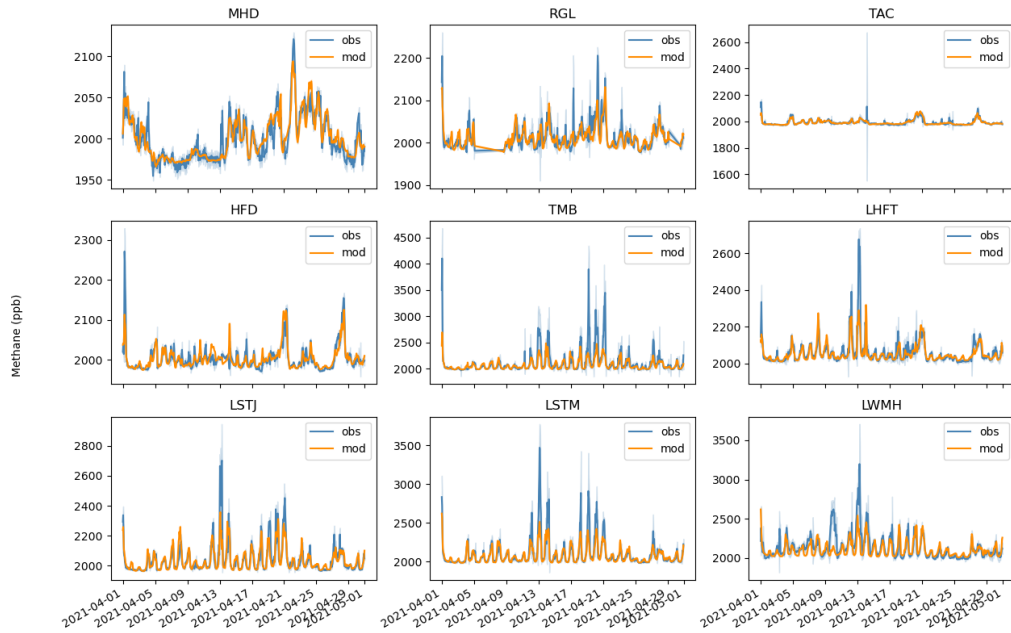


Figure 28: A set of typical observations and modelled values, shown for April for a run including nighttime values. Note that all y axes have separate scales.

5.5.1 Drift Correction

My next important question to ask is: how is the drift correction in this model performing? To give an answer to this I look into the difference in performance between the runs with different drift settings applied. I check to see what would happen if no drift correction was used, and I check to see what happens if drift correction is applied unnecessarily (to a calibrated site with no expected drift) - do these conditions give significantly different results?

Looking at Figure 30 (which shows emission estimates for various setups) - specifically the runs with TMB drift, and no LICOR drift, we see that adding drift to a non-drifting instrument does not change the results, while not solving for drift on the LICORs does impact the results. This impact is more significant in some months than others - as the true drift is random it is not unexpected that some months may have minimal problems from drift.

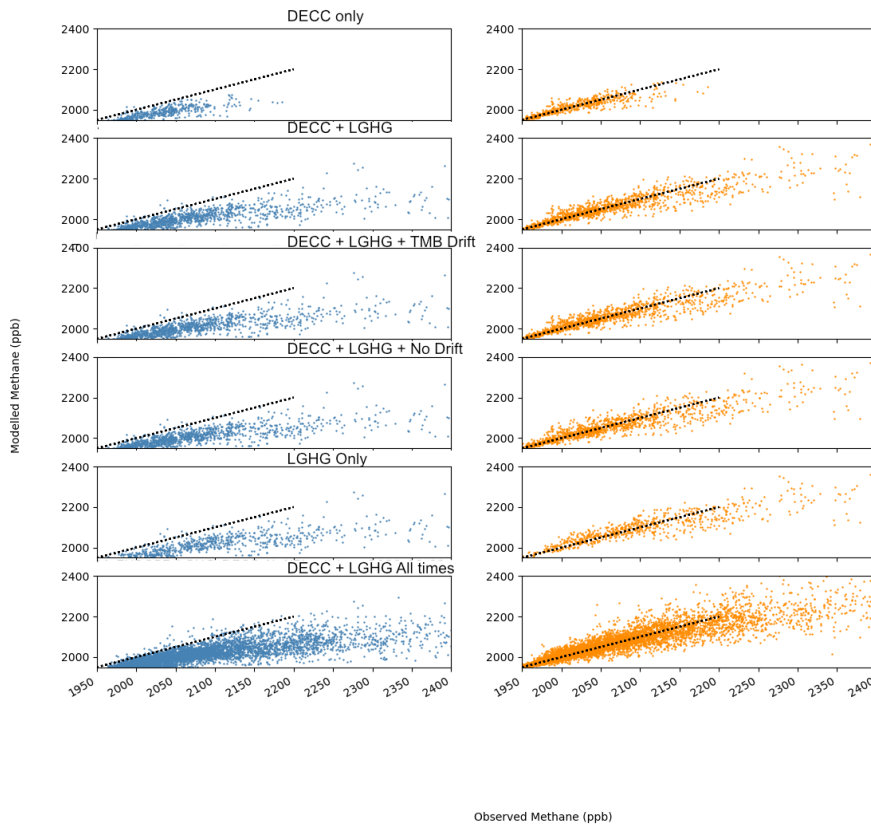


Figure 29: Prior (left) and posterior (right) scatter plots of modelled vs observed methane levels in January 2021. The black dotted line shows the 1:1 line.

The drift that is solved for the non-drifting Thames Barrier site is shown in figure 31. We can see that, while the priors for the monthly drift give a 0-centred drift and the instrument is calibrated daily, the model assigns some drift to the site each month. The drift is not continuous between months - each month is solved for independently. The gap in the drift values plotted is due to no data available for the Thames Barrier site at these times. All drift values are positive, meaning the model believes the observations are higher than what should be caused by emissions and background values. However, this assigned drift does not appear to change the retrieved emissions. There are several possibilities here: the drift may be balanced by a background offset as was seen in some of the initial tests, the drift is correcting for other time-varying effects not present in the priors, or a combination of the two. This

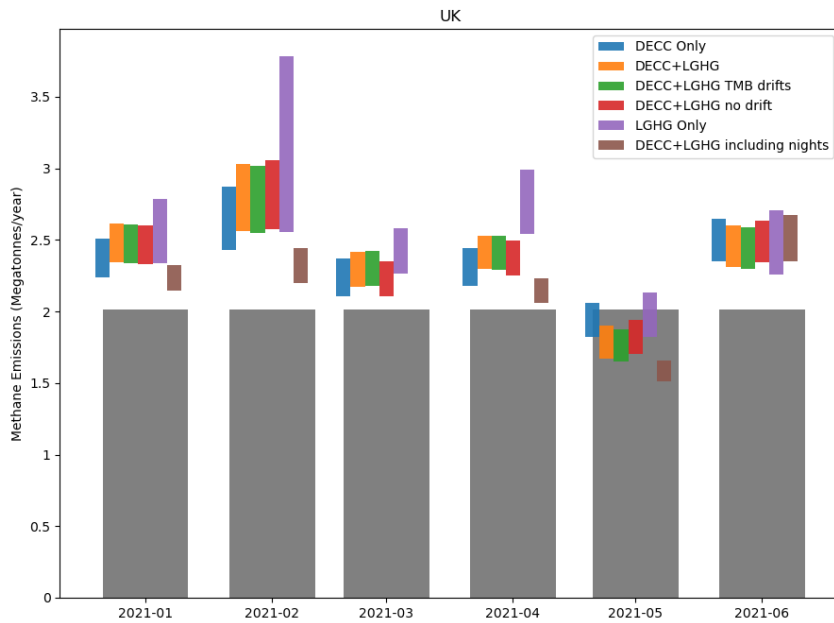
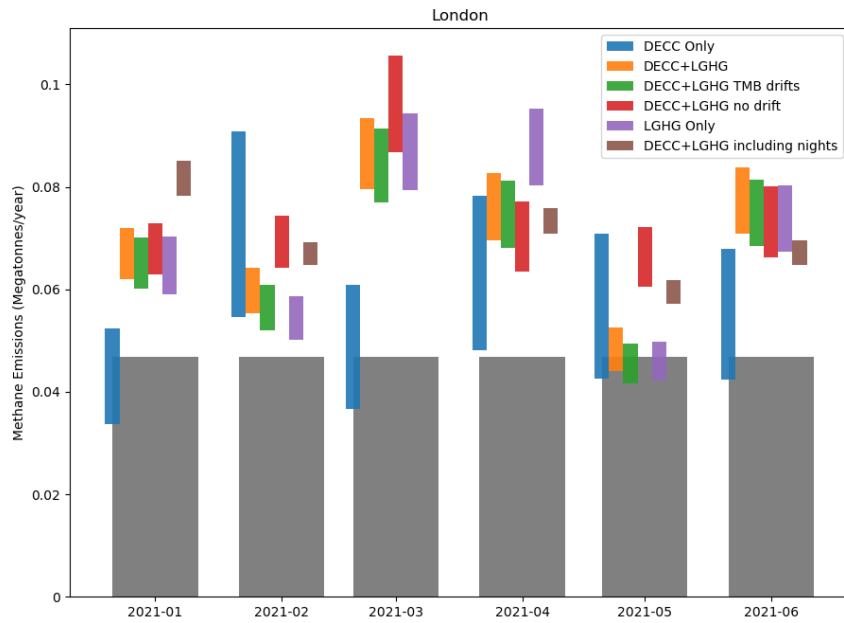


Figure 30: Emission priors (grey) and posterior estimates for the UK and London. Several different runs with different configurations are used for a sensitivity test.

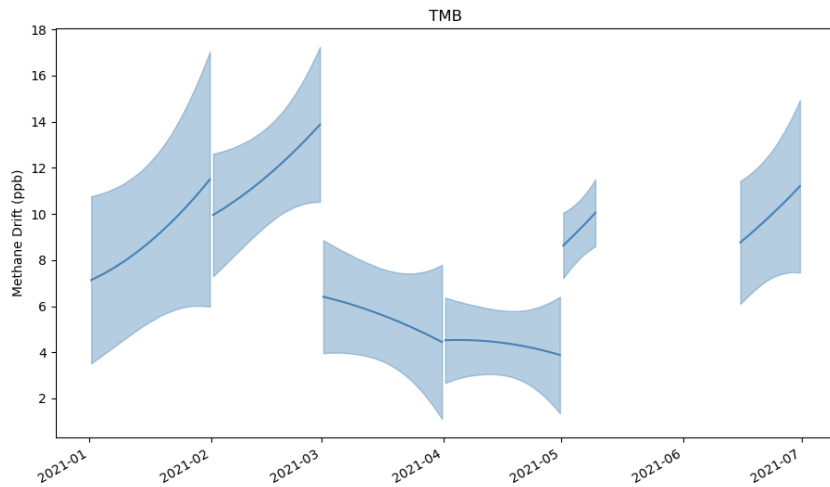


Figure 31: The Thames Barrier site is assumed not to drift as it is calibrated daily but the model is allowed to assign drift in one experiment, and the resulting drift is shown here.

unknown time-varying effect could be due to meteorological simulation errors in the transport model or time varying emissions that are not in the inventory.

There are several time-varying effects that could be present that are not accounted for in this model. The most likely effects are related to the emissions - which are assumed to be constant in time and space across the entire month for each inversion. While methane emissions are relatively stable across the year compared to a gas such as carbon dioxide, it is likely that there are changes over time, especially somewhere with dense emissions such as London. This could come, for instance, from gas leaks being fixed or worsening or from changes in decomposition rate at waste centres due to the weather or waste loads. Cataloguing these effects is beyond the scope of this project, but could be monitored by measuring local emissions through targeted campaigns in the city.

These results give us confidence that the drift correction in this model improves the skill at resolving emissions. While there is evidence that there are more effects than just instrument drift being captured by this part of the model, it does not appear to significantly affect the emissions estimates made for London.

Ideally, further tests would be done on the data to verify how accurate the drift correction is and there are several methods proposed to achieve this. The first is to run the inversion against the pre-calibration data for one of the calibrated sites and compare the drift correction against the calibration. However, the Picarro instruments drift at a rate of much less than 1ppb in a month, which is not a large enough for the model to distinguish from noise in the data. The second proposed method is to utilize a technique used from the Breathe London network, which uses raw observation data from a large number of sites to calculate the background drift between them, using similar principles but a much more direct method than the inverse model. Due to limited resources, this method has not been implemented in time for this thesis, but will be available to be trialled on the data at a later date.

5.5.2 Emission Values

Figure 30 shows the prior and posterior emissions for both London and the rest of the UK. A number of different runs are used to see how the setup effects the results, by which sites are included, which sites are drift corrected, and a run that includes the night time emissions that are expected to be poorly modelled just to confirm whether this is the case. The run using DECC and LGHG is considered to be the best setup, based on model skill and data availability, and is to be used as the final estimate. We can see that emissions are consistently estimated to be higher than the inventory values, with the exception of May 2021 where emissions are estimated to be consistent with inventory values. Emission differences for each run averaged over the months are shown in Table 5. Another expected feature is present: adding London sites does not significantly change estimates for the UK's total emissions, but has a large effect (in mean value and uncertainty range) on London's emissions.

In terms of UK total emissions, adding London sites only has a small change in magnitude, and little in uncertainty. The exception here is when the DECC sites are removed (using London-only sites does not get the same UK total emissions) or when nighttime values are used. These results suggest that adding a concentrated network of sites in London does not provide a benefit to modelling the UK total emissions directly. This in itself is not too surprising - on the UK scale each site would be largely redundant as they are located in a very similar place, and not too far from

Table 5: Mean difference between posterior and prior emissions totals for the various inversions averaged over first 6 months of 2021. Uncertainty is calculated from the 68% highest probability distribution.

Inversion	UK Difference (%)	London Difference (%)
DECC Only	16 \pm 11	19 \pm 20
DECC + LGHG	18 \pm 15	47 \pm 27
DECC + LGHG + TMB Drift	17 \pm 15	42 \pm 27
DECC + LGHG without Drift	17 \pm 15	57 \pm 22
LGHG Only	27 \pm 18	47 \pm 33
DECC + LGHG all times	7 \pm 15	49 \pm 16

an existing DECC site. However, if the results from modelling London’s emissions can enable inventory developers to gain new insights into London’s emissions this may have knock-on effects to the inventories for other urban areas, leading to more accurate national inventories.

I now take a look at the geographic distribution of the emissions, first to check they appear reasonable and physical, and secondly to interpret what this means for London’s emissions. When looking at these graphs, we must bear in mind that the spatial scale of adjustment to emissions is coarser than the original emissions map, and is applied at the scale of the Quadtree basis. The model also adjusts total emissions only: it cannot adjust emissions by sector or other variable. This means the fine details of London’s emissions will remain unchanged (we cannot easily allocate change in emissions to individual sources), and it is the larger scale changes we will see.

Maps showing the difference in emissions from prior (NAEI) to posterior for January’s inversions are shown in Figure 32. One common feature to all model runs here is that central London shows lower emissions in the posterior, suggesting the priors over-estimate of central London emissions is robust to the data we use in the inversions. Apart from this, there are broadly three different outputs across the 6 inversions here; a small decrease across all of London from DECC only, a large increase across most of London and to the north-west of London from including night time observations, and a moderate increase in London and to the north for the rest. It

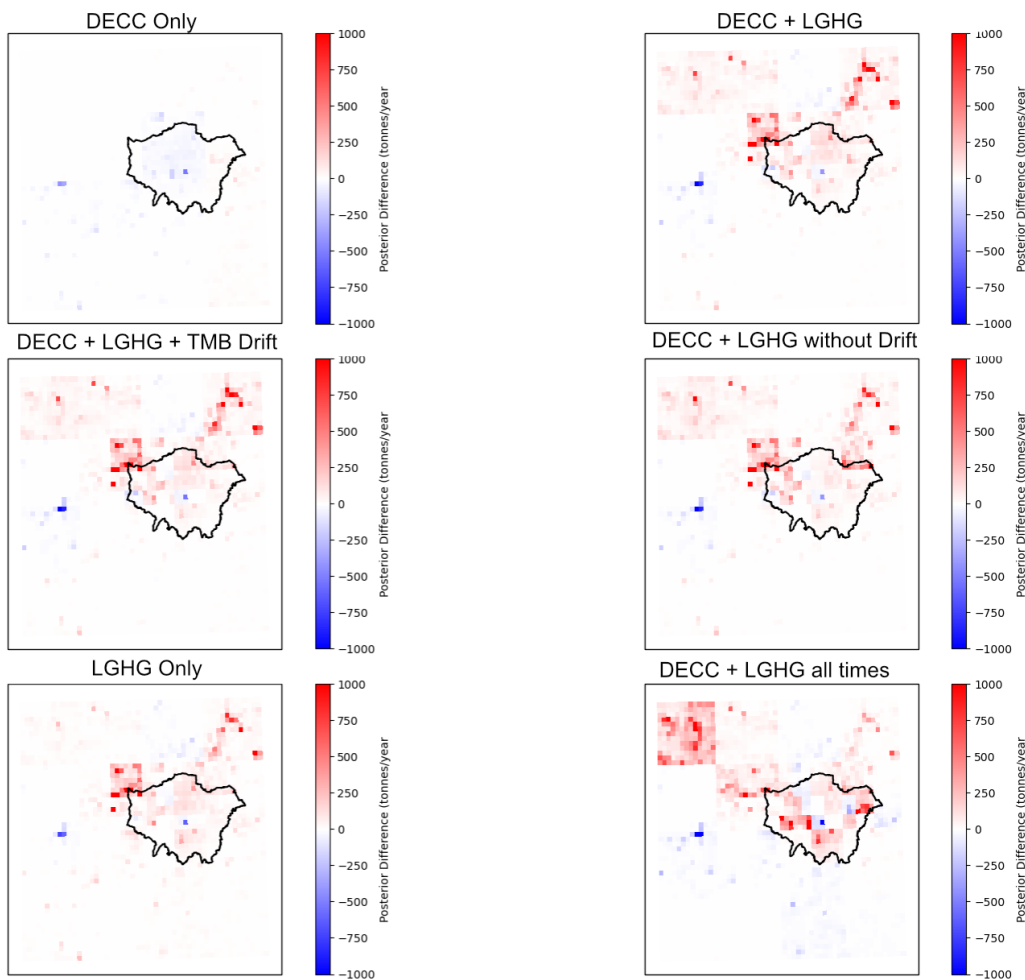


Figure 32: Difference in emissions between posterior and prior for the inner grid. Results are shown for each model run during January.

is not unexpected that including night time observations increases posterior emissions across London - we have already seen from the previous chapter that the model has a large underestimate of methane concentration during the nighttime compared to the city centre observations. It is quite possible this is a physics modelling error that the inversion is over-compensating for, especially as it is an outlier from the rest of the runs.

Taking a look at the same plots for February in Figure 33, we see some of the same patterns from January, but with some differences. All but the DECC-only run show the same central London decrease in emissions, and the 3 daytime drifting London site runs are in good agreement with each other. This time the DECC-only run shows

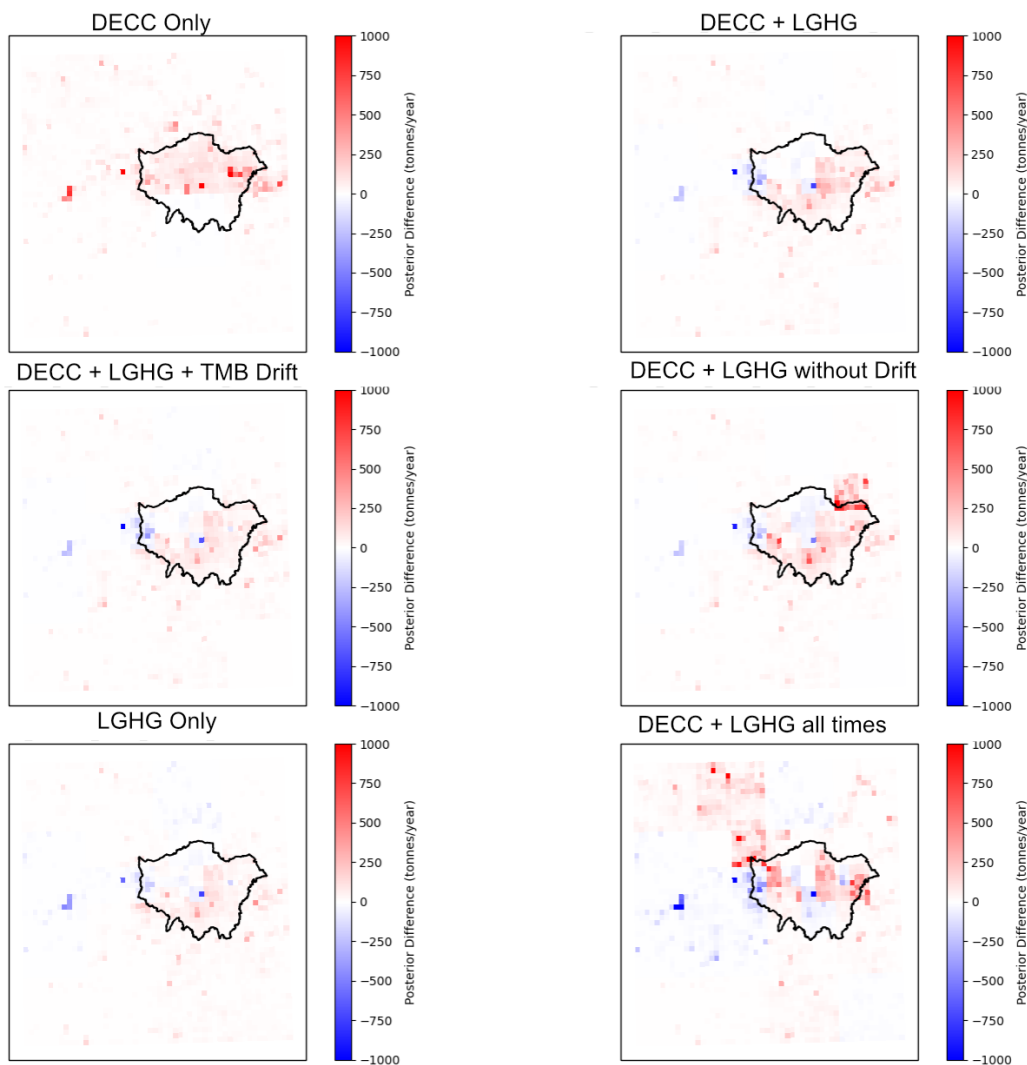


Figure 33: Difference in emissions between posterior and prior for the inner grid. Results are shown for each model run during February.

an increase, the non-drifting run shows a greater increase in emissions compared to drifting, and the all time run shows a different pattern of emission increases, with a greater overall increase.

Overall, the maps highlight differences between the solutions to the inverse model based upon the inputs, along with a persistent overestimate compared to NAEI emissions in central London. Otherwise they suggest a general increase in London's emissions, but not in any location in particular. As was seen in a previous chapter, most of London's methane emissions are allocated to waste and gas emissions, with gas emissions distributed by population density. It may be that the density in central

London reaches a saturation point where natural gas emissions do not scale linearly with population, and that across London these emissions are generally underestimated. It could also be that waste sector is underestimated, but the model is not able to resolve specific waste sites as that would require high resolution, which is not available with the level of data available here. To be more confident about what source is being underestimated further measurements would be needed, such as isotopes, co-emitted gasses or by taking local emission measurements at sites of interest.

5.5.3 Comparison to Other Work

A recent study using data from Imperial College London has also analysed methane emissions from London during 2018-2020 [82]. I do not have a temporal overlap between their results and the results I just presented, but I do not expect significant changes in methane emissions in a single year. This work also uses the NAME model and NAEI emissions priors, and finds that their observations suggest emissions are under-reported by 20-30%, mainly from the natural gas sector (attribution is gained by using isotope measurements). This magnitude of under-reporting is in agreement within uncertainty of the value of 47 ± 27 % obtained by my results. The agreement between both methods strengthens the claim that emissions are being under-reported.

5.6 Further Work

The work I have presented in this chapter only corresponds to 6 months of data, January-June of 2021, from a subset of all sites that have collected data on methane in London. This leaves some straightforward goals for further work: to analyse the full time series of work available and complete the original plan for a year long case study, and to run new inversions to estimate emissions that make use of all the Picarro sites across London. While further sites will provide diminishing returns in the inversion framework as their footprints overlap more, it does allow for some gaps in sensitivity to be reduced, to allow for site redundancy and to better analyse consistency between sites. However, it is not expected that more sites would allow source attribution as London's emissions are not geographically separated. As more data comes in it will eventually be possible to analyse longer trends and patterns such as seasonality and annual emissions change. Monitoring the change in emissions over time is a key

political goal from a monitoring network, as it will allow policy makers in London to verify that emission reduction plans are working at the expected rate.

While laying out the shortcomings of some of the results presented, I have mentioned several other possibilities for further work. Two key works that could help make this work more policy relevant include doing targeted hotspot campaigns similar to those performed before [51] but based on the presented inversions, and to include isotope or ethane measurements such as have been done in other studies [8, 82].

For the hotspot studies, this thesis has consistently found high levels of methane emissions appearing to come from north-east London, both from the original analysis of Thames Barrier data and from the inversions. North-east London contains several large point sources as listed within the NAEI inventory, including industry, gas and waste treatment facilities. One possibility is that these point sources are underestimated in the inventory - carrying out mobile measurement campaigns around these sources would help identify whether or not they are in fact underestimated in the inventory.

In order to be able to identify sector sources for the emissions, more data is required than is gathered by the LGHG network. This data could come in the form of isotope or ethane measurements, values of which differ by whether the methane source is fossil fuel or biogenic. Including this data would require substantial modelling work to update and test the inverse models, and both isotope and local measurements would require new instruments and logistical concerns. These additional complexities do not fit in with the original LGHG goal of proving a simple and cheap measurement system that could be used in the developing world, but would be useful for the goals of providing useful information for London policy makers.

It was also planned that in the future a round-robin calibration would be performed on all the London sites, which would allow the instrument drift at a given time to be directly measured, which could be compared against the modelled values to further validate the model. Such an event has not yet happened due to resource and logistical constraints.

5.7 Conclusion

In this chapter I have outlined the new measurement network in London, explored some of the observational data coming from the instruments, and discussed the

outcomes of various inversion setups using the network. I find that the network is able to provide useful methane estimates from the inverse modelling, and results consistently show that the inventory under-estimates London's emissions. Further work is required to pinpoint the source of these emissions that are unaccounted for, but the evidence is robust and makes a strong starting point for directly tracking London's emissions.

The results here show that this type of lower-cost, lower-maintenance measurement network, where sites are not regularly calibrated, can successfully be used to monitor methane emissions provided an appropriate model is used. This demonstration means that further networks of this description can be used to monitor more cities across the globe, and also demonstrate a good starting point for continuous monitoring of London's emissions. However, the results also point out the need to do more specific and targeted monitoring work to locate the individual sources of emissions that are not being accounted for in the inventory.

6 Summary and Final Remarks

And now we come to the final chapter in this thesis. Here I provide a brief summary of my thesis, highlighting key points from the main chapters, recapping my previous chapters.

6.1 State of the Field

I have shown that the study of urban-scale measurement networks for measuring greenhouse gas emissions is an active and evolving field. Numerous case studies have been set-up in cities across the world, with varying budgets, lifetimes and methods used. As this field is still establishing itself, and due to the great variation between the geographies of cities, there is not a single, best methodology used. However, an unofficial standard can be seen to begin emerging, with a large number of studies using a network of continuous in-situ measurements, combined with an atmospheric transport model and inverse model. However, each of these components still sees a great variation between each study. There are several points where I extend the current scientific knowledge in the field with this study.

One niche identified in the current literature is that the use of drifting instruments has not been greatly explored. By this, I refer to instruments that are not equipped with a gas standard and automatically calibrated against the standard on a regular basis as many measurement locations are. The instruments are calibrated before deployment, and may be manually calibrated several times a year, but drift in between these points. Drift in instrument measurements introduces a new source of uncertainty that can weaken the skill of the inverse model, but if this can be mitigated it would allow for smaller, cheaper instrument deployments. Such deployments could be vital for monitoring emissions in the developing world.

Another unique point of the LGHG network is that I seek to embed it within an existing national network. Many cities use the city limits (sometimes with a buffer zone) as the boundaries for the modelling work. However, the boundary conditions are potentially a large source of uncertainty as they have a great effect on emission estimates and they can be difficult to accurately quantify across all dimensions at all times. By embedding the urban model within a national model, the boundary conditions are greatly moved from the point of interest (reducing their impact on the

final result) and allowing the national model to solve for some of the information that would otherwise have to be input as boundary conditions.

6.2 The LGHG Instrument Network

The instruments and network was chosen and deployed by the instrument teams from the University of Cambridge and Cranfield University. The LGHG network is composed of two types of instruments: the drifting Licor instruments installed across London buildings as a part of the project grant, and calibrated Picarro instruments operated by various research groups who have agreed to share data with the project (although several sites were not available in time for this write up). The two instruments operate largely under the same principles, passing air samples through a laser cavity and recording changes in the absorbed light at the target gas absorption peaks. This allows them to make measurements at the second scale with good accuracy. This high resolution data is averaged to hourly to match with the modelling, but the high frequency allows for analysis of variability in the data which can be used to look for data that may be poorly modelled.

The instruments are sited largely opportunistically. I performed work was done to find optimal locations for the sites, such as identifying buildings that stood high above the local urban canopy to reduce the effect of small-scale atmospheric dynamics the models cannot reproduce. However, gaining access to ideal sites was difficult in practice and this method was largely abandoned, and instruments were placed wherever access could be gained, attempting to find higher buildings and avoiding placing instruments too close together. This process has led to a lack of instruments south London, but this is not of too much concern due to the prevailing south-westerly winds resulting in much of south London being seen by existing sites. The problem of site selection will be unique to each city that attempts to deploy a network such as LGHG, and my recommendation to anyone who seeks to do this should first attempt to gain the cooperation of people who can easily grant access to a large number of buildings. If this route is successful, your shortlist of potential sites would first be those you already have permission to use, and you could do atmospheric modelling to decide which sites provide the best overall coverage of the city.

6.3 Upgraded Models

I modified existing models primarily used for national level studies, adapting them to work in the high resolution urban environment. The atmospheric outputs have been collated using new high-resolution inputs and with the outputs using a multi-resolution grid to capture the details over London, but include the large geographic region from the previous work.

The inverse modelling has seen an even greater level of change, and I have developed it to be purpose built for the work presented in this thesis. The model is now written in a new programming environment, which is able to use Hamiltonian MCMC methods, which are more efficient at exploring the probability space, and is more easily adapted to account for new features. This has been used to include the new drift-correction terms to solve for instrument drift within the inverse model itself, as well as a new method to generate basis functions based upon the priors and input data that work with the multi-resolution grids.

I first trialled this new modelling setup in synthetic data experiments to assess how well the new features worked. This enabled an understanding of the new models, including finding out details such as the importance of an 'anchor site' - a calibrated site that can be used as a reference for the model when calculating instrument drift for other sites.

6.4 London's Emissions

The first 6 months of data (January-June 2021) from the complete London network has been collected and analysed. Taking a look at the original data, one of the sites (Woodgreen farm) has been discarded due to signs of contamination from a local source that would interfere with modelling, while the remaining sites look like good candidates for inverse modelling.

I ran inversion models on this data at a monthly time scale with a variety of different inputs, based upon which sites are used and whether instrument drift is accounted for. The inverse model is able to align the modelled data with observational data with good skill in all cases, with different posterior emissions for different scenarios. The experiment shows that excluding local sites, not allowing the uncalibrated instruments to drift, or including difficult to model nighttime observations can

significantly change the emissions. Allowing a calibrated instrument to drift in the model, or excluding national sites has a much smaller effect.

The final results of the inverse modelling is that the best configuration, using the London and national sites during the daytime, shows an increase of London emissions of $47 \pm 27\%$ on average (using uncertainty from 68% highest probability density) compared to NAEI emissions in the first half of 2021. These values are in agreement within uncertainty with an independent study [82] that used a different data source to estimate London's emissions in 2018-2020. This is strong evidence that London's emissions are under-reported, and the inventories need to be updated. However, further investigation will be needed to determine the source-sectors responsible for this increase. This study also demonstrates that this type of network, with drifting instruments, can be successfully combined with an appropriate model to monitor emissions. Removing the requirement of constant calibration means instruments can be cheaper and easier to install in a variety of locations, allowing these emission estimation systems to be used in a wider range of cities across the world.

6.5 Conclusion

And thus I come to the final conclusions of this thesis. I have taken a look at the transport models available, and deemed them to perform well (they produce sensible behaviour that correlates well with observational data) at the scales of the emissions data we have available. I have taken a look at the ways inverse models can be updated to include instruments that are uncalibrated and drift over time. And finally I have combined these, with a novel instrument network, to provide an estimate of London's emissions.

The results I have shown here demonstrate the inverse modelling setups in the style of the London GreenHouse Gas Network can be useful for providing estimates of city-scale emissions with a method that can mitigate the effects of drifting instruments. These achieves the projects goal of providing a potential modelling framework for cheaper instrument networks that could be deployed in the developing world. I have been able to show that, across the entire city, methane emissions are underreported in the NAEI emissions inventory. However, I have not been able to draw any conclusions about what may be the source of these emissions, by either sector or by geography.

To this end, further studies would be required. Isotope measurements could be used to differentiate between fossil fuel (natural gas) and biogenic (waste) emissions as these are the largest two sectors in London by reporting. A denser network may allow for a higher geographic resolution in solving for emissions, and be better able to pinpoint any hotspots around the city. Finally, more studies of the gas network and individual waste treatment facilities would be able to directly tell if that infrastructure is emitting more methane than the inventory reports.

Keeping the London network running would allow us to monitor London's emissions over the coming years. This could be powerful information for policy makers as reducing methane emissions is becoming more of a hot topic. Being able to monitor the effects of policy in near-real time would provide excellent evidence of policy impact, and help reduce emissions in a timely fashion.

This work also demonstrates that similar networks could be setup in other cities, using cheaper and lower-maintenance setups than previously expected. Being able to use lower cost instruments, that are not required to be constantly calibrated lowers the financial and logistical barriers for setting up such a network. This makes an urban greenhouse gas monitoring system more readily available for cities across the globe.

References

- [1] S. Arrhenius, “XXXI. On the influence of carbonic acid in the air upon the temperature of the ground,” *The London, Edinburgh, and Dublin Philosophical Magazine and Journal of Science*, vol. 41, no. 251, pp. 237–276, 1896.
- [2] IPCC, “Global warming of 1.5°C. an ipcc special report on the impacts of global warming of 1.5°C above pre-industrial levels and related global greenhouse gas emission pathways, in the context of strengthening the global response to the threat of climate change, sustainable development, and efforts to eradicate poverty,” 2018. [V. Masson-Delmotte, P. Zhai, H. O. Pörtner, D. Roberts, J. Skea, P.R. Shukla, A. Pirani, W. Moufouma-Okia, C. Péan, R. Pidcock, S. Connors, J. B. R. Matthews, Y. Chen, X. Zhou, M. I. Gomis, E. Lonnoy, T. Maycock, M. Tignor, T. Waterfield (eds.)].
- [3] London Assembly, “Assembly calls on the mayor to declare a climate emergency (press release),” 2018.
- [4] Greater London Authority, “Zero carbon London: A 1.5°C compatible plan (government report),” 2018.
- [5] IPCC, “2019 refinement to the 2006 IPCC guidelines for national greenhouse gas inventories,” 2019.
- [6] K. M. Stanley, A. Grant, S. O’Doherty, D. Young, A. J. Manning, A. R. Stavert, T. G. Spain, P. K. Salameh, C. M. Harth, P. G. Simmonds, W. T. Sturges, D. E. Oram, and R. G. Derwent, “Greenhouse gas measurements from a UK network of tall towers: technical description and first results,” *Atmospheric Measurement Techniques*, vol. 11, no. 3, pp. 1437–1458, 2018.
- [7] E. D. White, M. Rigby, M. F. Lunt, T. L. Smallman, E. Comyn-Platt, A. J. Manning, A. L. Ganesan, S. O’Doherty, A. R. Stavert, K. Stanley, M. Williams, P. Levy, M. Ramonet, G. L. Forster, A. C. Manning, and P. I. Palmer, “Quantifying the UK’s carbon dioxide flux: an atmospheric inverse modelling approach using a regional measurement network,” *Atmospheric Chemistry and Physics*, vol. 19, no. 7, pp. 4345–4365, 2019.
- [8] K. McKain, A. Down, S. M. Raciti, J. Budney, L. R. Hutyra, C. Floerchinger, S. C. Herndon, T. Nehrkorn, M. S. Zahniser, R. B. Jackson, N. Phillips, and S. C. Wofsy, “Methane emissions from natural gas infrastructure and use in the urban region of boston, massachusetts,” *Proceedings of the National Academy of Sciences*, 2015.
- [9] D. Say, A. J. Manning, S. O’Doherty, M. Rigby, D. Young, and A. Grant, “Re-evaluation of the UK’s HFC-134a emissions inventory based on atmospheric observations,” *Environmental Science & Technology*, vol. 50, no. 20, pp. 11129–11136, 2016.
- [10] D. J. Hamilton and A. J. Orr-Ewing, “A quantum cascade laser-based optical feedback cavity-enhanced absorption spectrometer for the simultaneous measurement of $\hat{\text{A}} \text{CH}_4$ and n_2o in air,” *Applied Physics B*, vol. 102, no. 4, pp. 879–890, 2010.

- [11] D. H. Cusworth, R. M. Duren, V. Yadav, A. K. Thorpe, K. Verhulst, S. Sander, F. Hopkins, T. Rafiq, and C. E. Miller, “Synthesis of methane observations across scales: Strategies for deploying a multitiered observing network,” *Geophysical Research Letters*, vol. 47, no. 7, 2020.
- [12] R. Parker, H. Boesch, A. Cogan, A. Fraser, L. Feng, P. I. Palmer, J. Messerschmidt, N. Deutscher, D. W. T. Griffith, J. Notholt, P. O. Wennberg, and D. Wunch, “Methane observations from the greenhouse gases observing SATellite: Comparison to ground-based TCCON data and model calculations,” *Geophysical Research Letters*, vol. 38, no. 15, 2011.
- [13] M. Frey, M. K. Sha, F. Hase, M. Kiel, T. Blumenstock, R. Harig, G. Surawicz, N. M. Deutscher, K. Shiomi, J. E. Franklin, H. Bösch, J. Chen, M. Grutter, H. Ohyama, Y. Sun, A. Butz, G. Mengistu Tsidu, D. Ene, D. Wunch, Z. Cao, O. Garcia, M. Ramonet, F. Vogel, and J. Orphal, “Building the collaborative carbon column observing network (COCCON): long-term stability and ensemble performance of the EM27/SUN fourier transform spectrometer,” *Atmospheric Measurement Techniques*, vol. 12, no. 3, pp. 1513–1530, 2019.
- [14] A. Kuze, H. Suto, K. Shiomi, S. Kawakami, M. Tanaka, Y. Ueda, A. Deguchi, J. Yoshida, Y. Yamamoto, F. Kataoka, T. E. Taylor, and H. L. Buijs, “Update on gosat tanso-fits performance, operations, and data products after more than 6 years in space,” *Atmospheric Measurement Techniques*, vol. 9, no. 6, pp. 2445–2461, 2016.
- [15] A. L. Ganesan, M. Rigby, M. F. Lunt, R. J. Parker, H. Boesch, N. Goulding, T. Umezawa, A. Zahn, A. Chatterjee, R. G. Prinn, Y. K. Tiwari, M. van der Schoot, and P. B. Krummel, “Atmospheric observations show accurate reporting and little growth in India’s methane emissions,” *Nat Commun*, vol. 8, no. 1, p. 836, 2017.
- [16] C. R. Martin, N. Zeng, A. Karion, K. Mueller, S. Ghosh, I. Lopez-Coto, K. R. Gurney, T. Oda, K. Prasad, Y. Liu, R. R. Dickerson, and J. Whetstone, “Investigating sources of variability and error in simulations of carbon dioxide in an urban region,” *Atmospheric Environment*, vol. 199, pp. 55–69, 2019.
- [17] A. Tarantola, *Inverse Problem Theory and Methods for Model Parameter Estimation*. Society for Industrial and Applied Mathematics, 2005.
- [18] W. K. Hastings, “Monte Carlo sampling methods using Markov chains and their applications,” *Biometrika*, vol. 57, pp. 97–109, 04 1970.
- [19] M. D. Hoffman and A. Gelman, “The no-u-turn sampler: Adaptively setting path lengths in hamiltonian Monte Carlo,” *Journal of Machine Learning Research*, vol. 15, pp. 1593–1623, 2014.
- [20] M. Saunio, A. R. Stavert, B. Poulter, P. Bousquet, J. G. Canadell, R. B. Jackson, P. A. Raymond, E. J. Dlugokencky, S. Houweling, P. K. Patra, P. Ciais, V. K. Arora, D. Bastviken, P. Bergamaschi, D. R. Blake, G. Brailsford, L. Bruhwiler, K. M. Carlson, M. Carrol, S. Castaldi, N. Chandra, C. Crevoisier, P. M. Crill, K. Covey, C. L. Curry, G. Etiope, C. Frankenberg, N. Gedney, M. I. Hegglin, L. Höglund-Isaksson, G. Hugelius, M. Ishizawa, A. Ito, G. Janssens-Maenhout, K. M. Jensen, F. Joos, T. Kleinen, P. B. Krummel, R. L. Langenfelds, G. G. Laruelle, L. Liu, T. Machida, S. Maksyutov, K. C. McDonald, J. McNorton, P. A. Miller, J. R. Melton,

- I. Morino, J. Müller, F. Murguía-Flores, V. Naik, Y. Niwa, S. Noce, S. O’Doherty, R. J. Parker, C. Peng, S. Peng, G. P. Peters, C. Prigent, R. Prinn, M. Ramonet, P. Regnier, W. J. Riley, J. A. Rosentretter, A. Segers, I. J. Simpson, H. Shi, S. J. Smith, L. P. Steele, B. F. Thornton, H. Tian, Y. Tohjima, F. N. Tubiello, A. Tsuruta, N. Viovy, A. Voulgarakis, T. S. Weber, M. van Weele, G. R. van der Werf, R. F. Weiss, D. Worthy, D. Wunch, Y. Yin, Y. Yoshida, W. Zhang, Z. Zhang, Y. Zhao, B. Zheng, Q. Zhu, Q. Zhu, and Q. Zhuang, “The global methane budget 2000–2017,” *Earth System Science Data*, vol. 12, no. 3, pp. 1561–1623, 2020.
- [21] S. Kirschke, P. Bousquet, P. Ciais, M. Saunois, J. G. Canadell, E. J. Dlugokencky, P. Bergamaschi, D. Bergmann, D. R. Blake, L. Bruhwiler, P. Cameron-Smith, S. Castaldi, F. Chevallier, L. Feng, A. Fraser, M. Heimann, E. L. Hodson, S. Houweling, B. Josse, P. J. Fraser, P. B. Krummel, J.-F. Lamarque, R. L. Langenfelds, C. Le Quéré, V. Naik, S. O’Doherty, P. I. Palmer, I. Pison, D. Plummer, B. Poulter, R. G. Prinn, M. Rigby, B. Ringeval, M. Santini, M. Schmidt, D. T. Shindell, I. J. Simpson, R. Spahni, L. P. Steele, S. A. Strode, K. Sudo, S. Szopa, G. R. van der Werf, A. Voulgarakis, M. van Weele, R. F. Weiss, J. E. Williams, and G. Zeng, “Three decades of global methane sources and sinks,” *Nature Geoscience*, vol. 6, pp. 813–823, Oct 2013.
- [22] M. Rigby, S. A. Montzka, R. G. Prinn, J. W. C. White, D. Young, S. O’Doherty, M. F. Lunt, A. L. Ganesan, A. J. Manning, P. G. Simmonds, P. K. Salameh, C. M. Harth, J. Muhle, R. F. Weiss, P. J. Fraser, L. P. Steele, P. B. Krummel, A. McCulloch, and S. Park, “Role of atmospheric oxidation in recent methane growth,” *Proceedings of the National Academy of Sciences*, vol. 114, no. 21, pp. 5373–5377, 2017.
- [23] P. J. Marcotullio, A. Sarzynski, J. Albrecht, N. Schulz, and J. Garcia, “The geography of global urban greenhouse gas emissions: an exploratory analysis,” *Climatic Change*, vol. 121, no. 4, pp. 621–634, 2013.
- [24] I. Tsagatakis, J. Richardson, C. Evangelides, M. Pizzolato, B. Pearson, N. Passant, M. Pommier, and A. Otto, “UK spatial emissions methodology: A report of the national atmospheric emission inventory 2020,” 2022.
- [25] A. Boon, G. Broquet, D. J. Clifford, F. Chevallier, D. M. Butterfield, I. Pison, M. Ramonet, J.-D. Paris, and P. Ciais, “Analysis of the potential of near-ground measurements of CO₂ and CH₄ in London, UK, for the monitoring of city-scale emissions using an atmospheric transport model,” *Atmospheric Chemistry and Physics*, vol. 16, no. 11, pp. 6735–6756, 2016.
- [26] S. J. O’Shea, G. Allen, Z. L. Fleming, S. J. B. Bauguitte, C. J. Percival, M. W. Gallagher, J. Lee, C. Helfter, and E. Nemitz, “Area fluxes of carbon dioxide, methane, and carbon monoxide derived from airborne measurements around greater London: A case study during summer 2012,” *Journal of Geophysical Research: Atmospheres*, vol. 119, no. 8, pp. 4940–4952, 2014.
- [27] E. G. Nisbet, M. R. Manning, E. J. Dlugokencky, R. E. Fisher, D. Lowry, S. E. Michel, C. L. Myhre, S. M. Platt, G. Allen, P. Bousquet, R. Brownlow, M. Cain, J. L. France, O. Hermansen, R. Hossaini, A. E. Jones, I. Levin, A. C. Manning, G. Myhre, J. A. Pyle, B. H. Vaughn, N. J. Warwick, and J. W. C. White, “Very strong atmospheric methane growth in the 4 years 2014–2017: Implications for the Paris agreement,” *Global Biogeochemical Cycles*, 2019.

- [28] J. R. Pitt, G. Allen, S. J.-B. Bauguitte, M. W. Gallagher, J. D. Lee, W. Drysdale, B. Nelson, A. J. Manning, and P. I. Palmer, “Assessing London CO₂, CH₄ and co emissions using aircraft measurements and dispersion modelling,” *Atmospheric Chemistry and Physics*, vol. 19, no. 13, pp. 8931–8945, 2019.
- [29] K. R. Verhulst, A. Karion, J. Kim, P. K. Salameh, R. F. Keeling, S. Newman, J. Miller, C. Sloop, T. Pongetti, P. Rao, C. Wong, F. M. Hopkins, V. Yadav, R. F. Weiss, R. M. Duren, and C. E. Miller, “Carbon dioxide and methane measurements from the Los Angeles megacity carbon project – part 1: calibration, urban enhancements, and uncertainty estimates,” *Atmospheric Chemistry and Physics*, vol. 17, no. 13, pp. 8313–8341, 2017.
- [30] E. A. Kort, C. Frankenberg, C. E. Miller, and T. Oda, “Space-based observations of megacity carbon dioxide,” *Geophysical Research Letters*, vol. 39, no. 17, 2012.
- [31] J. K. Hedelius, J. Liu, T. Oda, S. Maksyutov, C. M. Roehl, L. T. Iraci, J. R. Podolske, P. W. Hillyard, J. Liang, K. R. Gurney, D. Wunch, and P. O. Wennberg, “Southern california megacity CO₂, CH₄, and co flux estimates using ground- and space-based remote sensing and a lagrangian model,” *Atmospheric Chemistry and Physics*, vol. 18, no. 22, pp. 16271–16291, 2018.
- [32] A. A. Shusterman, J. Kim, K. J. Lieschke, C. Newman, P. J. Wooldridge, and R. C. Cohen, “Observing local co₂ sources using low-cost, near-surface urban monitors,” *Atmospheric Chemistry and Physics*, vol. 18, no. 18, pp. 13773–13785, 2018.
- [33] F. M. Bréon, G. Broquet, V. Puygrenier, F. Chevallier, I. Xueref-Remy, M. Ramonet, E. Dieudonné, M. Lopez, M. Schmidt, O. Perrussel, and P. Ciais, “An attempt at estimating paris area CO₂ emissions from atmospheric concentration measurements,” *Atmospheric Chemistry and Physics*, vol. 15, no. 4, pp. 1707–1724, 2015.
- [34] K. McKain, S. C. Wofsy, T. Nehrkorn, J. Eluszkiewicz, J. R. Ehleringer, and B. B. Stephens, “Assessment of ground-based atmospheric observations for verification of greenhouse gas emissions from an urban region,” *Proceedings of the National Academy of Sciences*, 2012.
- [35] L. E. Mitchell, E. T. Crosman, A. A. Jacques, B. Fasoli, L. Leclair-Marzolf, J. Horel, D. R. Bowling, J. R. Ehleringer, and J. C. Lin, “Monitoring of greenhouse gases and pollutants across an urban area using a light-rail public transit platform,” *Atmospheric Environment*, vol. 187, pp. 9–23, 2018.
- [36] M. Sargent, Y. Barrera, T. Nehrkorn, L. R. Hutyla, C. K. Gatley, T. Jones, K. McKain, C. Sweeney, J. Hegarty, B. Hardiman, and et al., “Anthropogenic and biogenic co₂ fluxes in the boston urban region,” *Proceedings of the National Academy of Sciences*, vol. 115, no. 29, p. 7491–7496, 2018.
- [37] D. Pillai, M. Buchwitz, C. Gerbig, T. Koch, M. Reuter, H. Bovensmann, J. Marshall, and J. P. Burrows, “Tracking city co₂ emissions from space using a high-resolution inverse modelling approach: a case study for berlin, Germany,” *Atmospheric Chemistry and Physics*, vol. 16, no. 15, pp. 9591–9610, 2016.

- [38] T. Lauvaux, N. L. Miles, A. Deng, S. J. Richardson, M. O. Cambaliza, K. J. Davis, B. Gaudet, K. R. Gurney, J. Huang, D. O’Keefe, Y. Song, A. Karion, T. Oda, R. Patarasuk, I. Razlivanov, D. Sarmiento, P. Shepson, C. Sweeney, J. Turnbull, and K. Wu, “High-resolution atmospheric inversion of urban CO_2 emissions during the dormant season of the Indianapolis flux experiment (influx),” *Journal of Geophysical Research: Atmospheres*, vol. 121, no. 10, pp. 5213–5236, 2016.
- [39] T. Lauvaux, K. R. Gurney, N. L. Miles, K. J. Davis, S. J. Richardson, A. Deng, B. J. Nathan, T. Oda, J. A. Wang, L. Huttyra, and J. Turnbull, “Policy-relevant assessment of urban CO_2 Emissions,” *Environmental Science & Technology*, 2020.
- [40] M. O. L. Cambaliza, P. B. Shepson, D. R. Caulton, B. Stirm, D. Samarov, K. R. Gurney, J. Turnbull, K. J. Davis, A. Possolo, A. Karion, C. Sweeney, B. Moser, A. Hendricks, T. Lauvaux, K. Mays, J. Whetstone, J. Huang, I. Razlivanov, N. L. Miles, and S. J. Richardson, “Assessment of uncertainties of an aircraft-based mass balance approach for quantifying urban greenhouse gas emissions,” *Atmospheric Chemistry and Physics*, vol. 14, no. 17, pp. 9029–9050, 2014.
- [41] C. Hu, S. Liu, Y. Wang, M. Zhang, W. Xiao, W. Wang, and J. Xu, “Anthropogenic CO_2 emissions from a megacity in the yangtze river delta of China,” *Environ Sci Pollut Res Int*, vol. 25, no. 23, pp. 23157–23169, 2018.
- [42] A. Nickless, P. J. Rayner, F. Engelbrecht, E.-G. Brunke, B. Erni, and R. J. Scholes, “Estimates of CO_2 fluxes over the city of cape town, South Africa, through Bayesian inverse modelling,” *Atmospheric Chemistry and Physics*, vol. 18, no. 7, pp. 4765–4801, 2018.
- [43] I. Super, H. A. C. Denier van der Gon, A. J. H. Visschedijk, M. M. Moerman, H. Chen, M. K. van der Molen, and W. Peters, “Interpreting continuous in-situ observations of carbon dioxide and carbon monoxide in the urban port area of rotterdam,” *Atmospheric Pollution Research*, vol. 8, no. 1, pp. 174–187, 2017.
- [44] I. Lopez-Coto, S. Ghosh, K. Prasad, and J. Whetstone, “Tower-based greenhouse gas measurement network design—the national institute of standards and technology north east corridor testbed,” *Adv Atmos Sci*, vol. 34, no. 9, pp. 1095–1105, 2017.
- [45] B. Gioli, M. F. Carfora, V. Magliulo, M. C. Metallo, A. A. Poli, P. Toscano, and F. Miglietta, “Aircraft mass budgeting to measure CO_2 emissions of rome, Italy,” *Environ Monit Assess*, vol. 186, no. 4, pp. 2053–66, 2014.
- [46] M. Nishihashi, H. Mukai, Y. Terao, S. Hashimoto, Y. Osonoi, R. Boer, M. Ardiansyah, B. Budianto, G. S. Immanuel, A. Rakhman, R. Nugroho, N. Suwedi, A. Rifai, I. M. Ihsan, A. Sulaiman, D. Gunawan, E. Suharguniyawan, M. S. Nugraha, R. C. Wattimena, and A. F. Ilahi, “Greenhouse gases and air pollutants monitoring project around jakarta megacity,” *IOP Conference Series: Earth and Environmental Science*, vol. 303, 2019.
- [47] A. J. Turner, A. A. Shusterman, B. C. McDonald, V. Teige, R. A. Harley, and R. C. Cohen, “Network design for quantifying urban CO_2 emissions: assessing trade-offs between precision and network density,” *Atmospheric Chemistry and Physics*, vol. 16, no. 21, pp. 13465–13475, 2016.

- [48] H. Peiro, S. Crowell, A. Schuh, D. F. Baker, C. O'Dell, A. R. Jacobson, F. Chevallier, J. Liu, A. Eldering, D. Crisp, F. Deng, B. Weir, S. Basu, M. S. Johnson, S. Philip, and I. Baker, "Four years of global carbon cycle observed from the orbiting carbon observatory 2 (oco-2) version 9 and in situ data and comparison to oco-2 version 7," *Atmospheric Chemistry and Physics*, vol. 22, no. 2, pp. 1097–1130, 2022.
- [49] D. Wu, J. C. Lin, T. Oda, and E. A. Kort, "Space-based quantification of per capita CO₂ emissions from cities," *Environmental Research Letters*, vol. 15, no. 3, p. 035004, 2020.
- [50] J. R. Pitt, I. Lopez-Coto, K. D. Hajny, J. Tomlin, R. Kaeser, T. Jayarathne, B. H. Stirm, C. R. Floerchinger, C. P. Loughner, C. K. Gately, L. R. Hutyra, K. R. Gurney, G. S. Roest, J. Liang, S. Gourджи, A. Karion, J. R. Whetstone, and P. B. Shepson, "New York City greenhouse gas emissions estimated with inverse modeling of aircraft measurements," *Elementa: Science of the Anthropocene*, vol. 10, 01 2022.
- [51] G. Zazzeri, D. Lowry, R. E. Fisher, J. L. France, M. Lanoisellé, and E. G. Nisbet, "Plume mapping and isotopic characterisation of anthropogenic methane sources," *Atmospheric Environment*, vol. 110, pp. 151–162, 2015.
- [52] G. Allen, P. Hollingsworth, K. Kabbabe, J. R. Pitt, M. I. Mead, S. Illingworth, G. Roberts, M. Bourn, D. E. Shallcross, and C. J. Percival, "The development and trial of an unmanned aerial system for the measurement of methane flux from landfill and greenhouse gas emission hotspots," *Waste Manag*, vol. 87, pp. 883–892, 2019.
- [53] C. Helfter, N. Mullinger, M. Vieno, S. O'Doherty, M. Ramonet, P. I. Palmer, and E. Nemitz, "Country-scale greenhouse gas budgets using shipborne measurements: a case study for the UK and Ireland," *Atmospheric Chemistry and Physics*, vol. 19, no. 5, pp. 3043–3063, 2019.
- [54] S. Ars, F. Vogel, C. Arrowsmith, S. Heerah, E. Knuckey, J. Lavoie, C. Lee, N. M. Pak, J. L. Phillips, and D. Wunch, "Investigation of the spatial distribution of methane sources in the greater toronto area using mobile gas monitoring systems," *Environmental Science & Technology*, 2020.
- [55] J. Fernandez, H. Maazallahi, J. France, M. Menoud, M. Corbu, M. Ardelean, A. Calcan, A. Townsend-Small, C. van der Veen, R. Fisher, D. Lowry, E. Nisbet, and T. Röckmann, "Street-level methane emissions of bucharest, romania and the dominance of urban wastewater.," *Atmospheric Environment: X*, vol. 13, p. 100153, 2022.
- [56] R. M. Duren and C. E. Miller, "Measuring the carbon emissions of megacities," *Nature Climate Change*, vol. 2, no. 8, pp. 560–562, 2012.
- [57] E. A. Kort, W. M. Angevine, R. Duren, and C. E. Miller, "Surface observations for monitoring urban fossil fuel co₂ emissions: Minimum site location requirements for the Los Angeles megacity," *Journal of Geophysical Research: Atmospheres*, vol. 118, no. 3, pp. 1577–1584, 2013.
- [58] J. Stauffer, G. Broquet, F.-M. Bréon, V. Puygrenier, F. Chevallier, I. Xueref-Rémy, E. Dieudonné, M. Lopez, M. Schmidt, M. Ramonet, O. Perrussel, C. Lac, L. Wu, and P. Ciais, "The first

- 1-year-long estimate of the paris region fossil fuel co2 emissions based on atmospheric inversion,” *Atmospheric Chemistry and Physics*, vol. 16, no. 22, pp. 14703–14726, 2016.
- [59] F. R. Vogel, M. Frey, J. Stauffer, F. Hase, G. Broquet, I. Xueref-Remy, F. Chevallier, P. Ciais, M. K. Sha, P. Chelin, P. Jeseck, C. Janssen, Y. Té, J. Groß, T. Blumenstock, Q. Tu, and J. Orphal, “Xco2 in an emission hot-spot region: the coccon paris campaign 2015,” *Atmospheric Chemistry and Physics*, vol. 19, no. 5, pp. 3271–3285, 2019.
- [60] L. E. Mitchell, J. C. Lin, D. R. Bowling, D. E. Pataki, C. Strong, A. J. Schauer, R. Bares, S. E. Bush, B. B. Stephens, D. Mendoza, D. Mallia, L. Holland, K. R. Gurney, and J. R. Ehleringer, “Long-term urban carbon dioxide observations reveal spatial and temporal dynamics related to urban characteristics and growth,” *Proceedings of the National Academy of Sciences*, 2018.
- [61] L. Kunik, D. V. Mallia, K. R. Gurney, D. L. Mendoza, T. Oda, and J. C. Lin, “Bayesian inverse estimation of urban CO₂ emissions: Results from a synthetic data simulation over Salt Lake City, UT,” *Elementa*, 2019.
- [62] Y. Huang, E. A. Kort, S. Gourdjji, A. Karion, K. Mueller, and J. Ware, “Seasonally resolved excess urban methane emissions from the baltimore/washington, DC metropolitan region,” *Environmental Science & Technology*, vol. 53, no. 19, pp. 11285–11293, 2019.
- [63] G. Janssens-Maenhout, M. Crippa, D. Guizzardi, M. Muntean, E. Schaaf, F. Dentener, P. Bergamaschi, V. Pagliari, J. G. J. Olivier, J. A. H. W. Peters, J. A. van Aardenne, S. Monni, U. Doering, A. M. R. Petrescu, E. Solazzo, and G. D. Oreggioni, “Edgar v4.3.2 global atlas of the three major greenhouse gas emissions for the period 1970–2012,” *Earth System Science Data*, vol. 11, no. 3, pp. 959–1002, 2019.
- [64] J. D. Maasackers, D. J. Jacob, M. P. Sulprizio, A. J. Turner, M. Weitz, T. Wirth, C. Hight, M. DeFigueiredo, M. Desai, R. Schmeltz, L. Hockstad, A. A. Bloom, K. W. Bowman, S. Jeong, and M. L. Fischer, “Gridded national inventory of u.s. methane emissions,” *Environmental Science & Technology*, vol. 50, no. 23, pp. 13123–13133, 2016.
- [65] X. Ren, O. E. Salmon, J. R. Hansford, D. Ahn, D. Hall, S. E. Benish, P. R. Stratton, H. He, S. Sahu, C. Grimes, A. M. F. Heimbürger, C. R. Martin, M. D. Cohen, B. Stunder, R. J. Salawitch, S. H. Ehrman, P. B. Shepson, and R. R. Dickerson, “Methane emissions from the Baltimore-Washington area based on airborne observations: Comparison to emissions inventories,” *Journal of Geophysical Research: Atmospheres*, vol. 123, no. 16, pp. 8869–8882, 2018.
- [66] G. Plant, E. A. Kort, C. Floerchinger, A. Gvakharia, I. Vimont, and C. Sweeney, “Large fugitive methane emissions from urban centers along the u.s. east coast,” *Geophysical Research Letters*, vol. 46, no. 14, pp. 8500–8507, 2019.
- [67] H. J. S. Fernando, D. Zajic, S. Di Sabatino, R. Dimitrova, B. Hedquist, and A. Dallman, “Flow, turbulence, and pollutant dispersion in urban atmospheres,” *Physics of Fluids*, vol. 22, no. 5, 2010.

- [68] D. Hoare, R. Jones, N. Harris, V. Ferracci, D. Carruthers, A. Stidworthy, E. Forsyth, and M. Rigby, “Development of an urban greenhouse gas modelling system to support a London monitoring network,” *Weather*, vol. 75, no. 11, pp. 353–359, 2020.
- [69] A. J. Manning, S. O’Doherty, A. R. Jones, P. G. Simmonds, and R. G. Derwent, “Estimating UK methane and nitrous oxide emissions from 1990 to 2007 using an inversion modeling approach,” *Journal of Geophysical Research*, vol. 116, no. D2, 2011.
- [70] A. L. Ganesan, A. J. Manning, A. Grant, D. Young, D. E. Oram, W. T. Sturges, J. B. Moncrieff, and S. O’Doherty, “Quantifying methane and nitrous oxide emissions from the UK and Ireland using a national-scale monitoring network,” *Atmospheric Chemistry and Physics*, vol. 15, no. 11, pp. 6393–6406, 2015.
- [71] A. L. Ganesan, M. Rigby, A. Zammit-Mangion, A. J. Manning, R. G. Prinn, P. J. Fraser, C. M. Harth, K. R. Kim, P. B. Krummel, S. Li, J. Mühle, S. J. O’Doherty, S. Park, P. K. Salameh, L. P. Steele, and R. F. Weiss, “Characterization of uncertainties in atmospheric trace gas inversions using hierarchical Bayesian methods,” *Atmospheric Chemistry and Physics*, vol. 14, no. 8, pp. 3855–3864, 2014.
- [72] A. Jones, D. Thomson, M. Hort, and B. Devenish, *The U.K. Met Office’s Next-Generation Atmospheric Dispersion Model, NAME III*, book section Chapter 62, pp. 580–589. 2006.
- [73] A. Inness, M. Ades, A. Agustí-Panareda, J. Barré, A. Benedictow, A.-M. Blechschmidt, J. J. Dominguez, R. Engelen, H. Eskes, J. Flemming, V. Huijnen, L. Jones, Z. Kipling, S. Massart, M. Parrington, V.-H. Peuch, M. Razinger, S. Remy, M. Schulz, and M. Suttie, “The CAMS reanalysis of atmospheric composition,” *Atmospheric Chemistry and Physics*, vol. 19, no. 6, pp. 3515–3556, 2019.
- [74] M. F. Lunt, M. Rigby, A. L. Ganesan, and A. J. Manning, “Estimation of trace gas fluxes with objectively determined basis functions using reversible-jump Markov chain Monte Carlo,” *Geoscientific Model Development*, vol. 9, no. 9, pp. 3213–3229, 2016.
- [75] C. D. Stocker J, Hood C and M. C, “ADMS-Urban: developments in modelling dispersion from the city scale to the local scale,” *International Journal of Environment and Pollution*, vol. 50, pp. 308–316, 2012.
- [76] C. Hood, I. MacKenzie, J. Stocker, K. Johnson, D. Carruthers, M. Vieno, and R. Doherty, “Air quality simulations for London using a coupled regional-to-local modelling system,” *Atmospheric Chemistry and Physics*, vol. 18, no. 15, pp. 11221–11245, 2018.
- [77] R. Stull, *An Introduction to Boundary Layer Meteorology*. Springer, 1988.
- [78] C. W. O’Dell, B. Connor, H. Bösch, D. O’Brien, C. Frankenberg, R. Castano, M. Christi, D. Eldering, B. Fisher, M. Gunson, J. McDuffie, C. E. Miller, V. Natraj, F. Oyafuso, I. Polonsky, M. Smyth, T. Taylor, G. C. Toon, P. O. Wennberg, and D. Wunch, “The ACOS CO₂ retrieval algorithm - part 1: Description and validation against synthetic observations,” *Atmospheric Measurement Techniques*, vol. 5, no. 1, pp. 99–121, 2012.

- [79] J. Salvatier, T. V. Wiecki, and C. Fonnesbeck, “Probabilistic programming in python using PyMC3,” *PeerJ Computer Science*, vol. 2, p. e55, apr 2016.
- [80] M. Crippa, D. Guizzardi, M. Muntean, E. Schaaf, F. Dentener, J. A. van Aardenne, S. Monni, U. Doering, J. G. J. Olivier, V. Pagliari, and G. Janssens-Maenhout, “Gridded emissions of air pollutants for the period 1970-2012 within EDGAR v4.3.2,” *Earth System Science Data*, vol. 10, no. 4, pp. 1987–2013, 2018.
- [81] K. Wu, T. Lauvaux, K. J. Davis, A. Deng, I. L. Coto, K. R. Gurney, and R. Patarasuk, “Joint inverse estimation of fossil fuel and biogenic CO_2 fluxes in an urban environment: An observing system simulation experiment to assess the impact of multiple uncertainties,” *Elementa*, vol. 6, p. 17, 2018.
- [82] E. Saboya, G. Zazzeri, H. Graven, A. J. Manning, and S. Englund Michel, “Continuous CH_4 and $\delta^{13}\text{C}_{\text{CH}_4}$ measurements in London demonstrate under-reported natural gas leakage,” *Atmospheric Chemistry and Physics*, vol. 22, no. 5, pp. 3595–3613, 2022.